Reversing GABA polarity corrects synaptic physiology and behaviour in young adolescents *Syngap1*$^{+/-}$ mice

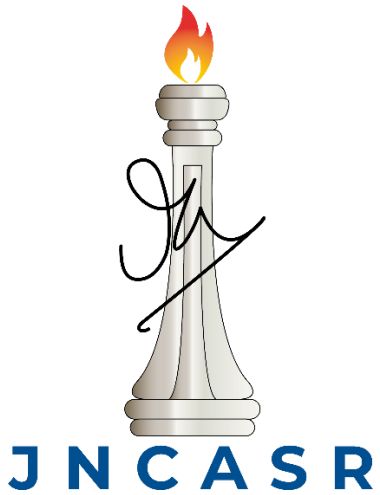

A thesis submitted for the degree of

DOCTOR OF PHILOSOPHY

by

Vijaya Verma,

Clement lab, Neuroscience Unit,

Jawaharlal Center for Advanced Scientific Research,

Jakkur, Bengaluru, Karnataka-560064, INDIA

April 2021

Table of Contents

Author's Declaration

I, Vijaya Verma, hereby declare that the thesis entitled **"Reversing GABA polarity corrects synaptic physiology and behaviour in young adolescents *Syngap1*$^{+/-}$ mice"** is a result of analysis carried out by myself under the guidance of Dr James P. Clement Chelliah, Neuroscience Unit, Jawaharlal Nehru Centre for Advanced Scientific Research (JNCASR), Bengaluru, India. This work has not been submitted elsewhere for the award of any academic degree. Keeping in consideration to report scientific observations, for the acknowledgements, references have been inserted wherever the work described has been based on other investigators.

Vijaya Verma

Certificate

This is to certify that the work described in this thesis entitled **"Reversing GABA polarity corrects synaptic physiology and behaviour in young adolescents *Syngap1*$^{+/-}$ mice"** is the result of investigations carried out by **Ms Vijaya Verma** under my guidance, and the results presented here have previously not formed the basis for the award of any other diploma, degree, or fellowship.

James P. Clement Chelliah,
Associate professor,
Clement lab,
Neuroscience Unit,
Jawaharlal Centre for Advanced Scientific Research,
Jakkur, Bengaluru, Karnataka-560064, INDIA
Date: 13 April 2021

Acknowledgement

Foremost, I would like to express my sincere gratitude to Dr James P. Clement Chelliah for providing me with an opportunity to work on this project in his lab. He has always been an encouraging mentor throughout my PhD. I am incredibly grateful for his insights on my work which have always helped me in developing a better scientist. His mentorship has a right balance of independence and security, which has let me grow as an independent researcher. He has been very supportive through all the challenges associated with this work. I admire him for his advice on time management and discipline in work-life balance. I look forward to taking the experience from my time in his lab for all my future endeavours.

I would like to thank Dr Thomas Behnisch, Fudan University, Dr Ravi Muddashetty, NCBS, and Dr Vidita Vaidya, TIFR, for their insightful guidance and support in this project.

My sincere thanks to Dr Ravi Manjithaya and Sheeba Vasu for their constant guidance and support in this project.

I would like to thank Prof. Ted Abel and Dr Joseph C. Glykys for the critical comments about the concept and the data. I would also like to thank Drs. Elizabeth Nicholson, Milos Petrovic, Emin Ozkan, and Jonathan Brown for valuable suggestions on perforated patch-clamp and LTP experiments.

I thank Ginni Khurana and Shruthi Sateesh for their technical inputs in immunoblotting and IHC experiments. I thank Zahid MD and M J Vijay Kumar for assisting in behavioural experiments.

I would further like to thank the NSU Chair, Prof. Anuranjan Anand, and MBGU Chairs, Prof. Manisha Inamdar, and Prof Ranga Udaykumar, for ensuring the smooth and efficient functioning of the departments and making sure all requirements were met for the students.

I am very grateful to all the faculty – Prof. M.R.S. Rao, Prof. Namita Surolia, Prof. Uday Kumar Ranga, Prof. Tapas Kumar Kundu, Prof. Hemalatha Balaram, Prof. Kaustav Sanyal, Dr Kushagra Bansal, Prof. V. K. Sharma, and Prof Amitabh Joshi for their insightful

guidance during work presentations and course work. Learning under each of them was a unique, adventurous experience that helped me develop the scientific temperament I have today. I would also like to thank Dr Sarit Agasti for their kind assistance in times of need during the project.

My immense thanks to MML, AL, CBL, HIV-AIDS lab, TDL, MPPEL, and Bansal lab for all the help in a time of need.

I would like to thank the administrative, academic, purchase, and support staff of JNCASR for making JNCASR a wonderful, calm, and tension-free environment to carry out science. I would like to especially thank Suma Madam for her patience and help with imaging studies. I am also very thankful to Dr Prakash and the animal house staff for the animal house maintenance.

Further, I am grateful to all present and past Clement lab members for their company and assistance throughout my project.

I would like to thank Vidita Vaidya`s lab members, Sthita, Ankit, Praachi, Toshali, Sonali, Sukrita, and Dwight, for making my stay at TIFR memorable.

I would also like to thank Dr Ravi Muddashetty lab members Preeti, Bharti, and Sarayu for providing me with the resources for IP experiments.

I would also like to thank Drisya Dileep, Ankita Kapoor, and Lakshmi Balasubramaniam for helping me with IHC image analysis. A very special thanks to Drisya Dileep and Sandeep for all the fun times we had in exploring places and food joints.

I am beyond thankful for having wonderful friends and companions in my JNC life.

Finally, I am greatly indebted to my family members - My Grandparents, Pitaji, Maate, Bhaiya, Bhabhi, Mayank, Dolly, and Shubham, for always being there for me and because of whom I am here. I am also grateful to my Bangalore family - Navodita, Rafay, Atif, Arbina, Mustafa, Vaibhav, Yogi aunty and uncle for making a memorable PhD journey for me.

Abbreviations

DSM: Diagnostic and statistical manual and mental disorders

ASD: Autism spectrum disorder

ID: Intellectual disability

MR: Mental retardation

NS: Non-syndromic

NDD: Neurodevelopmental disorder

SYNGAP1: Synaptic RAS-GTPase activating protein

GABA: γ-aminobutyric acid

KCC2: Potassium chloride cotransporter

NKCC1: Sodium potassium chloride cotransporter

GABAR: γ-aminobutyric acid receptor

KAR: Kainate receptor

NMDAR: N-methyl D-aspartate receptor

AMPAR: α-amino-3-hydroxy-5-methyl-4-isoxazolepropionicacid receptor

BDNF: Brain-derived neurotrophic factor

CaMKII: Calcium-calmodulin-dependant protein kinase II

PSD: Post synaptic density

F-ACTIN: Fibrous-Actin

GSK-3: Glycogen synthase kinase-3, multifunctional serine/threonine kinase

6BIO: 6-bromoindirubin-3`-oxime

CA: Cornu ammonis

DG: Dentate gyrus

EC: Entorhinal cortex

E/I: Excitatory/inhibitory

PND/P: Post natal day

WT: Wild type

fEPSP: Field excitatory post synaptic potential

LTP: Long-term potentiation

mEPSC: Miniature excitatory post synaptic current

GDP: Giant depolarization potential

OFT: Open field test

NOR: Novel object recognition

SI: Social interaction

SP: Social preference

DI: Discrimination Index

Thesis Synopsis

Introduction: Differential regulation of the strength of synapses through the process of synaptic plasticity is a fundamental phenomenon regulating neuronal development and function, primarily during the early stages of development (Bliss and Collingridge 1993). Mutations in gene encoding proteins that regulate synaptic function disrupt this phenomenon and have been linked to the onset of neurodevelopmental brain-related disorders such as Autism Spectrum Disorders (ASD) and Intellectual Disability (ID) (Bear, Huber et al. 2004, Penzes, Cahill et al. 2011). One of the genes implicated in ASD/ID is *SYNGAP1* that encodes for RAS-GTPase-activating protein SYNGAP1 (Hamdan, Daoud et al. 2011, Berryer, Hamdan et al. 2013, Kilinc, Creson et al. 2018, Kimura, Akahira-Azuma et al. 2018, Vlaskamp, Shaw et al. 2019). Enhanced excitatory neurotransmission, premature development of synapses, and Excitation/Inhibition (E/I) imbalance during development are the neuropathophysiological hallmarks of heterozygous *Syngap1* mouse strain (*Syngap1*$^{+/-}$) that disturbs synaptic function and cognitive and social behaviours (Komiyama, Watabe et al. 2002, Guo, Hamilton et al. 2009, Muhia, Yee et al. 2010, Clement, Aceti et al. 2012, Clement, Ozkan et al. 2013, Ozkan, Creson et al. 2014, Jeyabalan and Clement 2016).

Syngap1$^{+/-}$ mice display improper glutamatergic synapse development and function; however, the trophic role of GABA in shaping synaptic function during development is unknown (Ben-Ari 2002, Clement, Aceti et al. 2012, Clement, Ozkan et al. 2013, Kepecs and Fishell 2014, Ozkan, Creson et al. 2014, Jeyabalan and Clement 2016). Studies have shown that GABA exhibits trophic function - excitatory and inhibitory in early and late stages of development, respectively - regulated by chloride (Cl^-) co-transporters like KCC2 and NKCC1, and their expression is regulated developmentally. NKCC1 is highest in the early stages of the development that allows influx of Cl^-. In contrast, the KCC2 expression increases in the later stages of development, thereby, extrudes Cl^- from the neuron. Hence, the intracellular Cl^- concentration determines GABA-mediated responses that can further regulate the synaptogenesis during development (Rivera, Voipio et al. 1999, Ben-Ari 2002, Gamba 2005, Rivera, Voipio et al. 2005, Blaesse, Airaksinen et al. 2009, Ben-Ari, Khalilov et al. 2012). Alteration in the intracellular basal Cl^- concentration modulates the electrochemical gradient of the Cl^- ion flow through the chloride conductive $GABA_A$ receptor/channels (GABAR), affecting the strength of inhibitory action in a neuronal

network. The chloride co-transporters expression level mediates the switch between excitatory or inhibitory action of $GABA_A$ receptor/channels. The disruption of the precise expression during the critical period of development impairs synapse formation and function as it has been reported in several ID/ASD animal models (Hyde, Lipska et al. 2011, Duarte, Armstrong et al. 2013, Ozkan, Creson et al. 2014, Deidda, Allegra et al. 2015). Besides, reversing the polarity of $GABA_A$ mediated chloride flow before the end of the critical period of development by bumetanide corrected E_{GABA}, synaptic function and phenotypes in Down's, Fragile -X and Rett syndrome-like animal models (Deidda, Allegra et al. 2015, Banerjee, Rikhye et al. 2016, Vlaskamp, Shaw et al. 2019). Thus, correcting the reversal potential of Cl^- (refers to GABA polarity), a common node in the neuronal network activity, is a crucial candidate for therapeutic intervention in ID/ASD.

GSK-3β (Glycogen synthase kinase-3, multifunctional serine/threonine kinase) has been suggested to have the potential to restore GABA polarity due to its pivotal role in modulating synaptic plasticity (Yao, Shaw et al. 2002, Salcedo-Tello, Ortiz-Matamoros et al. 2011). The increased activity of GSK-3β is a contributor to the pathophysiology of ID/ASD, and inhibiting GSK-3β reversed the phenotypes (Guo, Hamilton et al. 2009, Mines and Jope 2011). Yet, finding potent therapeutics that can target GSK-3β and restore phenotypes, when administered after a critical period of development, has been elusive. The opportunity, therefore, exists to develop a therapeutically viable GSK-3β inhibitor that can restore the phenotypes. We report a GSK-3β inhibitor, 6-bromoindirubin-3`-oxime (6BIO), that has been described to cross the blood-brain barrier and to be neuroprotective in an MPTP-based model of Parkinson's disease (Meijer, Skaltsounis et al. 2003, Polychronopoulos, Magiatis et al. 2004, Vougogiannopoulou and Skaltsounis 2012, Suresh, Chavalmane et al. 2017).

Given the minimal knowledge of GABAergic function during development in *Syngap1*$^{+/-}$, we hypothesise that the GABA-mediated processes regulated by Cl^- co-transporter expression and function are disrupted during development in *Syngap1*$^{+/-}$. Thus, reversing the GABA function may restore phenotypes to the Wild-type level, particularly when the hard-wiring of neurons are well-established after the critical period of development.

Aims and Scopes of study:

Until now, there are a few drugs that can be used to cure or alleviate all the symptoms in adult stages for individuals suffering from ASD/ID but with limited efficacy. The biggest

challenge is to induce rewiring of the already formed hard-wired synaptic connections in the brain in ASD/ID without causing significant secondary effects. Restoring the protein level of SYNGAP1 in adult stages reinstated synaptic function (LTP) but not behaviour, suggesting that these neurons are hard-wired during development (Ozkan, Creson et al. 2014). Nevertheless, genetic restoration of *Syngap1* in the adult stages has restored some of the phenotypes, implying that not all deficits related to *Syngap1*$^{+/-}$ can be ascribed to neuronal circuit damage caused by aberrant neurodevelopment (Creson, Rojas et al. 2019).

A significant caveat evaluating the efficacy of drugs in pre-clinical models is either the lack of investigation on the effectiveness of drugs after the critical period of development (during hard-wiring) or the inability of the drug to restore the synaptic function after the critical period of development (after hard-wiring of neurons) (Vlaskamp, Shaw et al. 2019, McCamphill, Stoppel et al. 2020). Selective pharmacological modulations in GABAergic circuits during development have shown promising results in rescuing several physiological and behavioural deficits in ID/ASD models (Braat and Kooy 2015, Deidda, Allegra et al. 2015, Banerjee, Rikhye et al. 2016, Vlaskamp, Shaw et al. 2019), thus, a key candidate target for the therapeutic intervention. However, these studies have not observed promising results when administered after a critical period of development. Therefore, concise therapeutics to correct deficiencies observed in *Syngap1*$^{+/-}$-mediated ID/ASD is unfounded and provides the platform to find a candidate target for therapeutics that can restore phenotypes after the neurodevelopment period.

To study the proposed hypothesis, we investigated the electrophysiological properties of the circuits mediated by GABA. We measured the Giant depolarisation potentials to understand how network activity is affected in *Syngap1*$^{+/-}$. Further, tonic currents were measured that would indicate the altered level of inhibition in *Syngap1*$^{+/-}$. We also investigated the reversal potential of GABA and its dual function in neurons during development which was disrupted in *Syngap1*$^{+/-}$. Additionally, mRNA and protein expression levels using qPCR, immunoblotting and immunohistochemistry were investigated. The other part of the project involved investigating whether the pharmacological intervention can restore E/I balance and several behavioural and synaptic functions to that of WT level, particularly when administered after the critical period of development, which remains a challenge to date.

Chapter 1 starts with the general introduction of the brain, its circuitry, and the impact of mutations on physiological functions and possible therapeutics. The importance of the hippocampus as a model, its circuitry, pathways, layers and cell types considered for the study is discussed in detail. I briefly mentioned the use of the hippocampus to study synaptic transmission and synaptic plasticity. I have extensively discussed neurodevelopmental disorders such as ASD/ID caused by mutations in specific genes encoding proteins necessary for synaptic functions. Besides, I have highlighted the incidence, aetiology, the number of genes implicated, and a few common examples of ASD/ID, mainly *Syngap1*$^{+/-}$, as this project involves using *Syngap1*$^{+/-}$ as a model to study ASD/ID. Most of the discussion about ASD/ID is converged to specific proteins considered in the study, SYNGAP1, GABA, NKCC1, and KCC2. Biogenesis, subunits, isoforms and their role in synaptic plasticity are discussed in detail for the proteins mentioned above. Besides, related signalling pathways by which they execute their functions are discussed in detail. SYNGAP1, GABA, NKCC1, and KCC2 expression are developmentally regulated, and mutations in them result in ASD/ID, indicating that they have a significant role in the critical period of brain development. Thus, the critical period of development and its relation to early GABA network activity are discussed later in the introduction. Further, the discussion is extended to therapeutic interventions prescribed to treat ASD/ID. It covers therapeutics used earlier and, to date, their functions and limitations. Additionally, the use of GSK-3β inhibitors as a potential and emerging therapeutics involving the targeting of $GABA_A$ receptors is discussed in detail.

Chapter 2 describes the materials and methods used for the study. All the electrophysiological recordings were performed in the Dentate gyrus granule cells of the hippocampus. Giant depolarisation potentials were recorded using the whole-cell patch-clamp method to study GABA-mediated network activity. Tonic inhibition mediated by GABA were recorded by whole-cell patch-clamp. The reversal potential of GABA was measured by a gramicidin-based perforated patch-clamp. After studying the functional properties of the neuronal network, protein and mRNA expression of NKCC1 and KCC2 were elucidated using immunoblotting, immunohistochemistry, and qPCR. Since we found out GABA-mediated functional properties of neurons altered in *Syngap1*$^{+/-}$ mice, we wanted to check whether reversing GABA reversal potential by pharmacological intervention could correct synaptic and behavioural deficits. We tested the effect of 6BIO, GSK-3β inhibitor, on synaptic and behavioural paradigms. It was injected intraperitoneally in three different age groups: 1) only critical period injection, 2) critical period and adulthood injection, and 3)

adulthood injections. These groups were chosen as they would facilitate the evaluation of the efficacy and potency of 6BIO in restoring synaptic and behavioural deficits observed in this mouse model of ASD/ID. LTP and GABA reversal potential from acute hippocampal slices were performed as a measurement of synaptic function in mice treated with 6BIO and vehicle (saline). Further, hallmark behaviours such as open field activity (total distance covered and the number of entries in the centre), novel object recognition, and social interaction and preference were tested in *Syngap1*$^{+/-}$ mice treated with 6BIO. Vehicle-treated and 6BIO treated mice. In this chapter, I have discussed all the reagents, salts and chemicals used in this study.

Chapter 3 describes the results obtained in the study. GABA-mediated network activity was found to be decreased in the first and second postnatal stages of development in *Syngap1*$^{+/-}$ mice. Less network activity indicates altered Excitation-Inhibition balance, which prompted us to check the tonic inhibition and found it to be significantly changed in two weeks in *Syngap1*$^{+/-}$ mice. GABA-mediated change in neuronal function (depolarised or hyperpolarised) can be correlated to the abnormal functioning of chloride co-transporters, NKCC1 and KCC2. GABA reversal potential was investigated during the development, and increased depolarised neurons having a reversal potential of around -45 mV was observed in two weeks in *Syngap1*$^{+/-}$ mice as compared to WT having a reversal potential of -65 mV. As the excitatory neurons were found to be depolarised in *Syngap1*$^{+/-}$ mice, the expression of NKCC1 and KCC2 was checked using immunoblotting and immunohistochemistry during different stages of development. NKCC1 expression was found to be high at P8, similar to KCC2 expression as a means of compensation to altered neuronal activity. KCC2 expression was decreased as compared to WT in PND14-16 *Syngap1*$^{+/-}$ mice. Though protein levels were found to be altered, there was no change observed in mRNA in two-week-old mice, suggesting dysregulated translational of NKCC1 and KCC2 during development. Since GABA-mediated function was affected, we examined whether reversing GABA reversal potential could correct synaptic, behavioural, and cognitive deficits observed in *Syngap1*$^{+/-}$ mice by therapeutic intervention. GSK-3β has been shown to play an essential role in learning and memory. Therefore, we injected 6BIO, a GSK-3β inhibitor, intraperitoneally in three age groups, as discussed in Chapter 2. Remarkably, the administration of 6BIO in adulthood restored most of the behavioural deficits and synaptic dysfunction, particularly LTP, to WT levels. Thus, based on these results, 6BIO is an excellent candidate to treat ASD/ID.

Chapter 4 includes discussion, interpretation of results, limitations of the compound, and future directions of the study. The compensatory mechanism for survival of *Syngap1*$^{+/-}$ mice have been elucidated by observed changes in selective age groups, mainly in the first and second postnatal weeks. This compensation is vital for survival, but it underlies the synaptic, behavioural, and cognitive deficits observed in *Syngap1*$^{+/-}$ mice. Briefly, decreased GDP and GABA-mediated activity at 1) P8 is being compensated by increased spiking rate, increased NKCC1 and KCC2 expression, 2) P14 is being counterbalanced by increased AMPAR/NMDAR ratio and decreased KCC2 expression along with depolarised neurons. Besides, the need for novel therapeutics and significance has been elucidated in this chapter. Special emphasis is provided on the side-affects and demerits of the available therapeutics, and how the GSK-3β inhibitor, 6BIO, has the potential to overcome all those demerits is debated. As a game-changer in neurodevelopmental disorders like ASD/ID, the GABA receptor has been concisely-structured and presented as a future potent therapeutic target. Additionally, the study's limitations, including water insolubility of 6BIO and intraperitoneal injections instead of oral gavaging, have been discussed. Future directions include introducing water-soluble derivatives of 6BIO, elucidation of the whole molecular signalling pathway of action of 6BIO, the study of a converged signalling pathway connecting GSK-3β, KCC2, BDNF, and SYNGAP1.

List of Publications

Manuscripts:

- Identification of an individual with a *SYNGAP1* pathogenic mutation in India. **Verma V**, Mandora A, Botre A, Clement JP. Mol Biol Rep. 2020 *10.1007/s11033-020-05915-4*.
- Chronic postnatal chemogenetic activation of forebrain excitatory neurons evokes persistent changes in mood behaviour. Pati S, Saba K, Salvi SS, Tiwari P, Chaudhari PR, **Verma V**, Mukhopadhyay S, Kapri D, Suryavanshi S, Clement JP, Patel AB, Vaidya VA. eLife 2020 *10.7554/eLife.56171.*
- Reversing developmental switch of GABA evoked chloride ion current flow corrects synaptic and behavioural deficits in *Syngap1*$^{+/-}$ mice. **Verma V**, MJ Vijay Kumar, Kavita Sharma, Sridhar Rajaram, Ravi Muddashetty, Ravi Manjithaya, Thomas Behnisch, Clement JP (submitted in Journal of Neuroscience).
- Generation of neuroprotective reactive astrocytes in the mouse brain is regulated by SRF. Monika Jain, Surya Chandra Rao Thumu, **Verma V**, Paul P. Y. Lu, Sumitha Soman, David H. Gutmann, Deepak Nair1, Clement JP, Narendrakumar Ramanan (submitted in Science).
- Supramolecular microenvironment for attachment and growth of primary neurons. Monica Swetha Bosco, **Verma V**, James P Clement, Sarit Agasti (to be submitted).

Reviews:

- Neurodegenerative diseases: model organisms, pathology and autophagy. Suresh SN, **Verma V**, Sateesh S, Clement JP, Manjithaya R. Journal of Genetics. 2018 Jul;*97(3):679-701.*
- Understanding Intellectual Disability and Autism Spectrum Disorder from common mouse models: synapses to behaviour. **Verma V**, Abhik Paul, Anjali AV, Bhupesh Vaidya, Clement JP. Open Biology 2019 *10.1098/rsob.180265.*

Chapter- 1 General Introduction

“There is no scientific study more vital to the human than the study of their brain. Our entire view of the universe depends on it. The brain makes each human unique and defines us,” modified from Francis Crick and Stanley B. Prusiner. The understanding of the human brain, a masterpiece of creation, has captivated scientists since the Neolithic era (~10,000 BC) based on archaeological evidence of `trepanation`, which has consequently led to the current era of machine learning and artificial intelligence, although it is in the juvenile stage. The intricacies and awe-inspiring facts that a three-pound of tissue mass can possess approximately 86 billion neurons and 85 billion non-neuronal cells and yet can store and encode the information in circuitry to determine one’s behaviour is remarkable and beyond comprehension (Azevedo, Carvalho et al. 2009). The accomplishment of the same is done by long term alteration of synaptic strength, which is the cellular correlation of learning and memory.

Differential regulation of the strength of synapses through synaptic plasticity is a fundamental phenomenon regulating neuronal development and function, primarily during the early stages of development (Bliss and Collingridge 1993). The strength of the synapse is dependent on the activity pattern from the external stimuli—the more the strength of the synapse, the stronger the neuronal connections for the stimulus. Daily normal activities like walking, talking, and more complex activities like decision-making, mathematics, and computation are coordinated by neuronal connections in the brain, which is the central processing unit of the body. One of the ways to recall the above activities require persistent stimulus to associated synaptic connections, the gradual integration of acquired information to neocortical areas resulting in the formation of stronger memory (Squire 1992, Shastri 2002). At the time of birth, there is very sparse neuronal circuitry, but as the brain matures, there is a huge increase in the complexity of the circuitry elucidated by dense dendritic arbours, which enables a baby to learn things quickly (Levitt 2003). However, at the end of adolescence, only active connections will be strengthened, and less active connections will be removed; therefore, it is hard to learn new things after adolescence (Stiles and Jernigan 2010).

The formation, maintenance, and elimination of these connections require proper functioning of many pre- and post-synaptic proteins and protein kinases like CaMKII (Calcium Calmodulin dependant protein kinase II), PSD95 (Post Synaptic Density), DENSIN-180, F-ACTIN (Fibrous Actin), NMDAR (N-methyl D-aspartate receptors), and AMPAR (α-amino-3-hydroxy-5-methyl-4-isoxazolepropionicacid receptor) (Vaillend, Poirier et al. 2008, Boda, Dubos et al. 2010). Alterations or imbalances in any of the genes encoding for the proteins involved in regulating synaptic function is shown to cause cognitive and developmental disorders such as impairment of cognition, mental illness, and developmental disorders (Chechlacz and Gleeson 2003, Verpelli and Sala 2012).

1.1 Brain, synapses, and synaptic plasticity:

A coordinated joint endeavour of the Frontal lobe, Temporal lobe, Parietal lobe, Occipital lobe, Cerebellum, and limbic system is the determinant of the cognitive, motor, social, emotional, and sensory behaviour of an individual. I would be discussing the hippocampus (a region in the temporal lobe) in detail as it is chosen as a model for this study. Hippocampus is widely used as a model system to study synaptic plasticity, learning and memory; hence, most thoroughly studied area of the nervous system. The reason for it to be used as a model system got attention in the 1950s when the famous patient HM (Henry Molaison) was diagnosed with memory loss (Scoville and Milner 1957). Since then, it has attracted scientists to explore learning and memory mechanisms that lie within the brain.

The structural formation of the hippocampus is unique due to distinctive and readily identifiable areas such as Cornu Ammonis (CA) and Dentate Gyrus (DG), which provides scientists to explore neuroanatomical and electrophysiological studies at ease. DG consists of three layers, the principal or granule cell layer, largely acellular molecular layer located above the granular layer and diffusely cellular polymorphic layer (also known as hilus), located below the granular layer. The pyramidal cell layer, which is the principal cell layer of the hippocampus, has been divided into three regions CA1, CA2, and CA3, based on the size and appearance of neurons. The primary input to DG originates from the entorhinal cortex (EC), known as the perforant pathway, which is further subdivided into the medial and lateral perforant pathway. CA3 pyramidal neurons receive a mossy fibre input from DG known as the mossy fibre pathway. From CA3, axons project to the contralateral hippocampus, known as the associational commissural pathway, and other to CA1 neurons, known as Schaffer

collateral pathway. Together Perforant, mossy fibre and Schaffer collateral pathway are known as the trisynaptic circuit of the hippocampus (Andersen, Bliss et al. 1969, Amaral and Witter 1989) (**Figure 1.1**).

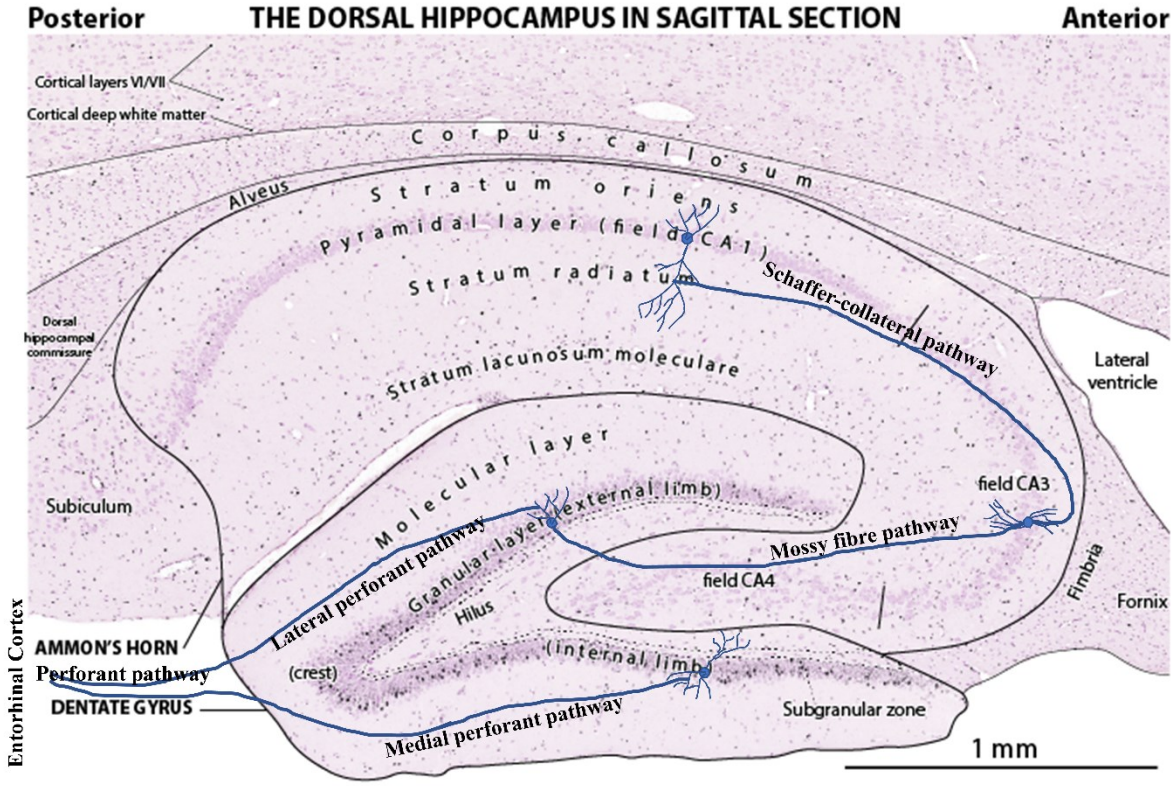

Figure 1.1 Diagram depicts different hippocampal layers and the trisynaptic circuit.
A sagittal section of the brain was injected with ^{3}H-thymidine to check neurogenesis in the hippocampus during development. The dark purple dotted structures making lines represents the neurons cell body layer. Blue coloured lines represent different pathways that form the trisynaptic circuit of the hippocampus. Major input comes from layer II of EC to DG forming perforant pathway, which is further divided into the lateral and medial perforant pathway. Granule cells of DG project and form synapses project onto CA3 pyramidal neurons through the mossy fibre pathway. Additionally, CA3 neurons project onto CA1 neurons dendrites forming Schaffer collateral pathway. All these circuits together form a trisynaptic circuit of the hippocampus. The diagram is modified from braindevelopmentmaps.org

Bliss and colleagues demonstrated persistent long-term potentiation (LTP) in DG when provided tetanic stimulation, suggesting DG's, thus hippocampus, importance in synaptic plasticity (Bliss and Lomo 1973). LTP is the cellular correlate of learning and memory. Various receptors such as AMPAR, NMDAR, KAR provide the platform for synaptic and structural changes in a neuron upon activation externally or pharmacologically. These

changes led to permanent structural change if the frequency of stimulation increases with time. Thus, the hippocampus is essential in synaptic plasticity and, thus, learning and memory in the brain. Since many brain-related disorders such as ASD/ID are associated with deficits in learning and memory, the hippocampus has been used as a model system to study the synaptic and cellular mechanisms of the disorders.

1.2 ASD/ID

As early as 1943, Leo Kanner was the first person to report and name a pattern of behaviour observed in 11 children, like Autism, meaning the self in Greek. However, the concept prevailed since the 18th century, where people had described the characteristics features of children, that time unknown, which can be quoted today as autism (Wolff 2004). Autism Spectrum Disorder (ASD) and Intellectual disability (ID) are the two major brain-related disorders to have abnormal synaptic connections in the brain. According to WHO, based on DSM-5 criteria (a system to classify ID), "*Intellectual disability means a significantly reduced ability to understand new or complex information and to learn and apply new skills (impaired intelligence). This results in a reduced ability to cope independently (impaired social functioning), and begins before adulthood, with a lasting effect on development*".

ID is characterised into two types: Syndromic (visible phenotypic characters present) and Non-Syndromic (NSID) (Kaufman, Ayub et al. 2010, Ellison, Rosenfeld et al. 2013). According to WHO, 1 in 160 children worldwide is reported to have ASD/ID (http://www.who.int/mediacentre/factsheets/autism-spectrum-disorders/en/). ID patients have deficits in intellectual and adaptive functioning, which are often comorbid with ASD traits that generally begins before adulthood. Mutations in several genes such as *NRXN1* and *NRXN2*, *FMR1*, *SHANK2*, *CHRNA7*, *SYNGAP1* are implicated in ASD and ID (summarised in **Table 1.1**) (Hamdan, Daoud et al. 2011, Chilian, Abdollahpour et al. 2013, Tassone, Choudhary et al. 2013). According to SFARI (Simons Foundation Autism Research Initiative) gene database, there are ~1231 genes encoding proteins regulating neuronal function that are implicated in ID/ASD, and one amongst them is *SYNGAP1* (Hamdan, Gauthier et al. 2009).

Table 1.1 Tabulation of behavioural, synaptic, and biochemical alterations in used transgenic mouse models of different ID/ASD related genes (*Fmr1, Syngap1, Shank, Neuroligin3, and Mecp2*).

↓Indicated down-regulation or reduced expression. ↑Indicates up-regulation or increased expression. mEPSP: Miniature Excitatory post-synaptic potential. N/D: Not determined. MGI: Mouse genome information. KO: Knock-out

Genetic modification	Behavioural changes	Changes in synaptic morphology and function	Biochemical alterations	References
Syngap1 mutation				
Exon 7/8 in *Syngap1*$^{+/-}$mice, B6;129-*Syngap1*^{tm1Rlh}/J MGI: 3822367	Stereotypic behaviour, anxiety ↓, memory deficits and social interaction ↓	LTP,↓ AMPAR/NMDAR↑	N/D	(Kim, Lee et al. 2003, Guo, Hamilton et al. 2009)
Exon 4-9 in *Syngap1*$^{+/-}$mice, *Syngap1*$^{tm1.1Mabk}$ MGI: 3511175		mEPSCs↑ Early maturation of the spines	Altered clustering of PSD-95 protein and their movement into the spine head, dysregulation of Ras, activation of the Rho family of GTP-binding proteins	(Vazquez, Chen et al. 2004)

			and phosphatidylinositol-3- kinase	
Exon 5/6 and 7/8 in *Syngap1*$^{+/-}$ mice B6;129S2 *Syngap1*^{tm2Geno}/RumbJ MGI: 5796355 STOCK *Syngap1*$^{tm1.1Geno}$/RumbJ MGI: 5796354	Seizure threshold↓, altered context discrimination behaviour, locomotor activity↑	Early spine maturation, AMPAR/NMDAR↑ LTP↓	N/D	(Clement, Aceti et al. 2012)
Syngap1^{tm1Grnt} MGI: 3581299	Reduced memory persistence in spatial learning	No change in basal synaptic trnsmission, and NMDA-mediated currents. Reduced LTP in CA1 synapses	NMDAR-mediated enhanced ERK activation	(Komiyama, Watabe et al. 2002)
Fmr1 mutations				
Fmr1-KO (neomycin cassette inserted into exon 5)	Cognition↓ and activity↑ Seizure threshold↓ Sensitivity to	Spine density, immature thin, elongated spines↑	Group I mGluR mediated LTD↑ local protein synthesis ↑	(Oostra, Bakker et al. 1994), (Dahlhaus

B6.129P2-*Fmr1*^{tm1Cgr}/J MGI: 2162650	sensory stimuli, anxiety↑, social interaction↓			2018)
Fmr1-KO2 (germline ablation of promoter and first coding exon) *Fmr1*$^{tm1.1Cidz}$ MGI: 3808885	Hyperactivity Altered emotional processing Memory deficits Hypersensory response Ultrasonic vocalizations↓	Spine heads↓ and wider spine necks	AMPAR/NMDAR↓ NMDAR-mediated LTP↓	(Mientjes, Nieuwenhuizen et al. 2006), (Gaudissard, Ginger et al. 2017), (Wijetunge, Angibaud et al. 2014)
Fmr1-CKO (promoter and first coding exon are floxed, can be removed with conditional cre-expression) *Fmr1*^{tm1Cidz} MGI: 3603442	Hippocampus-dependent learning deficits Cerebellar eyelid conditioning↓	Immature spines number ↑	LTD↑	(Koekkoek, Yamaguchi et al. 2005), (Guo, Allan et al. 2011)
Mecp2 mutation				
Mecp2 KO B6.129P2(C)-*Mecp2*$^{tm1.1Bird}$/J	locomotor activities,↓ improper gait,	Number of Dopaminergic neurons,↓	The deficit in GABA and Glutamate synthesis	(Blue, Kaufmann et al. 2011, El-Khoury,

MGI: 2165230	hind limb clasping. Respiratory disorder,	Soma size,↓ Precocious opening of the critical period in the visual cortex and accelerated maturation of GABAergic PV (+) neurons.	pathway, Spatiotemporal alteration of NMDAR expression, Alteration in activity-dependent global chromatin dynamics.	Panayotis et al. 2014) (Guy, Hendrich et al. 2001, Abdala, Dutschmann et al. 2010, Carouge, Host et al. 2010, Singleton, Gonzales et al. 2011, Krishnan, Wang et al. 2015)
Mecp2-CKO TH-Cre, *Mecp2 flox* B6;129P2-*Mecp2*^{tm1Bird}/J MGI:3702570	Total distance and vertical activity in the open field test,↓ performance in Dowel walking test↓	Dopamine, Norepinephrine, Serotonin release ↓	Expression of *TH* and *Tph2* ↓	(Samaco, Mandel-Brehm et al. 2009)
MeCP2 KI FVB-Tg(MECP2)1Hzo/J MGI: 3817212	Homozygous animals show tremors, gait-ataxia.↑ Heterozygous animals show rescue from RTT	Neuronal cell number and brain size is rescued to wild-type littermates.	N/D	(Luikenhuis, Giacometti et al. 2004)

	like symptoms			
MeCP2^{R168X} Point mutation; STOCK *Mecp2*$^{tm1.1Jtc}$/SchvJ MGI: 5568127	Stereotyped behaviour↑ hypoactivity, breathing problems	N/D	No change in the *Ube3A* mRNA level	(Lawson-Yuen, Liu et al. 2007)
Shank3 Mutation				
Shank3^{e4-9} homozygous B6.129S7-*Shank3*^{tm1Yhj}/J MGI: 5295948	Social interaction↓, repetitive behaviour, ↑ impaired memory	Activity-dependent redistribution of GluA1 AMPAR↓, thin long dendritic spines↑, LTP↓.	GKAP, PSD95, Homer protein level ↓	(Hamdan, Daoud et al. 2011)
Shank3^{e4-9} heterozygous B6-*Shank3*$^{tm1.2Bux}$/J MGI: 5317118	Social behaviour, social sniffing, ultrasonic vocalisation ↓	mEPSC, basal neurotransmission, LTP↓	AMPAR expression↓	(Bozdagi, Sakurai et al. 2010)
Shank3B$^{-/-}$ B6.129-*Shank3*^{tm2Gfng}/J MGI: 5444207	Repetitive grooming↑ social interaction↓	Complexity of dendritic length, dendritic arborization, and surface area of MSN↑ . Caudate volume ↑ .Cortico-	SAPAP3, PSD93, Homer, NR2B, GluA2, NR2A expression↓	(Peça, Feliciano et al. 2011)

		striatal synaptic transmission, mEPSC frequency in MSN↓		
Neuroligin				
Neuroligin3 R451C knock-in mice B6;129-*Nlgn3*^{tm1Sud}/J MGI: 3820515	Rotarod mediated motor behaviour↑	Dendritic complexity ↑and dendritic branching in hippocampus ↑. mEPSC in CA1, mIPSC in somatosensory cortex, LTP ↑. mIPSC in CA3, GABA release, GDP frequency ↑. GABAergic synaptic transmission ↑and IPSC amplitude in barrel cortex and hippocampus↓ . IPSC↓ and E/I ratio in D1-MSN↑ .	NLGN3 protein misfolding and trafficking defects, NLGN3 expression was 90% ↓ . Alteration of NMDAR subunit composition and expression of NMDAR subunit 2B ↑ . IPSC amplitude and success rate at the same synapse failed to respond to AM251 (CB1 receptor antagonist).	(Tabuchi, Blundell et al. 2007, Etherton, Foldy et al. 2011, Foldy, Malenka et al. 2013, Pizzarelli and Cherubini 2013, Cellot and Cherubini 2014, Rothwell, Fuccillo et al. 2014)
Neuroligin3 R704C knock-in mice STOCK		AMPAR mediated synaptic response↓ and unaltered NMADR or GABAR mediated	Levels of AMPAR subunits GluA1 and GluA3↑.	(Etherton, Foldy et al. 2011)

Nlgn3$^{tm3.1Sud}$/J MGI: 5437466		response↑ Unaltered NMDAR mediated LTP, EPSC frequency and NMDAR/AMPAR, in cultured hippocampal neurons		

1.3 *SYNGAP1*:

Mental retardation (MR; nowadays termed as Intellectual Disability (ID)) affects 1-3% of the population and often occur in a non-syndromic (NS) form where associated morphological, radiological, and metabolic features will be absent (Ropers and Hamel 2005, Chelly, Khelfaoui et al. 2006). Most cases are reported as *de novo* autosomal point mutations because of the vast genetic heterogeneity of NSMR. Genes associated with MR has been shown to regulate synaptic strength and spine morphogenesis, thus regulating synaptic plasticity (Purpura 1974, Ropers and Hamel 2005, Chelly, Khelfaoui et al. 2006, Laumonnier, Cuthbert et al. 2007). *De novo* truncating mutations in *SYNGAP1* represents a common cause of autosomal dominant NSID. *SYNGAP1*-mediated ID/ASD appears to be equally prevalent for all ethnic groups and among males and females. It is considered a rare disorder with 173 females, 158 males, and 3 with no gender affected by mutation in *SYNGAP1* in the world hitherto (**Figure 1.2**). These numbers are merely the registered numbers, but the actual numbers may be higher (#SyngapCensus: 535. +51 in #1Q20 - SynGAP Research Fund).

Hamdan et al were the first to show that *SYNGAP1* disruption is a cause of autosomal dominant non-syndromic mental retardation in human patients. They recruited 94 patients (45 males, 49 females), including 63 French Canadians, 6 European whites, 9 non-Europeans whites, 2 South Americans, 6 non-whites, and 8 of mixed ethnic backgrounds. They identified *de novo* truncating mutations (*K138X*, *R579X*, and *L813RfsX22*) in three of these

patients (Hamdan, Gauthier et al. 2009). Details of the mutations identified in *SYNGAP1* is summarised in **Figure 1.3**

Two groups independently identified a novel synaptic RAS-GTPase activating protein, SYNGAP1. SYNGAP1 has a RAS-GAP domain (N-terminus, position 393 to 717, and contain FLR… PA… P motifs important for the catalytic function of RAS-GAPs) and present

Figure 1.2 Represented figure demonstrates the distribution of the registered number of SYNGAP1 patients all over the world.

The country-wise distribution of the patients suffering from *SYNGAP1* mutations, ranging from child to adult, is marked with a total of 163 males, 173 females, and 3 with no gender at the time of writing this thesis. The data is taken from Syngap1 WorldMap.

at excitatory and inhibitory synapses (Chen, Rojas-Soto et al. 1998, Kim, Liao et al. 1998, Berryer, Chattopadhyaya et al. 2016). Conserved residues of SYNGAP1 with other RAS-GAPs, suggests its participation in interaction with RAS and GTP catalysis. SYNGAP1 has RAS-GAP activity that was further demonstrated by GST fusion protein assay where the GAP domain of SYNGAP1 was shown to stimulate H-RAS-GTPase activity (Kim, Liao et al. 1998). These studies suggest the potential interaction of SYNGAP1 and RAS-GAP to facilitate the GTP hydrolysis. Most of the Arginine present in FLR motifs are stabilized by their guanidinium group and carbonyl oxygens, mostly localised in the conserved catalytic domains of the SYNGAP1 (Scheffzek, Lautwein et al. 1996, Scheffzek, Ahmadian et al.

1997). It helps in protein stabilization (core stabilization), catalysis, and formation of transition-state (an important step in catalysis of GTP).

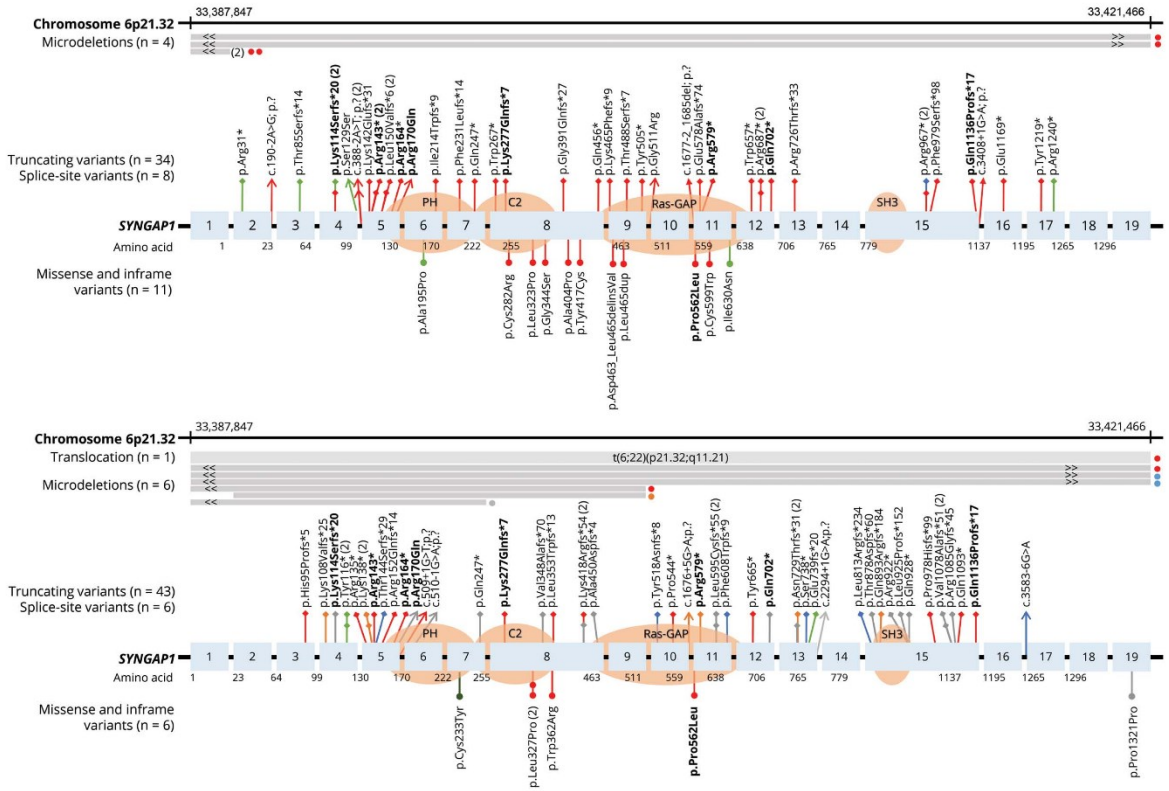

Figure 1.3 Schematic representation of *SYNGAP1* mutations and microdeletion identified to date.

Different types of mutations in chromosome 6p21.32 were identified in children with *SYNGAP1*-related ASD/ID. Truncating (♦) and splice-site (→) mutations are presented above the gene, and missense and in-frame (•) mutations are shown underneath the gene. Red lines represent moderate to severe developmental and epileptic encephalopathy, Orange indicates moderate to severe developmental encephalopathy with epilepsy, blue represents moderate to severe developmental encephalopathy with no epilepsy, light green shows mild developmental and epileptic encephalopathy, dark green is for mild developmental encephalopathy with no epilepsy, and grey is to denote unknown/unclassified epilepsy. Picture source (Vlaskamp, Shaw et al. 2019)

As shown by mutations in the conserved C2 and RAS-GAP domains (Arginine) are predicted to be deleterious as they affect the RAS-GTPase activity of SYNGAP1. pArg621*, sequence change in the catalytic domain, may create a premature translational stop signal in the *SYNGAP1*, which might result in a disrupted or truncated protein product (Berryer, Hamdan et al. 2013, Carvill, Heavin et al. 2013, Mignot, von Stulpnagel et al. 2016). Most of the point

mutation in the catalytic domain, for example, in Arginine, may result in loss of function of the protein by either destabilization of protein or because of formation of truncated protein product that might not bind to the substrate resulting in a potential disruption in the interaction of RAS-GAP with SYNGAP1, thereby, hampering the downstream protein signalling mechanisms. The RAS family GTPases, along with the upstream and downstream proteins present in biochemical signalling cascades, are key regulators of synaptic plasticity (Qin, Zhu et al. 2005). The fact that SYNAGP1 is a RAS-GTPase activating protein and *de novo* mutations in *SYNGAP1* cause NSID exemplifies its role in synaptic plasticity (Hamdan, Gauthier et al. 2009, Hamdan, Daoud et al. 2011, Berryer, Hamdan et al. 2013).

SYNGAP1 is downstream of NMDAR, and calcium influx through the NMDA receptor is the key event in the transfer of the information through neurons, which activates several downstream protein signalling targets such as CaMKII (Jeyabalan and Clement 2016, Verma, Paul et al. 2019). Intracellular increase in calcium phosphorylates CaMKII, which in turn, phosphorylates SYNGAP1 (**Figure 1.4**). SYNGAP1 is a synaptic RAS-GTPase activating protein, an important component of post synaptic density, which is closely associated with the NMDA receptor. CaMKII predominantly inhibits the RAS-GTPase activity of SYNGAP1 by phosphorylating it when there is no activity, but upon stimulation, this inhibition on RAS-GTPase is lost, thereby increasing RAS activity. It has also been shown that SYNGAP1 associates with the PSD-95 and SAP-10 protein family, which is important for the formation of synaptic connections (Kim, Liao et al. 1998). Studies have shown that SYNGAP1 is expressed predominantly in the brain, particularly in Hippocampus, Cortex, and less in the striatum and brainstem. Colocalization studies illustrate the presence of SYNGAP1 in excitatory synapses along with NMDAR and PSD-95; however, the presence of SYNGAP1 in inhibitory neurons (GABAergic) was demonstrated recently contradicting previous studies (Chen, Rojas-Soto et al. 1998, Kim, Liao et al. 1998, Berryer, Chattopadhyaya et al. 2016).

Upon NMDAR activation, SYNGAP1 is phosphorylated by CaMKII, followed by RAS and RAC activation that in turn activates ERK/ MAPK and the PAK pathway (Komiyama, Watabe et al. 2002). Followed by this, LIMK will be phosphorylated, which in turn will inactivate and phosphorylate p-COFILIN that would lead to an increase in the stability of actin cytoskeleton in spines (Carlisle, Manzerra et al. 2008). Studies have shown that using biochemical and electrophysiological techniques, *Syngap1* is a key player in neuronal

development and survival as homozygous mutant mice died within 48 hours after birth (Komiyama, Watabe et al. 2002, Kim, Lee et al. 2003).

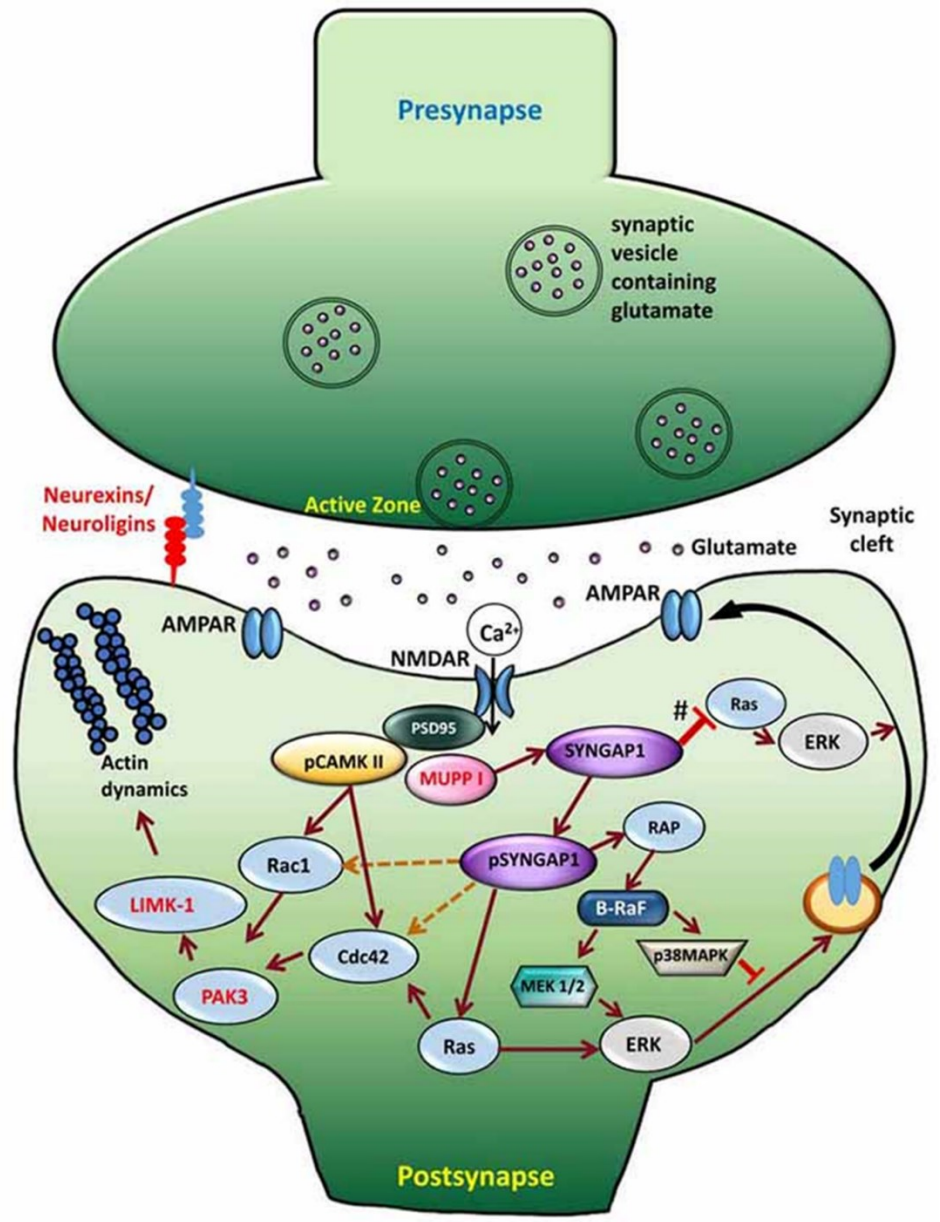

Figure 1.4 represents the biochemical signalling pathway of SYNGAP1.

Upon NMDAR activation, Ca^{2+} influx through NDMAR resulting in phosphorylation of CAMKII, which in turn phosphorylates SYNGAP1. Phosphorylated SYNGAP1 triggers downstream signalling to lead to increased RAS activity and phosphorylation of ERK, which ultimately leads to AMPAR insertion onto the postsynapses. In the case of haploinsufficiency of SYNGAP1, increased RAS activity leads to more AMPAR insertion to postsynapses, thus creating an imbalance in E/I. Picture source (Jeyabalan and Clement 2016)

Besides, increased clusters of AMPA receptors were observed in mutant mice suggesting that SYNGAP1 regulates glutamate receptor synaptic targeting during learning or synaptic activity. Physiologically, it has been observed that reduced Long Term Potentiation (LTP), a cellular correlate of memory *in vivo*, was observed in mutant mice, further confirming the significant role of SYNGAP1 in learning and memory (Ozkan, Creson et al. 2014).

Studies have shown that SYNGAP1 is consistently present in the dendritic spines in a dormant state, but upon activation by NMDAR-mediated Ca^{2+} influx and phosphorylation by CaMKII, it is dispersed towards the dendritic shaft that renders potentiation of synapses (**Figure 1.5**) (Araki, Zeng et al. 2015).

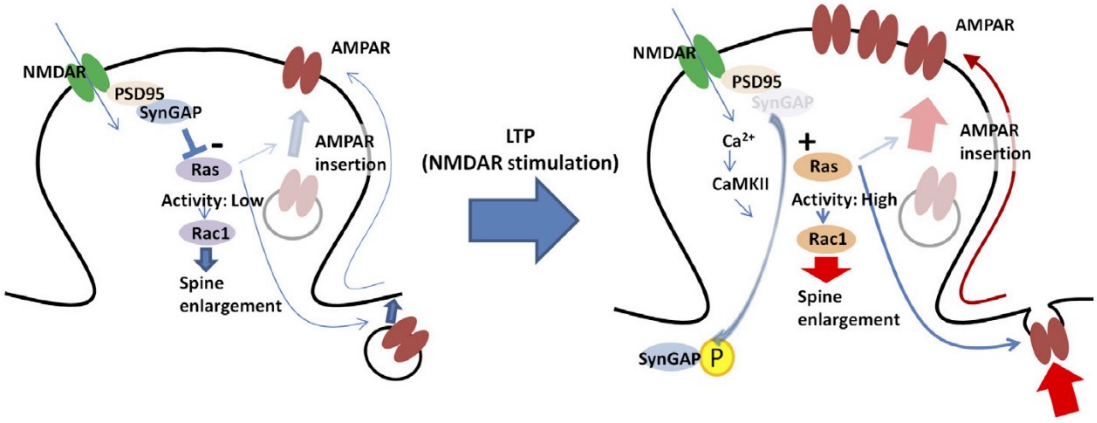

Figure 1.5 Schematic demonstration of CAMKII-mediated phosphorylation of SYNGAP1 leading to cellular changes upon LTP induction.

LTP induction leads to NMDAR-dependent calcium influx and activation of CAMKII, which in turn phosphorylates SYNGAP1, which get dispersed from synapses (spine head to spine shaft), thus, regulating synaptic plasticity (learning and memory). This leads to increased RAS activity, and activation of the RAC1 pathway leads to spine head enlargement. Figure source (Araki, Zeng et al. 2015)

Using a robust mouse model of *Syngap1* Heterozygous mutation (*Syngap1*$^{+/-}$), Clement *et al.* have shown that *Syngap1*$^{+/-}$ leads to early maturation of excitatory dendritic spines, abnormal Excitatory/Inhibitory balance leading to a dysregulated critical period of plasticity (Clement, Aceti et al. 2012, Clement, Ozkan et al. 2013, Aceti, Creson et al. 2015). Thus, alterations in dendritic spine activity and critical period of plasticity leads to various cognitive and social impairments. These cognitive abnormalities might be a consequence of enhanced excitatory

synaptic function in mature cortical pyramidal cells, which disrupts synaptic homeostasis resulting in brain dysfunction in adulthood (Ozkan, Creson et al. 2014).
Recently Llamosas N. et al has demonstrated the impact of *SYNGAP1* loss of function on the development and function of human neurons using CRISPR/Cas9 technology. SYNGAP1 protein expression was ablated in neurons derived from iPSC obtained from a human donor. They observed enhanced dendritic morphogenesis and prominent excitatory synaptic connections, and early elevated network spiking as well as synaptic activity in the neurons where SYNGAP1 expression was ablated (Llamosas, Arora et al. 2020). These results corroborated with existing literature but provided us with a broader and more confirmative platform to test therapeutics to alleviate deficits observed in *SYNGAP1* haploinsufficiency.

In this study, we have used a mouse model of *Syngap1*$^{+/-}$. To consider it as a good model to understand ASD/ID, studies have demonstrated that *Syngap1*$^{+/-}$ mice display the following behaviour traits similar to what is observed in patients (Guo, Hamilton et al. 2009, Nakajima, Takao et al. 2019):

1) Increased locomotor activity (hyperactivity)
2) Decrease anxiety-like behaviour
3) Decrease depression-like behaviour
4) Decrease in sensitivity of pain stimuli
5) Impaired working and reference spatial memory
6) Disrupted cognitive processes associated with cued fear conditioning eventually indicating deficits in fear-associated behaviours and dysregulated emotional disruptions in the amygdala
7) Impaired motor function as latency to fall on the rotarod was more
8) Enhanced acoustic startle (insignificant between WT and *Syngap1*$^{+/-}$ in Nakajima R. et al., 2019) and reduced prepulse inhibition suggesting general inhibition of related circuits may be disrupted, leading to abnormal auditory processing
9) Impaired social behaviour: Do not prefer social novelty (insignificant between WT and *Syngap1*$^{+/-}$ in Nakajima R. et al., 2019, no social preference), do not prefer social interaction

Studies discussed above place *SYNGAP1* as a major risk gene associated with ASD/ID and elucidate its critical role in synaptic development, structure, function, and plasticity. When

any of the disease models is studied to uncover the molecular and cellular mechanism causing the pathology, the ultimate far fetch goal is to cure or ameliorate the symptoms observed in the disease model. Reintroduction of recombinant WT SYNGAP1 in *Syngap1* knock out neurons was able to rescue the mutant cellular phenotypes. For example, an increase in SYNGAP1 expression and decreased spine protrusions to WT levels was observed, suggesting the restoration of SYNGAP1 expression levels in the brain might be able to correct the synaptic, morphological, behavioural, and cognitive deficits observed in *Syngap1*$^{+/-}$ mice (Vazquez, Chen et al. 2004). Clozapine, a neuroleptic, was injected and abolished hyperactivity, but no change in prepulse inhibition was observed in *Syngap1*$^{+/-}$ mice, suggesting clozapine might be effective for some brain regions but not all to correct the phenotype (Guo, Hamilton et al. 2009).

Temporal induction of *Syngap1* haploinsufficiency demonstrated that function of SYNGAP1 protein is critical in the first two weeks of hippocampal development, i.e., the critical period of SYNGAP1 is 2 weeks old mouse hippocampus. This was further confirmed by conditional reversal of *Syngap1* haploinsufficiency in adult mice where no rescue was observed for behavioural deficits present in *Syngap1*$^{+/-}$ mice, although SYNGAP1 protein expression was restored (Clement, Aceti et al. 2012). In contrast, reversing mutation at the first week of development corrected core behaviour deficits such as risk-taking, novelty-induced hyperlocomotion, and long-term memory when checked at 12 weeks of age. Reversal at third week did not rescue above mentioned behaviours but, the contextual fear memory was completely rescued. This suggests that there are different time points for critical period regulation of the SYNGAP1 function that may differ for phenotypes. One reason could be the maturation of cortical circuits associated with different behaviours varies for different regions of the brain (Aceti, Creson et al. 2015, Chakraborty, Vijay Kumar et al. 2021). Adult reversal of SYNGAP1 also eliminated interictal events and restored the seizure threshold to WT levels (Creson, Rojas et al. 2019). Additionally, reversing the *Syngap1* haploinsufficiency exclusively in forebrain glutamatergic neurons in adult mice was sufficient to correct few behaviour deficits such as anxiety, risk-taking, working, and contextual memory (Ozkan, Creson et al. 2014). These results suggest tight critical period regulation of SYNGAP1 protein function, which can vary for different behaviour, which when disrupted, leads to early spine synapse defects resulting in disorganized neural circuits and information processing that direct the behaviour and synaptic function in adulthood.

Apart from protein or gene re-expression-based rescue experiments, literature also emphasizes converged common cellular pathways in genetically diverse ID and ASDs, such as synaptic pathophysiology associated with deletion of *Fmr1* gene and *Syngap1* haploinsufficiency. Barnes et al were able to normalize basal protein synthesis to WT levels by administration of negative regulators (lovastatin) of mGluR5 and RAS-ERK1/2 pathway, which is common in deletion of *Fmr1* gene and *Syngap1* haploinsufficiency, suggesting a common pathway modulator that could be used to ameliorate the disorders of the ASD/ID (Barnes, Wijetunge et al. 2015).

In the view of rescue studies done for *Syngap1* haploinsufficiency, it is observed that Cre-mediated conditional temporal increase in SYNGAP1 level was able to restore core synaptic and behavioural deficits in adult mice (Vazquez, Chen et al. 2004, Ozkan, Creson et al. 2014, Aceti, Creson et al. 2015, Barnes, Wijetunge et al. 2015). For model systems, it is easy to manipulate the gene or protein expression levels at any developmental time point. However, to treat human patients, one should seek a way to ease the associated general religious and ethical concerns. Using molecules that can be taken orally or in the form of injections, which can either increase the SYNGAP1 expression or target a pathway that is critical yet indirect in regulating the SYNGAP1 function, would be a convincing method to treat them. A common characteristic when it comes to ASD/ID, such as *SYNGAP1* haploinsufficiency, is an imbalance in excitation to inhibition ratio. GABA, one of the major inhibitory neurotransmitters in an adult's central nervous system, shapes the neural circuits in the early stages of development which aid the future synaptic functions and behaviour of the individual, could serve as a potential therapeutic target for ASD/ID (Braat and Kooy 2015).

1.4 GABA:

Excitation to Inhibition balance (E/I balance) is important for the development, function, and maturation of synaptic connections in the initial stages of development and normal function of the brain (Ben-Ari 2002). E/I balance is maintained by extra- and intracellular concentration of various ions like Cl^-, Na^+, K^+. During the early stages of development, GABAergic (γ-aminobutyric acid) inhibitory neurons activate excitatory neurons and suppress the excitatory neurons during later stages of development. Besides, synaptic network maturation is driven by GABAergic excitation in the early stages of development that helps in the optimal maturation of synaptic connections (Pfeffer, Stein et al. 2009). This

excitatory action of GABA is determined by Cl^- ion concentration inside the neuron (Ben-Ari 2002, Gaiarsa, Caillard et al. 2002, Ben-Ari, Khalilov et al. 2012).

Studies have shown that two chloride cotransporters are important in maintaining Cl^- ion concentration inside the neurons, NKCC1 (Sodium Potassium Chloride Cotransporter) and KCC2 (Potassium Chloride Cotransporter), encoded by *SLC12a* (**Figure 1.6**) (Ben-Ari 2002, Gamba 2005, Rivera, Voipio et al. 2005).

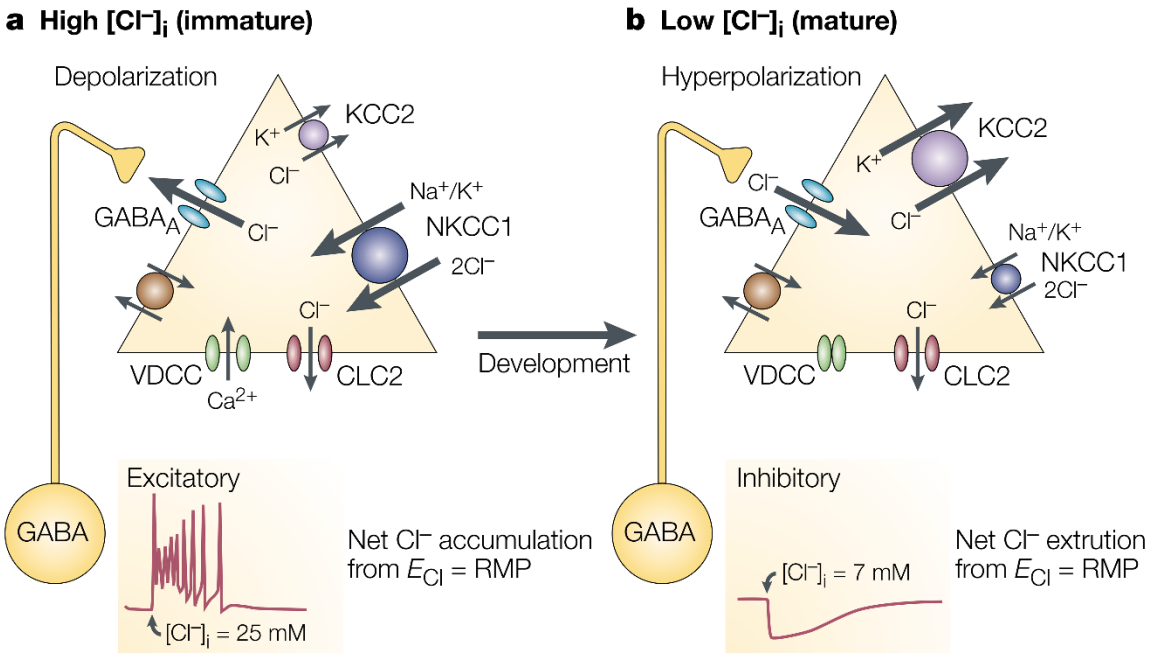

Figure 1.6 represents the dual function of GABA during the development, which is tightly regulated by the temporal expression of chloride cotransporters, NKCC1 and KCC2.

In immature neurons, chloride concentration inside is high at the resting stage. When activated, GABA binds to its receptor leading to the efflux of chloride from GABARs and hence depolarises neurons. Whereas, in mature neurons, chloride is less inside the neuron at resting state. GABA activation allows chloride to enter the neuron and thus hyperpolarises neurons. Figure source (Ben-Ari 2002)

These Cl^- transporters utilize energy from the electrochemical gradient of Na^+ and K^+ ions to transport Cl^- ions (Glykys and Mody 2007, Chamma, Chevy et al. 2012). Studies have shown that NKCC1 increases the Cl^- ion concentration inside the neuron at rest in the early stages of development, thus, depolarizes the neuron during early stages of development, whereas KCC2 extrude Cl^- ions at rest during later stages of development (towards the end of the

critical period of development), thereby, maintaining the hyperpolarizing state of the cell. (Ben-Ari 2002, Rivera, Voipio et al. 2005, Blaesse, Airaksinen et al. 2009, Ben-Ari, Khalilov et al. 2012). This developmental switch (or GABA polarity) is a prerequisite to maintain E/I balance in the brain. Failure to switch from NKCC1 to KCC2 expression during development can lead to various neurodevelopmental disorders as observed in Fragile X Syndrome (expression of NKCC1 in PND10 is more), Schizophrenia (expression of KCC2 is less in adults), and Rett, and contribute towards the pathophysiology of these disorders (Hyde, Lipska et al. 2011, Duarte, Armstrong et al. 2013, Ozkan, Creson et al. 2014).

1.4.1 GABA and Critical period of plasticity:

Neuronal circuit formation in the brain is shaped by experiences in the early stages critical period of development (Hensch 2005). The critical period of development is the time during which various sensory experiences shape neuronal development and refinement of neuronal circuits important for memory consolidation. If the neuronal circuit is untouched or unstimulated, the function served by that circuit of the brain will be compromised, which would be irreversible. Studies have demonstrated the existence of an inhibitory threshold using the gene disruption method to prevent the increase in the levels of GABA, the major inhibitory neurotransmitter of the central nervous system, suggesting the onset of the critical period of plasticity can be delayed for a long time if GABA release is kept low (Fagiolini and Hensch 2000). In contrast, precious enhancement of GABA accelerated the natural plasticity profile, such as visual acuity resulting in an early closure of the critical period of plasticity for ocular dominance (Huang, Kirkwood et al. 1999, Fagiolini and Hensch 2000). A study by Ventencourt et al. has used drugs like benzodiazepine to enhance the effect of GABA and fluoxetine to reverse the critical period of plasticity via regulating E/I balance (Maya Vetencourt, Sale et al. 2008). This suggests an important role of GABA in determining the fate of neuronal circuits in the brain during and after the critical period of development (Hensch 2005, Duarte, Armstrong et al. 2013, Hubener and Bonhoeffer 2014, Ozkan, Creson et al. 2014, Verma, Paul et al. 2019).

Alteration in the timing of sensitive periods could underlie various neurodevelopmental disorders, including ASD, ID and Schizophrenia (Bavelier, Levi et al. 2010, Baroncelli, Braschi et al. 2011). In all these disorders, one common feature is an imbalance of E/I ratio, which can serve as a key factor to understand the major cause of these disorders, and how

manipulating critical period would help to resolve the assisted defects. This is one of the major problems observed in *Syngap1* Heterozygous mutation.

During development, especially during the critical period of development, synapse formation and pruning occurs, assisted by cytoskeletal proteins in developing dendritic spines (Hensch 2005, Glykys and Mody 2007). As the neurons mature gradually, dendritic spine morphology changes from thin to stubby and to mushroom-shaped spines due to an increase in the number of AMPA receptors on the postsynaptic membrane. (Dickstein, Weaver et al. 2013). Therefore, based on these studies, for proper development of dendritic spines during development, cytoskeletal proteins are required, and, since KCC2 also interacts with one of these proteins, for example, via FERM domain protein 4.1N (Walensky, Blackshaw et al. 1999), KCC2 may have a role in the insertion of AMPA receptor to the post synaptic membrane during development. Consistent with this, it has been reported that loss of interaction of 4.1N protein leads to reduction of efficiency of excitatory synapses as well as aggregation of GluR1 subunit of AMPA receptor (Glykys and Mody 2007). Besides, KCC2 helps in spines morphogenesis rather than its maintenance which is independent of its function (Tardin, Cognet et al. 2003, Glykys and Mody 2007, Petrini, Lu et al. 2009). Thus, based on these studies, KCC2 could regulate optimal dendritic spine development and function during and after the critical period of development.

Based on the above studies and that *Syngap1*$^{+/-}$ mice display early maturation of dendritic spines along with the altered critical period of plasticity during development, these changes may affect the maturation and function of other neurons such as GABAergic neurons. A report has shown that heterozygous knockout of *Syngap1* in GABAergic interneurons alter the functions of these neurons (Berryer, Chattopadhyaya et al. 2016). As stated earlier, the function of GABAergic neurons is dependent on Cl^- transporters (NKCC1 and KCC2). Therefore, the altered maturation of dendritic spines could affect the function and development of Cl^- transporters, thereby modifying the function of GABAergic inhibitory neurons in the initial stages of development. By understanding how GABA function and polarity switch is affected by accelerated excitatory dendritic spines in *Syngap1*$^{+/-}$, potential therapeutic targets can be obtained.

1.5 NKCC1:

SLC12A2, also known as NKCC1 present on chromosome 5q23.3, has been implicated in ASD (Marchese, Valvo et al. 2016, Anazi, Maddirevula et al. 2017). Recently one patient

with complete absence of NKCC1 was diagnosed which was presented with intellectual disability, respiratory weakness, and gastrointestinal issues (Macnamara, Koehler et al. 2019). NKCC has two isoforms, NKCC1 and NKCC2, encoded by two different genes of the *SLC* family (Solute Carrier Family), *SLC12A2* and *SLC12A1*, which are formed by either the presence or absence of exon 21 respectively in the final gene product (Hebert, Mount et al. 2004). NKCC1 is expressed in almost all parts of the body, mainly in secretory epithelia (Haas and Forbush 2000) and the brain (Dzhala, Talos et al. 2005). NKCC2 is majorly expressed on the apical membrane of the thick ascending limb of Henle`s loop of nephron (Gamba and Friedman 2009). In the brain, NKCC1 is expressed in the neocortex, hippocampus, cerebellum, thalamus, brainstem, olfactory bulb, and on the apical membrane of choroid plexus, epithelial cells and its expression in these areas are seen to be regulated developmentally (Delpire and Mount 2002, Wang, Shimizu-Okabe et al. 2002, Dzhala, Talos et al. 2005).

The function of the NKCC1 cotransporter was determined from the NKCC1 knock out studies in various models like *shaker/waltzer*, null mice for NKCC1 (Delpire, Lu et al. 1999). Knock-out of *NKCC1* resulted in sensorineural deafness, intestinal phenotype, salivary gland phenotype, blood pressure/renin phenotype, male infertility, and sensory perception phenotype (Delpire, Lu et al. 1999, Evans, Park et al. 2000, Grubb, Lee et al. 2000, Sung, Kirby et al. 2000). (Delpire, Lu et al. 1999, Dixon, Gazzard et al. 1999, Flagella, Clarke et al. 1999, Pace, Madden et al. 2001). Sensory perception phenotype mainly accounts for depolarizing/excitatory effect of NKCC1. Khirug and group have studied NKCC1 dependent depolarising GABAergic effect at Axon Initial Segment (AIS: considered to be the main site for action potential generation) by measuring E_{GABA} gradient in Wild type and *NKCC1*$^{-/-}$ mice. AIS E_{GABA} values were found to be more positive as compared to soma and dendrite in WT, and this gradient was lost in *NKCC1*$^{-/-}$ mice, suggesting spatially distinct regulation of GABA function by NKCC1, dependent on differential chloride gradient in the cell (Khirug, Yamada et al. 2008). This effect is due to the presence of a high concentration of Cl^- in the presynaptic axonal compartment than soma. Given that NKCC1 expression is higher in the early stages of development, there is a higher level of uptake of Cl^- mediated by NKCC1, resulting in depolarisation of neurons (Stell, Rostaing et al. 2007, Khirug, Yamada et al. 2008).

In the visual cortex, NKCC1 inhibitor bumetanide in the early and late time window was administered to evaluate the plasticity of the cortical circuits by monocular deprivation and LTP experiments. It was found that early depolarizing GABA may have a critical role in cortical inhibition and plasticity later in development (Deidda, Allegra et al. 2015). The same group elucidated the importance of early depolarizing GABA in the Down`s syndrome mouse model. CA1 pyramidal neurons exhibit less negative E_{Cl^-} which was restored by NKCC1 inhibitor bumetanide, along with synaptic plasticity and hippocampal-dependent memory in adult mice. LTP deficits, associative memory, spatial memory, novel object recognition memory were completely restored in *Ts65Dn* mice. These effects on behaviour or synaptic plasticity were not permanent, as shown by bumetanide washout experiments, suggesting its beneficial effects rely on direct cotransporter antagonism (Deidda, Allegra et al. 2015).

The GABA-mediated reversal potential of chloride shifts towards more negative values affecting presynaptic inhibition in NKCC1-KO mice (Laird, Garcia-Nicas et al. 2004). Increased intrinsic excitability of glutamatergic neurons and increased pharmacologically isolated glutamatergic network activity was observed in NKCC1 null mice. Additionally, developmental upregulation of KCC2 was unperturbed in these mice, suggesting homeostatic regulation of neuronal activity during development in the hippocampus, which is not affected by the absence of NKCC1 (Sipila, Huttu et al. 2009). Pharmacological inhibition of NKCC1 by bumetanide in juvenile stages of development (in critical period) corrected reversal potential of chloride in the somatosensory cortex in *Fmr1* KO mice (Vlaskamp, Shaw et al. 2019). The above-discussed studies highlight the importance of early depolarizing GABA activity and NKCC1 function in shaping neuronal circuits.

1.6 KCC2:

SLC12A5, also known as KCC2, present on chromosome 20q13.12, has been implicated in ASD. 2 out of 5 reports wherein one, exonic mosaic mutations, and other with CpG site variations were presented in ASD samples (Merner, Chandler et al. 2015, Krupp, Barnard et al. 2017). Variants were categorized under rare single gene mutation. KCC2 has two isoforms: KCC2a and KCC2b, encoded by alternative splicing of *SLC12A5*gene (Blaesse, Guillemin et al. 2006, Uvarov, Ludwig et al. 2009). KCC2a is dominant in the embryonic brain, and KCC2b is foremost in the mature brain (Uvarov, Ludwig et al. 2009). KCC2 occurs not only as non-functional monomers, which is observed in the early stages of development, as well as functional oligomers that are observed in the adult stages. Usually,

oligomers vary from ~270, ~400, and ~500 kDa, which are sensitive to sulfhydryl-reducing agents and resistant to SDS. KCC2 is expressed in different parts of the brain, such as the olfactory bulb, cerebellum, brainstem, spinal cord, cortex, and hippocampus.(Payne 1997, Uvarov, Pruunsild et al. 2005, Blaesse, Guillemin et al. 2006, Takayama and Inoue 2010). Studies have shown that KCC2 is distributed along the somatodendritic axis of thalamocortical neurons (Bartho, Curto et al. 2009), dentate gyrus granule cells (Baldi, Varga et al. 2010), cortical neurons (Szabadics, Varga et al. 2006), cerebellum (Williams, Sharp et al. 1999), brainstem (Blaesse, Guillemin et al. 2006), and dendritic spines (Gulyas, Sik et al. 2001).

E_{GABA} gradient studies and immunohistochemistry studies have shown the presence of ion transport inactive KCC2 (monomers) in immature neurons (Casula, Shmukler et al. 2001, Blaesse, Guillemin et al. 2006). Biochemical analysis from the same study had shown that the oligomers to monomers ratio increases as the neuron matures. Besides, the focal GABA uncaging experiment under constant Cl^- load revealed that ion transport active form of KCC2 are oligomers and ion transport inactive form is a monomer. Transformation of monomers to oligomers is site-specific and depends on developmental stages (Blaesse, Guillemin et al. 2006). Therefore, to remove Cl^- from neurons at rest, KCC2 must be oligomerized, which is predominantly observed from the end of the critical period of development and continues throughout adulthood (Blaesse, Guillemin et al. 2006, Uvarov, Ludwig et al. 2009).

Primary neuron culture from cortical regions of KCC2 deficient mice showed prominent morphological deficits in neurons and a reduction in the number of functional synapses in immature neurons. This was independent of its cotransporter function but rather involves KCC2 carboxy-terminal domain (CTD) interaction with 4.1N (Neuronal FERM domain actin-binding protein) (Walensky, Blackshaw et al. 1999, Glykys and Mody 2007). In mature neurons, suppressing KCC2 expression decreases the efficacy of excitatory synapses as observed by reduced GluR1-containing AMPAR on post synapse, which was found to be independent of its cotransporter function (Gauvain, Chamma et al. 2011). These studies place KCC2 as a critical candidate for the development and function of glutamatergic synapses at the early and late stages of development. KCC2 is required for LTP expression as suppression of KCC2 expression and not function precludes LTP in hippocampal neurons.

Activity-driven AMPAR exocytosis was also compromised when KCC2 expression was suppressed, which was not dependent on 4.1N expression. Further, KCC2 suppression enhances ACTIN polymerization through RAC1 and LIMK-mediated inhibition of COFILIN through recruitment of βPIX-GIT1 complexes., hence, increasing phosphorylated COFILIN, thereby precluding synaptic and structural LTP expression (**Figure 1.7**). This suggests the critical role of KCC2 in the regulation of spine actin cytoskeleton and vital regulator of long-term plasticity at excitatory synapses (Chevy, Heubl et al. 2015). Studies from Mahadevan and the group have shown that KCC2 and Kainate-type glutamate receptors (KAR) subunits coexist, which contributes significantly to hyperpolarizing neurons due to the differential function of oligomerized KCC2 (Mahadevan, Pressey et al. 2014). These studies suggest that KCC2 is important in regulating neuronal development, maturation, and function.

1.7 Therapeutics:

Currently, there is no cure or specific treatment for individuals with *SYNGAP1* mutations. However, most strategic therapies target the symptoms such as seizures, hypotonia, sleeplessness, mania, euphoria, etc. Cholesterol-lowering statins, such as lovastatin or atorvastatin, has been proven to ameliorates deficits in global behaviour and cognitive behaviour in a 31-year-old patient as well as a 2-year-old child, respectively (Cook, Masaki et al. 2019, Verma, Mandora et al. 2020). However, care should be taken while prescribing these drugs, as pre-clinical studies have shown high dosage of atorvastatin for the long-term could cause significant deficits in cognitive capabilities and basic exploratory behaviour.

Up until now, preclinical studies have mostly targeted RAS-ERK signalling or, more recently, GSK-3 as therapeutics for ASD/ID. Since the historical period, late bronze age, Tyrian purple dye was processed from gastropod molluscs and prescribed for treatment. Bromine-substituted Indigo and Indirubin isomers are the main constituents of Tyrian purple dye. 6-bromoindirubin along with its synthetic derivative 6-bromoindirubin-3`-oxime (6BIO) (permeable to the cell membrane) were found out to be potent GSK-3 (Glycogen synthase kinase-3, multifunctional serine/threonine kinase) inhibitors (Meijer, Skaltsounis et al. 2003, Polychronopoulos, Magiatis et al. 2004, Vougogiannopoulou and Skaltsounis 2012).

Inactivation of GSK-3 (GSK-3α and GSK-3β) through S21/S9 phosphorylation leads to dephosphorylation of its substrates resulting in their functional activation (Culbert, Brown et al. 2001, Doble and Woodgett 2003).

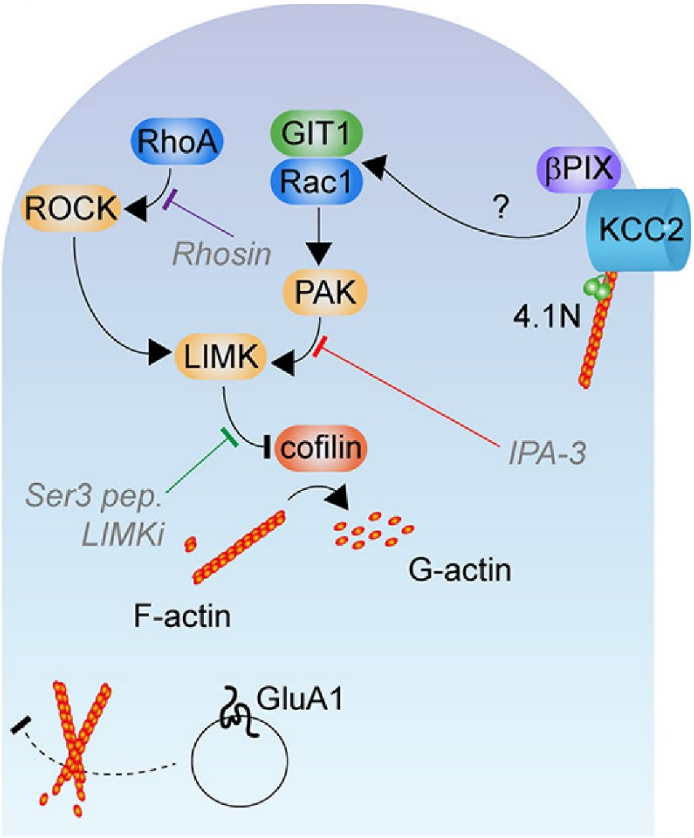

Figure 1.7 represents KCC2 mediated ACTIN depolymerization by COFILIN through RAC1 and LIMK pathway.

COFILIN activity is inhibited by its phosphorylation by LIMK. RhoA and RAC1 pathway activates LIMK. βPIX interaction with KCC2 could deactivate the RAC1 pathway, thus could inhibit LIMK to phosphorylates COFILIN. Here, disruption of KCC2 interaction with βPIX leads to RAC1 and, in turn, activation of the LIMK pathway, which phosphorylates COFILIN. This would enhance ACTIN polymerization and subsequently prevents LTP-induced AMPAR trafficking to postsynapses. Image source (Chevy, Heubl et al. 2015)

GSK-3 (Leclerc, Garnier et al. 2001), CDKs (Hoessel, Leclerc et al. 1999), Aurora kinase (Myrianthopoulos, Magiatis et al. 2007), Aryl hydrocarbon receptor (Knockaert, Blondel et al. 2004), STAT3 (Beurel and Jope 2008, Etherton, Foldy et al. 2011), could be considered as major interacting targets of indirubins (majorly 6BIO) thus placing them in most promising therapeutic candidate category (Vougogiannopoulou and Skaltsounis 2012). GSK-3 is abundant in the mouse brain, particularly in the hippocampus, neocortex, and cerebellum and play an important role in synaptic plasticity and memory during the development (Yao, Shaw et al. 2002, Salcedo-Tello, Ortiz-Matamoros et al. 2011). Homozygous GSK-3β deletion is embryonically lethal, but heterozygotes survive with increased anxiety and decrease

exploration (O'Brien, Harper et al. 2004, Kimura, Yamashita et al. 2008, Salcedo-Tello, Ortiz-Matamoros et al. 2011).

Children with ASD are often found comorbid with psychiatric disorders. One of them is Schizophrenia, where GSK-3β levels were found to be 40-45% lower in the post-mortem frontal cortex samples, which was further replicated in a rat model where hippocampal lesions were performed in the prefrontal cortex and effect was studied. This suggests a possible role of the GSK-3β signalling pathway in Schizophrenia (Kozlovsky, Belmaker et al. 2000, Kozlovsky, Belmaker et al. 2001, Nadri, Lipska et al. 2003). Commercially available Lithium or its derivatives are primarily used for the treatment of psychiatric disorders. Patient-based studies have proven Lithium to be the potent drug for ameliorating mood disorders commonly found in ASD (Siegel, Beresford et al. 2014). Lithium (inhibit both GSK-3 α and β) along with other GSK-3β inhibitor was able to restore elevated GSK-3β levels in the FXS mice model. Audiogenic seizures and hyperactivity and anxiety were found to be reduced in the FXS model upon administration of GSK-3β inhibitors, suggesting GSK-3β as a potent therapeutic target for the FXS model(Guo, Hamilton et al. 2009). However, several side effects have been reported as Lithium toxicity, including vomiting, tremor or fatigue, enuresis, or irritability in ASD patients. The increased dosage might also cause acute renal failure, seizures, altered mental status, confusion, and coma. Given the toxic effect, the development of paralog selective inhibitors demonstrated that inhibition of GSK-3α and not GSK-3β is responsible for corrected aberrant protein synthesis, audiogenic seizures, and sensory cortex hyperexcitability in *Fmr1*$^{-/y}$ mice (McCamphill, Stoppel et al. 2020).

Human neurons differentiated from induced pluripotent stem cells from patients with Rett syndrome showed a deficit in KCC2 expression leading to impaired GABAergic functions by delayed GABA polarity switch from excitatory to inhibitory. Remarkably, KCC2 overexpression in *MeCP2* deficient neurons rescued GABA functional deficits, suggesting an important role of KCC2, thus GABA receptors in Rett syndrome (Banerjee, Rikhye et al. 2016). Screening of more than 900 small-molecule chemicals narrowed down a group of KCC2 expression enhancing compounds (KEECs). These compounds increased KCC2 expression in human WT and isogenic *MECP2* mutant neurons. This increased expression restored the reversal potential of GABA, mEPSC frequency, morphological deficits observed in *MECP2* mutant neurons. Administration of these compounds also restored breathing issues and locomotory deficits observed in *MeCP2* mutant mice (Tang, Drotar et al. 2019). These

results suggest KCC2 and thus GABA receptor as a potential therapeutic target for ASD/ID. Braat S. and Kooy R.F. in 2015 summarized the GABA receptor as a potential therapeutic target for neurodevelopmental disorders such as ASD/ID, which is not explored much in the case of ASD/ID (Braat and Kooy 2015).

Based on preclinical and clinical studies conducted for Fragile-X syndrome, a few points are worth incorporating in future research for NDDs. Inclusion of electroencephalogram (EEG) recordings, functional magnetic resonance imaging (fMRI) in preclinical studies would link disorder directly with functional brain changes. Windows for therapeutic interventions differ with different genetic defects. Thus, a thorough investigation of plasticity windows, timepoints for interventions or gene reinstatement should be carried out for all NDDs in preclinical studies for better translatable research. Similarly, for clinical research, proper behaviour assessment and refined methods to evaluate cognition are required for a broad range of the population. Pharmacokinetics of drugs for the treatment of early-onset NDDs should rely on excessive safety and efficacy when administered to children as compared to adolescents or adults. Therefore, evaluation of paediatric development should be done case-by-case considering scientific rationale, preclinical and clinical efficacy, safety, severity data and ethical risk benefits. These measures would certainly improve the efficacy of drug development for NDDs (Berry-Kravis, Lindemann et al. 2018).

Hypothesis

1. There might be an alteration of function and expression of Cl^- cotransporters, NKCC1 and KCC2, during development in *Syngap1*$^{+/-}$ mice

2. Reversing GABA polarity might restore physiological and behavioural deficits in *Syngap1*$^{+/-}$ mice

Aims

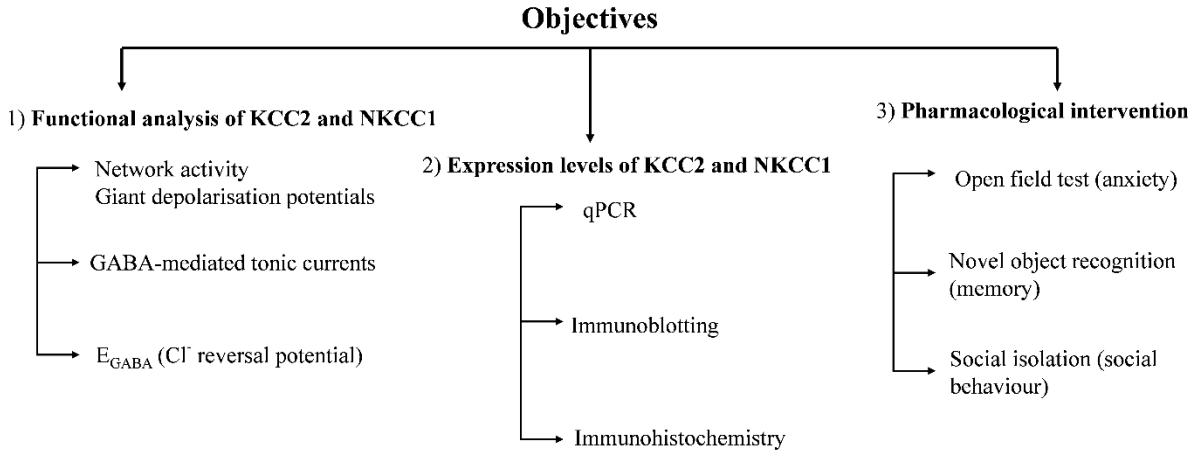

Chapter- 2 Materials and Methods

2.1 Experimental mice

C57BL/6J (#000664) wild type (WT), *Syngap1* Heterozygous Knock Out (*Syngap1*$^{+/-}$) (B6;129-*Syngap1*^{tm1Rlh}/J) (#008890) and B6.Cg-Tg(Thy1-YFP)HJrs/J (#003782) mice were obtained from The Jackson Laboratory (https://www.jax.org/strain/008890; https://www.jax.org/strain/003782) (Feng, Mellor et al. 2000, Kim, Lee et al. 2003), bred and maintained in the Institute's animal house under 12-hour dark and light cycle. Food and water were available ad libitum. All the experiments were performed following the Institutional Animal Ethics Committee (IAEC) and Committee for the Purpose of Control and Supervision of Experiments on Animals (CPCSEA). The experimenter was blind to the experimental conditions and during analysis.

B6.Cg-Tg(Thy1-YFP)HJrs/J mice were constructed by using a transgenic construct containing a *Yfp* gene under the regulation of mouse *Thy1* gene (6.5 kbp fragment obtained from the 5' portion of the *Thy1* gene, extending from the promoter to the intron following exon 4) which was injected into fertilized B6CBAF1 mouse eggs. Founder animals were obtained and crossed with WT C57BL/6J mice. For B6;129-*Syngap1*^{tm1Rlh}/J mice, Exons 7 (common to all splice variants) and 8 (encodes part of C2 domain) were replaced with a neomycin resistance cassette in the opposite direction creating a knock out allele. The construct was electroporated into (129X1/SvJ x 129S1/Sv) F1- *Kitl*$^{+}$-derived R1 embryonic stem (ES) cells. ES cells were injected into recipient blastocysts. The resulting chimeric animals were crossed to C57BL/6J mice and then maintained on a mixed C57BL/6J and 129 genetic background.

2.1.1 Genotyping of experimental mice

2.1.1.1 DNA isolation

Mice ear was tagged with Monel ear tags procured from Kent Scientific, USA (INS10005-1Z). A 1.5-3 mm tail clip was taken for DNA isolation from respective mice. The clipped tail was further chopped into small pieces and suspended in 180 µl of 50 mM NaOH (HiMedia, #GRM467) in the 1.5 ml tube and heated at 95°C in thermomixer (Thermo Scientific, #88871003) to facilitate lysis of cell membrane so that DNA would get exposed. Further, 20

µl of 1M Tris-HCl (Tris: 15965, Thermo Fisher Scientific; HCl: HC301585, Merck), pH 8.0 was added to each tube for stabilization of DNA (soluble form) and maintenance of pH of the solution throughout the process of extraction and later. Samples were centrifuged at 12000 rpm (Eppendorf, #5430R) for 10-minute for sedimentation of the debris. The supernatant containing the genomic DNA was aliquoted to fresh 0.5 ml tubes and stored at -20°C till further use.

2.1.1.2 Polymerase chain reaction (PCR) and gel electrophoresis:

Following DNA isolation, PCR by using a thermocycler (Mastercycler nexus GX2, Eppendorf) was used to detect the presence of neomycin cassette placed in place of Exon 7 and 8 for *Syngap1*$^{+/-}$ mice. A master mix [1 X Taq buffer (Kapa biosystems, #KK1015), 0.2 mM dNTP (G-Biosciences, #IBS-786-442), 1 µM of each primer (S1, S2, S3), 1.5 U Taq polymerase (Kapa Biosystems, #KK1015), 1.5 µl of gDNA, and autoclaved Milli-Q (Merck Millipore, #ZRX003IN)] of 20 µl was used to set up PCR. Amplicons were yielded by the PCR setup containing initial denaturation at 95°C for 3-minute, 35 cycles of 3-steps: denaturation at 95°C for 30-second, annealing at 61.9°C for 45-second, extension at 72°C for 35-second, the final extension at 72°C for 2-minute, and holding at 4°C. Primer (Sigma Aldrich) sequence S1 (Forward): 5`ACCTCAAATCCACACTCCTCTCCAG3`, and primer sequence S2 (Reverse): 5`AGGGAACATAAGTCTTGGCTCTGTC3`, specific to *Syngap1,* gave 500 bp PCR amplified product corresponding to Wild Type (WT) allele. Primer sequence S3 (Reverse): 5`ATGCTCCAGACTGCCTTGGGAAAAG3`, specific to neomycin cassette, with S1 (Forward) gave 300 bp PCR amplified product, because of the absence of Exon 8 and 9, S2 (Reverse) failed to bind, thus, corresponding to *Syngap1*$^{+/-}$ allele. 12 µl PCR amplified products with 2 µl of 6 X DNA dye [Diluent: autoclaved Milli-Q, 30 % glycerol (V/V) (Amresco, #0854), 0.25 % bromophenol blue (W/V) (Fischer scientific, #39121), 0.25 % xylene cyanol (W/V) (Amresco, #0819)] were electrophoresed on 1 % agarose (Lonza, #50004) gel prepared in 1 X TAE buffer (G-Biosciences, #R023) with 0.1 µg/ml ethidium bromide (HiMedia, #MB071). Bands were visualized using Gel Doc XR (Bio-Rad) imaging system, and three sets of bands were observed: a) around 500 bp (WT), b) 500 bp and 300 bp (*Syngap1*$^{+/-}$), and c) around 300 bp (*Syngap*$^{-/-}$). Since homozygous mice pups do not survive for more than a week, we generally observe scenario a) and b) in gel upon illumination. **Figure 2.1** represents the potential primer binding on the gene, and **Figure 2.2** demonstrates different genotypes in a gel.

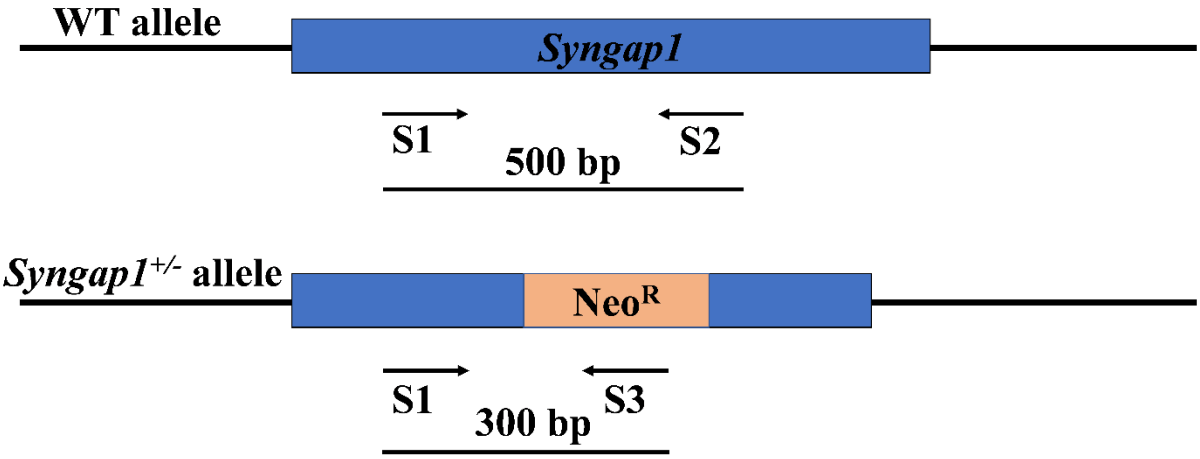

Figure 2.1 Genotyping strategy for *Syngap1*$^{+/-}$ mice

Primer sequence S1 and S2 detect the WT allele to generate a 500 bp amplicon, whereas primer sequences S1 and S3 detect a knock out allele to generate a 300 bp amplicon.

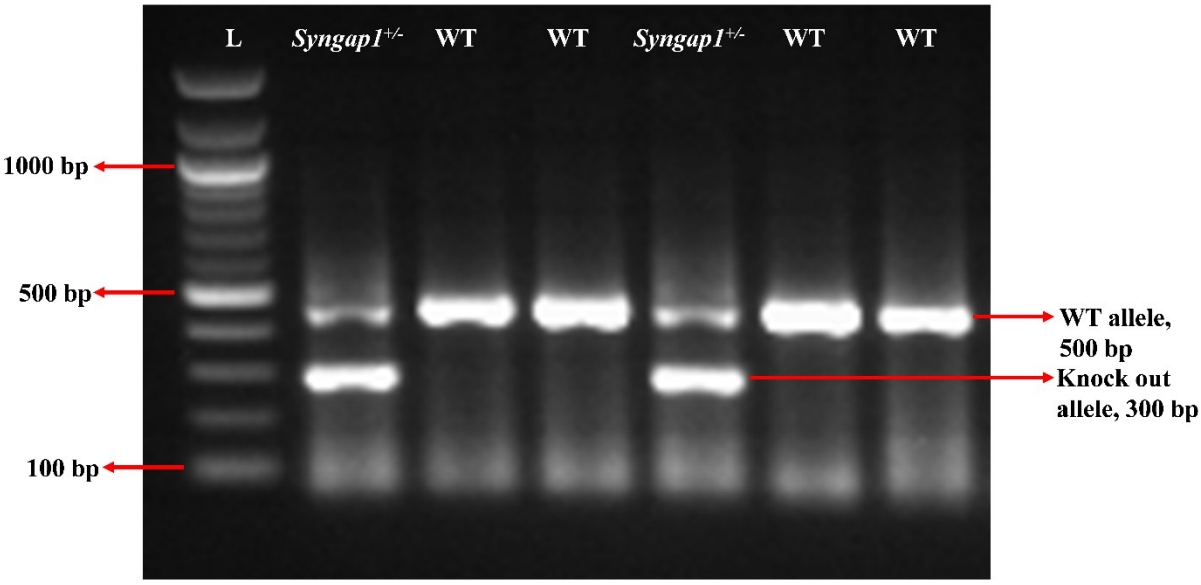

Figure 2.2 A representative image of an agarose gel demonstrating genotyping of *Syngap1*$^{+/-}$ mice

Individual lane illustrates PCR amplified products from different mice gDNA. Lanes consisting of 500 bp amplicon corresponds to WT mice, whereas lanes consisting of both 500 bp as well as 300 bp amplicon corresponds to *Syngap1*$^{+/-}$ mice.

For *Yfp* mice, a mastermix [1 X Taq buffer, 0.2 mM dNTP, 1 µM of each primer
[YFP FP (Yellow florescent protein forward primer (5`ACAGACACACACCCAGGACA3`),
YFP RP (Reverse primer) (5`CGGTGGTGCAGATGAACTT3`),
IPC FP (Internal positive control) (5`CTAGGCCACAGAATTGAAAGATCT3`),

IPC RP (5`GTAGGTGGAAATTCTAGCATCATC3`)],

1.5 U Taq polymerase, 1.5 µl of gDNA, and autoclaved Milli-Q] of 20 µl was used to set up PCR. Amplicons were yielded by the PCR setup containing initial denaturation at 94°C for 2-minute, 10 cycles of 3-steps: denaturation at 94°C for 30-second, annealing at 67°C for 30-second, extension at 68°C for 30-second, 28 cycles of 3-steps: denaturation at 94°C for 20-second, annealing at 60°C for 30-second, extension at 72°C for 30-second the final extension at 72°C for 3-minute, and holding at 4°C. 12 µl PCR amplified products with 2 µl of 6 X DNA dye were electrophoresed on 1 % agarose gel prepared in 1 X TAE buffer with 0.1 µg/ml ethidium bromide. Bands were visualized using Gel Doc XR (Bio-Rad) imaging system, and two sets of bands were observed: a) around 400 bp (*Yfp*), b) around 300 bp (WT). **Figure 2.3** demonstrates different genotypes in a gel.

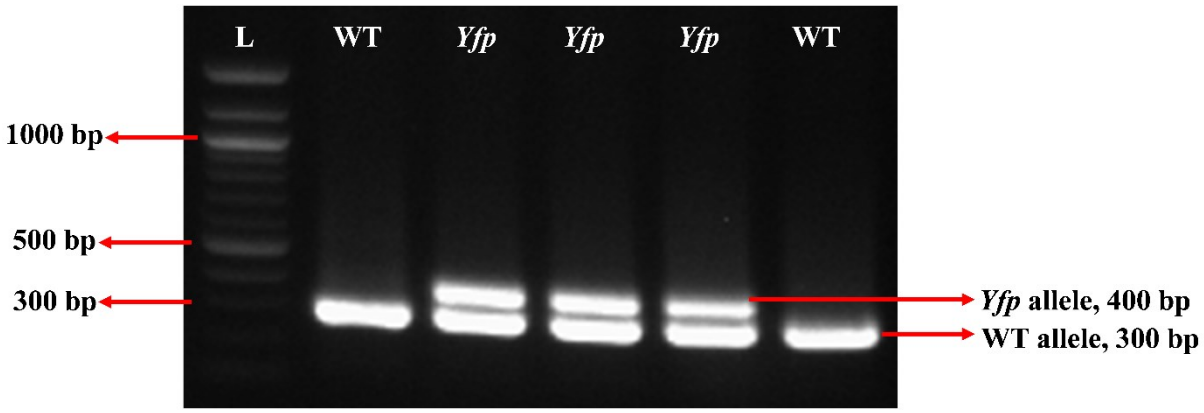

Figure 2.3 An agarose gel-image demonstrating genotyping of *Yfp* mice

Individual lane illustrates PCR amplified products from different mice gDNA. Lanes consisting of only 300 bp amplicon corresponds to WT mice, whereas lanes consisting of both 400 bp as well as 300 bp amplicon corresponds to *Yfp* mice.

2.2 Mice brain tissue lysate preparation:

Mice were sacrificed by cervical dislocation. Post brain isolation in ice cold 1 X PBS (Diluent: autoclaved Milli-Q, 139 mM NaCl (Qualigens, #Q15915), 2.7 mM KCl (Fisher Scientific, #13305), 10 mM $Na_2HPO_4.2H_2O$ (Fisher Scientific, #14105), 2 mM KH_2PO_4 (HiMedia, #GRM1188), pH-7.4 (by NaOH or HCl), hippocampus and cortex were dissected and homogenised in 7 ml KIMBLE Dounce tissue grinder (Sigma Aldrich, #D9063) with RIPA (Radio immunoprecipitation assay) Buffer [(mM): 150 NaCl (increase ionic strength of buffer and reduce non-specific ionic interaction between the protein), 50 Tris-Cl (HCl, pH 7.4) (buffering agent, prevents protein denaturation), 0.25 % Sodium deoxycholate (Sigma

Aldrich, #D6750) (ionic detergent, disrupt protein interaction), 5 EDTA (Merck Millipore, #324502) (chelates divalent ions and inhibits metalloproteases), 0.10 % SDS (BioRad, #1610302) (ionic detergent, disrupt protein interaction), 0.10 % Triton X (HiMedia, #RM845) (non-ionic detergent, solubilises membrane), 10 µl/100 ml protease-inhibitor cocktail (Roche, #11836170001) (inhibits protease activity), 2 µl/100 ml phosphatase inhibitor cocktails (Sigma Aldrich, cocktail 1, #P2850, cocktail 2, #P5726, cocktail 3, #P0044) (inhibits phosphatase activity) in ice. After homogenisation, tissue was kept on ice for 30-minute. Then, lysates were centrifuged (Eppendorf, #5920R) at 4˚C (prevent protein degradation) at 16,000 g for 30-minute (for sedimentation of debris, insoluble protein fraction). The supernatant was collected, aliquoted, and stored at -80˚C (Panasonic, #MDF U55V-PE) until further use. Hippocampal lysates were prepared from male and female Wild Type (WT) and *Syngap1*$^{+/-}$ littermates of (P: Post-natal day) P4, P7, P8, P14-15, P21-23, and P≥90.

2.2.1 Protein estimation by Bradford method:

Bovine serum albumin (BSA, 1 mg/ml) (HiMedia, #TC194) was used to prepare the standard solutions to estimate the unknown concentration of protein lysates obtained. The total volume of 100 µl each, diluent autoclaved Milli-Q, containing standard solutions of (µl) 0.5, 1, 2, 4, 6, 8, 10, 12 of 1mg/ml BSA, along with 2 µl of unknown protein samples was prepared in 96-well plate. 200 µl of 1 X Bradford reagent (Bio-Rad, # 5000006) was aliquoted in each well and kept in the dark for 5-minute (to give enough time for dye binding to protein). Using ELISA plate reader (Versamax, Molecular devices), total protein concentration in given unknown samples were measured at 595 nm, keeping BSA as the standard solution. Absorbance values were used to plot the standard curve, and using the linear equation y = m x + c, the concentration of unknown protein samples were obtained. **Figure 2.4** represents the standard curve obtained from BSA standards.

2.2.2 SDS-PAGE (Sodium dodecyl sulphate-Polyacrylamide gel electrophoresis) and Immunoblot:

50 µg of protein sample was mixed with 4 µl of 5 X dye [Diluent: autoclave Milli-Q, 250 Mm Tris-Cl pH 6.8, 0.005 % bromophenol blue, 40 % glycerol, 5 % DTT (dithioetriol) (HiMedia, #RM525) or 2-Mercaptoethanol (Himedia, #MB041), and 5 % SDS] for 20 µl of total volume. Proteins were electrophoresed and separated based on the molecular weight on SDS-PAGE (BioRad, # 1703812) with 1 X, 1l running buffer [5.3 mM Tris, 192 mM Glycine

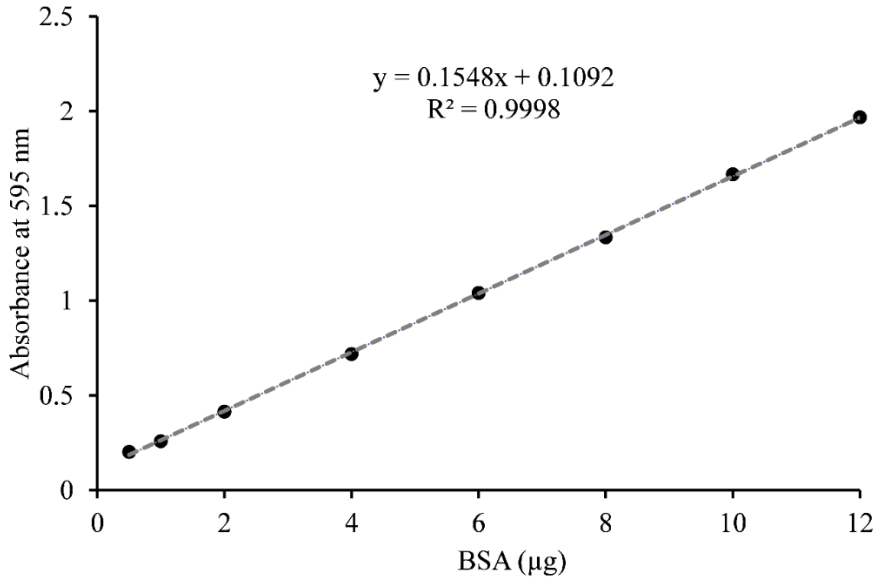

Figure 2.4 Standard curve for BSA standards used in Bradford assay.

The filled circle represents the concentration of BSA standard used and its absorbance at 595 nm obtained to plot the standard curve.

(Fisher Scientific, #15428), 0.1 % SDS (BioRad, #1610301)]. For NKCC1, samples were resolved in 5 % stacking gel and 8 % resolving gel and electrophoresed for approximately 3-hour. The separated proteins were transferred onto PVDF (Polyvinylidene fluoride) (BioRad, #162-0177) for 3-hour at 80 V in 1 X, 1l transfer buffer [5.3 mM Tris, 192 mM Glycine, 20 % methanol (Fisher Scientific, #17790)]. Transfer efficiency was analysed by Ponceau [0.1 % Ponceau S, (HiMedia, #RM977), in 5 % glacial acetic acid (SDFCL, #37013)] imaging (**Figure 2.5**), followed by blocking in 5 % skimmed milk (Himedia, #M530) in 1 X PBS (prevents non-specific binding of primary antibody) for 1-hour. Three washes at room temperature (RT) (1 with 1 X PBST and two with PBS) were given to remove milk traces for 5-minute each, followed by incubation in anti-NKCC1 (Sigma Aldrich, #AV43805), anti-β-ACTIN (Thermo Fisher Scientific, #GX2781) primary antibodies for 12-hour in 4°C. To remove the background caused by primary antibody incubation, blots were given 3 washes, 10-minute each with PBST (PBS and 1 % Tween20 (Himedia, # GRM156) at RT. Then, 1-hour incubation in secondary antibody conjugated with Horse-radish-peroxidase, Goat Anti-rabbit (BioRad, #1721019) in 1 % skimmed milk at RT. Again, to remove the background caused by secondary antibody incubation, three washes with PBST were given for 10-minute each at RT. ECL (Enhanced chemiluminescence) method was used to detect the protein bound to the PVDF membrane using Clarity ECL substrate (BioRad, # 1705060), and signals

were visualized using CCD-imaging system, Versadoc (BioRad, #MP4000). Blots were quantified using ImageJ software. Briefly, the intensity of individual bands for the corresponding molecular weight of protein in consideration was taken and converted to the intensity bell curve. Excluding ends of the curves remaining area was marked for intensity, and values were stored. The normalised intensity of protein of interest to the control protein was plotted for the graph. For KCC2, the same procedure was followed except that samples were prepared in dye without DTT but in 3 % 2-Mercaptoethanol and resolved in 3-8 % Tris-acetate gel (Thermo Fisher Scientific, #EA03752), and transferred overnight (16-hour) followed by Ponceau imaging. The reason for using 3 % 2-Mercaptoethanol is KCC2 oligomers are sensitive to sulfhydryl-reducing agents and sensitive to SDS; thus their presence may disrupt the protein and may hamper the final results (Blaesse, Guillemin et al. 2006). Blots were probed with anti-α-TUBULIN (CST, #2144S) and anti-KCC2 (Sigma Aldrich, #C2366) antibodies and visualised as mentioned earlier. The combined intensity of both the bands observed in the case of KCC2 after chemiluminescent assay were considered for the analysis and normalized to control protein, and plotted in the graph.

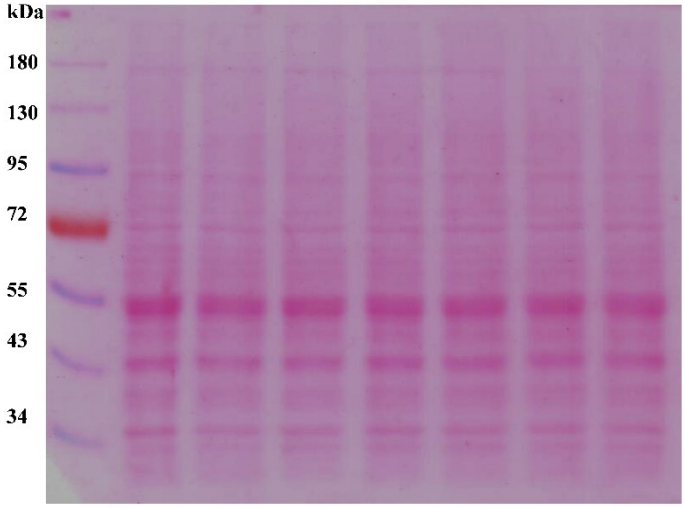

Figure 2.5 Post transfer representative image of a blot stained with Ponceau S

Scanned image of a Ponceau stained gel illustrating the transfer of proteins to PVDF membrane with good efficacy.

2.3 Quantitative Reverse Transcriptase Polymerase Chain Reaction (qPCR) analysis:

mRNA expression levels of *Nkcc1*, *Nkcc2*, *Kcc1*, *Kcc2*, *Kcc3*, *Kcc4*, *Bdnf*, *Gluk2* and *Neto2* were measured in male and female WT and *Syngap1*$^{+/-}$ from P4-5, P7, P8, P14-15, P21-23, and P≥90 mice. All primers procured from Eurofins and summarised in **Table 2**. Briefly,

hippocampus samples were frozen immediately after dissection in liquid nitrogen (N_2) and kept in different vials and stored at -80ºC till further use. Tissue was homogenised in 1 ml Dounce homogeniser (Wheaton, #357538) having 1000 ml of Trizol (ThermoFisher, #15596026) (maintains the integrity of RNA with simultaneous disruption of cells and its components and inhibition of RNAase activity) at room temperature (RT) for 5-minute and 200 µl of $CHCl_3$ (Fisher Scientific, # BP1145-1) (helps in phase separation and allow RNA to remain in aqueous phase) was added and kept at RT for 10-minute. The whole mix was centrifuged at 4ºC at 12,000 rpm for 20-minute (phase separation). The upper aqueous phase was transferred to a fresh tube, and 500 µl of 95 % isopropanol (Sigma Aldrich, #59304) (due to high dielectric constant than water, it excludes water atoms from the phosphate backbone and allows cations to form an ionic bond with phosphate thus forcing RNA to precipitate out) was added to 500 µl of the aqueous phase and incubated at RT for 1-hour followed by centrifugation at 4ºC at 10,000 rpm for 20-minute. The white pellet was washed with 1 ml of 70 % ethanol (Merck Millipore, #100983) (precipitate RNA, dissolves excess salts and evaporates faster than isopropanol) and centrifuged at 4ºC at 10,000 rpm for 10-minute. The washing step was repeated twice, and the pellet was air-dried till it becomes invisible. Pellet was resuspended in 20 µl of nuclease-free water (Thermo Fisher Scientific, #AM9932) and kept at 55°C for resuspension, and RNA concentration was assessed in nanodrop (Thermo Fisher, #ND-ONE-W). Based on RNA concentration for 1 µg of RNA volume was calculated, and the total volume was made up to 7 µl with nuclease-free water. A master mix (10 µl) containing 0.2 µl buffer, 0.5 µl enzyme, 0.5 µl of random hexamers, and 7 µl of RNA with nuclease-free water was used for reverse transcriptase PCR (initial denaturation at 95°C for 2-minute, 39 cycles of 3-steps: denaturation at 95°C for 15-second, annealing at 60°C for 30-second, extension at 72°C for 20-second, the final extension at 65°C for 5-second, and holding at 4°C) for cDNA synthesis by using cDNA synthesis kit (Takara, #TP600). cDNA was aliquoted and stored at -80ºC till further use. For setting up qPCR reaction, cDNA was diluted to 1:40 or 1:50 ratio, and reaction (10 µl: 2.5 µl nuclease-free water, 5 µl SYBR, 0.25 µl forward primer, 0.25 µl reverse primer, 2 µl cDNA) was set up in duplicates using SYBR Mix (Roche, #light cycler 480), and probes for the genes mentioned in Table 2. Cq values were calculated by the ddC_t method, in which dC_t was calculated by subtracting the test gene value from the housekeeping gene value and then taking 2^{-dC_t} as the Cq value. Relative mRNA level, 2-ddCt, was plotted for the graph.

Table 2 List of primers used in qPCR experiments

Gene Name	Primer Sequence 5` to 3`
Slc12a1 (FP)	TGCCTCCGAAACAAGCTGAA
Slc12a1 (RP)	GTTAACACCGCGGCTCATCA
Slc12a2 (FP)	ATCCGCCTGAAGGAAGGACT
Slc12a2 (RP)	TGCCATCCTCTTCCTCATCTTTC
Slc12a4 (FP)	ACGGTGAGGGACAGGGTAAC
Slc12a4 (RP)	AGCTTGCCCAGGAGAGATGA
Slc12a5 (FP)	CCTTCTAATGCTCGGCTCCC
Slc12a5 (RP)	CACACCCCCTGAGAACTTGT
Slc12a6 (FP)	GGACCTCAGCTCTCGGTCTA
Slc12a6 (RP)	ACTCGGGTCCTCCGTAACAT
Slc12a7 (FP)	GGGACAGCAGAGTCTAACGG
Slc12a7 (RP)	GTTTCCATCTCCCGGCGTAG
Bdnf (FP)	CCTGCATCTGTTGGGGAG
Bdnf (RP)	GCCTTGTCCGTGGACGTTTA
Neto2 (FP)	GCAGAATCGTCTCGCCCTC
Neto2 (RP)	GCATTCACGACCACCACTGT
Gluk2 (FP)	TGCCAAAGTGGTAGTGATCCA
Gluk2 (RP)	TTTGTTTAAAAAGTGCATGTGAAGT

2.4 Histology:

2.4.1 Transcardial perfusion:

For immunohistochemical analysis, P8, P14-15, and P≥90 male and female mice were anaesthetised with halothane (Alem, #M14A). The chest cavity was cut open, and the heart was carefully exposed, with the heartbeat intact. Butterfly needle (0.55 x 19 mm, scalp van)

whose one end was attached to the heart and one end to the PBS/paraformaldehyde (PFA) (Sigma Aldrich, #158127) solution was inserted into the left ventricle (so that PBS/PFA will go to other organs) and a nick was made in the right atrium (all blood will come out) and perfused with ice-chilled 150 ml PBS (remove blood from vessels and maintain pH). For checking the efficacy of PBS perfusion, the liver should gradually turn whitish during the process. Then the other end of the tube (previously placed in PBS) was connected to 4 % of 150 ml PFA (fix the tissues and preserves morphology) solution and perfused at ~50 ml/minute speed using a peristaltic pump (Ravel Hiteks #RH-P110S-25). Successful perfusion was noted by concurrent tail wagging as PFA has reached the extremities. The brain was dissected out without making any nicks and incubated in 4 % PFA overnight, followed by incubation in 30 % sucrose (Sigma Aldrich, #S9378) till it submerged to the bottom and stored at -80ºC until further use.

2.4.2 Cryosectioning:

The brain in the sucrose solution was thawed at 4°C one day before the start of cryosectioning. The chamber temperature (CT) of the cryotome (Leica, #CM3050) was maintained at -20°C, and the object temperature (OT) was maintained at -22°C before the start of the experiment and throughout the experiment. Now, the brain was embedded in Optimum Cutting Temperature (OCT) solution (Trivitron, Tissue Tek #DIG-46181) (water-soluble, provide convenient specimen matrix, eliminate undesirable background staining) and incubated for 20-minute inside cryotome at mentioned OT and CT. 30 µm coronal sections were obtained and stored in 1 X PBS in a 24-well plate.

2.4.3 Immunohistochemistry (IHC):

Antigen retrieval was performed by treating sections with Sodium citrate buffer (Fisher Scientific, #27625) pH 6.0 (break protein cross-links, unmask antigen and epitopes, enhance staining intensities) for 30-minute followed by three washes, 10-minute each, by 0.1 % PBSTx [0.1 % Triton X 100 in PBS] and then blocking [2 % BSA (Himedia, #GRM105) (prevents non-specific binding of antibodies to tissue or Fc receptors) + 1 % Goat Serum (MP Bio, #0219135680) (prevent non-specific binding of the antibody to tissue) + 0.1 % PBSTx incubation for 4-hour at RT]. Sections were washed thrice with 0.1 % PBSTx for 10-minute each and then incubated in anti-KCC2 and anti-SYNGAP1 antibody for 2-hour at RT and 34-hour at 4ºC followed by three washes with 0.1 % PBSTx and kept in secondary antibody (Thermo Fisher Scientific, Alexa Flour 633 goat anti-mouse, #A21052 and Alexa Flour 555

goat anti-rabbit, #A21428) for 4-hour at RT in the dark to avoid bleaching of fluorescence. Secondary incubation was followed by three washes with 0.1 % PBSTx and then incubation in Hoechst (Thermo Fisher Scientific, #H3570) for 10-minute followed by a wash of 10-minute with PBS in the dark. Sections were mounted in Vectashield (Vector, #H-1000) on slides. All the imaging was performed in a confocal laser scanning microscope (LSM 880, Zeiss, India) and analysed using ImageJ software. Background subtraction was performed as an initial step for all the images, followed by thresholding of KCC2 intensity. Then integrated density was measured, keeping the threshold value similar within the genotypes for all age groups. Mid 15 stacks were considered for the Z projected image in which all the analysis was performed.

2.5 Preparation of Hippocampal Slices:

Acute brain slices were prepared from WT and *Syngap1*$^{+/-}$ mice from P4-5, P7, P8, P14-15, P21-23, and P≥90. Mice were sacrificed by cervical dislocation. Following decapitation, the brain was removed and kept in an ice-cold (almost frozen) cutting solution containing [(mM): 189 Sucrose (Sigma Aldrich, #S9378) (prevents Na^+ and Cl^- influx and swelling, preserve excitatory and inhibitory neurons better), 10 D-Glucose (Sigma Aldrich, #G8270) (metabolic fuel, required for synaptic activity and long-term memory, preserves morphology and function of astrocytes and other cells), 26 $NaHCO_3$ (Sigma Aldrich, #S5761) (buffering agent, maintains pH), 3 KCl (Sigma Aldrich, #P5405) (required for synaptic activity), 10 $MgSO_4.7H_2O$ (Sigma Aldrich, #M2773) (provide balanced inhibition, neuroprotective), 1.25 NaH_2PO_4 (Sigma Aldrich, #S8282) (buffering agent), and 0.1 $CaCl_2$ (Sigma Aldrich, #21115) (required for neuronal activity)] continuously bubbling with carbogen (5 % CO_2 and 95 % O_2, Chemix, India). After 30-second, the brain was placed over a petri-dish to dissect out the cerebellum, frontal lobe, and olfactory bulb, followed by glueing to the brain holder of a vibratome (Leica, #VT1200S). Subsequently, 350 µm thick slices were prepared, and the cortex was dissected to isolate the hippocampus. Dissection of mice as well the step containing glueing of the brain to holder must be quick (within 40-45 second) to preserve the cell responses and neurons or other cells from dying. All the slices were kept at 37ºC in a water bath (Thermo Fisher Scientific, #2842) for 50-minute in a slice chamber with custom made small chambers within, having mesh beneath, containing aCSF (artificial cerebrospinal fluid) composed of (mM): 124 NaCl (Sigma Aldrich, #S6191) (required for neuronal activity, excitation), 3 KCl, 1 $MgSO_4.7H_2O$, 1.25 NaH_2PO_4, 10 D-Glucose, 24 $NaHCO_3$, and 2 $CaCl_2$ bubbled with carbogen. Following recovery, slices were maintained at RT until transferred to

a submerged chamber of ~1.5 ml volume, in which individual slice was perfused continuously (2-3 ml/minute) with warmed (34ºC) and carbogenated aCSF during the recording.

2.5.1 Extracellular and intracellular recording rig:

aCSF for extracellular recording is stored in a customised chamber that has a tube connected to a solution heater pencil with a single outlet (Harvard, #SH-27B). aCSF is heated in pencil to 34ºC and flown to the recording chamber (Scientifica), where slices are placed. 34ºC is maintained in the chamber with the help of a thermocouple placed in the chamber and connected to an automated temperature controller (Warner Instruments, #TC-324C). A Tygon tubing outlet (LongerPump) is connected to a perfusion system (LongerPump, #YZ1515x) which brings back the aCSF into the customised storage chamber, thus complete the flow. The recording chamber also consists of the replaceable Ag/AgCl bath earth wire attached to the headstage (Axon Instruments). For fEPSP or patch-clamp recordings, mice acute brain slices were transferred to a submerged chamber mounted on an Olympus WI-DICD upright microscope (Scientifica) equipped with infrared differential interference contrast optics to enable visual identification of neurons. The whole recording setup is placed inside a Faraday cage and placed over an anti-vibration table (TMC, Ametek, #63P-541) to ensure minimum noise and vibrations during recordings. Signals acquired were amplified by an internal gain of 10 for field recordings, whole-cell patch-clamp experiments, and 5 for perforated-patch-clamp experiments. Signals were filtered at 10kHz using a low pass filter. All this were performed by MultiClamp 700B (Axon CNS), and final signals were then digitised using Digidata 1440A (Axon CNS). **Figure 2.6** demonstrates the schematic of signal transmission wiring for extracellular as well as intracellular experiments using the electrophysiology set-up.

2.5.2 Extracellular Field Recordings:

Field excitatory postsynaptic potential (fEPSP) were elicited from pyramidal cells of CA1 regions of stratum radiatum by placing a concentric bipolar stimulating electrode (CBARC75, FHC, USA) connected to a constant current isolator stimulator unit (Digitimer, UK) at Schaffer-collateral commissural pathway, and recorded from stratum radiatum of CA1 area of the hippocampus, with 3-5 MΩ resistance glass pipette (ID: 0.69mm, OD: 1.2mm, Harvard Apparatus) filled with aCSF. Signals were amplified using an Axon Multiclamp 700B amplifier (Molecular Devices), digitised using an Axon Digidata 1440A (Molecular Devices)

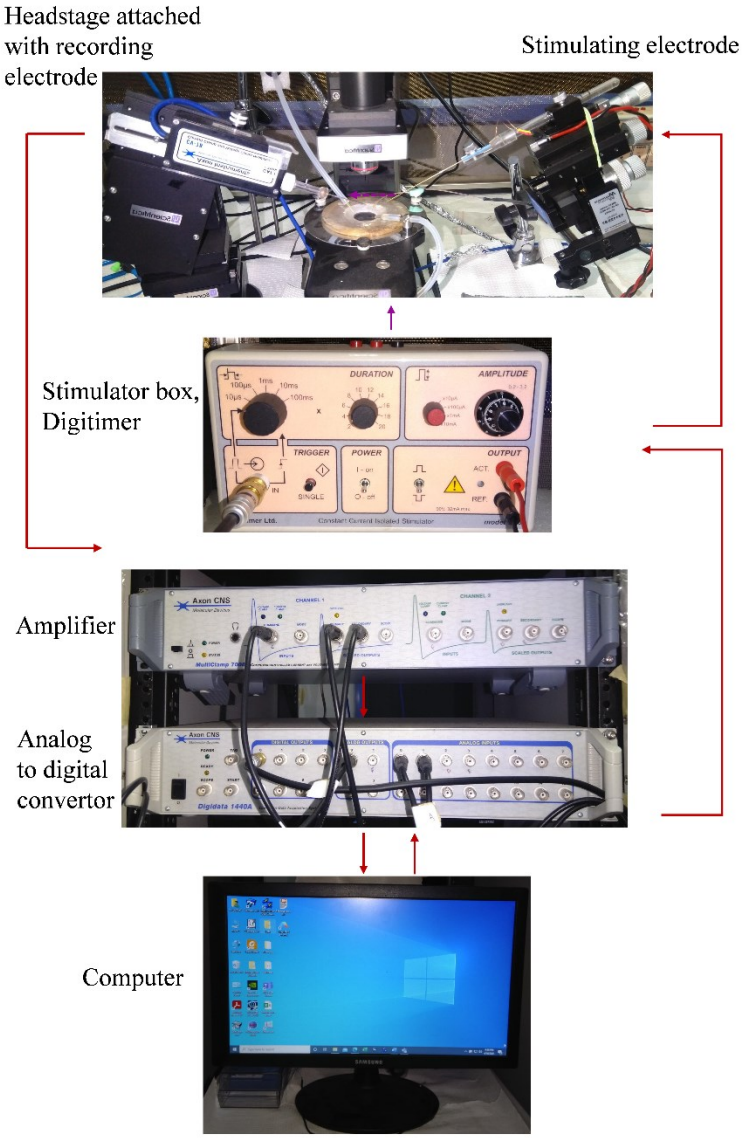

Figure 2.6 A schematic representation of extracellular field and intracellular patch-clamp recording set up.

The stimulus protocol is generated by the computer and fed to the Analog to Digital convertor. Then, the signals were fed to the stimulator box for the extracellular field recordings. For the intracellular patch-clamp rig, the analogue step signals were fed to the recording electrode from the Analog to Digital converter via the amplifier. The signals in response to stimulation were picked up by the recording electrode in the head stage. In the extracellular field, whole-cell patch-clamp, the signals were amplified 10 times, and for perforated-patch-clamp 5 times by the amplifier. Then the analogue signals were converted to digital signals by Analog to Digital converter and then fed to the computer for storage and further analysis. Red lines represented is a common pathway for extra and intracellular recordings, whereas violet lines are for intracellular recordings.

and stored on a computer using pClamp10.7 software (Molecular Devices). Stimulation frequency was set at 0.05 Hz. A baseline period of 15-minute fEPSP was recorded at a stimulation intensity that elicited an approximately half-maximal response. Stimulation intensity remained constant throughout the experiment, including during theta-burst stimulation (TBS), by which long term potentiation (LTP) was induced, and 45-minute post-potentiation. Following the baseline period, the TBS was delivered consisting of five bursts at 5 Hz (theta frequency), repeated four times at an interval of 20 s (Booth, Brown et al. 2014). fEPSP after TBS were recorded for 45 minutes. Slices with a high FV/fEPSP ratio and with unstable baseline were discarded from the analysis. Data analysis were performed using Clampfit 10.7 and Excel 2019. Data are represented as Mean ± SEM. Two-Way ANOVA was performed to determine the statistical significance for the last 3-minute of baseline and post-LTP. Example traces are those recorded for 5-minute around the time point indicated.

2.5.3 Perforated and Whole-Cell Patch-Clamp Recordings:

The reversal potential of $GABA_AR$ (E_{GABA}) was measured using Gramicidin (Sigma Aldrich, #G5002) based perforated patch-clamp of DGGC (Dentate Gyrus Granule Cells) from WT and *Syngap1*$^{+/-}$ littermates at P4-5, P7, P8, P14-15, P21-23, and P≥90. 5-6 MΩ glass electrode (Harvard, USA) tip was filled with an internal solution containing (mM): 130 K-Gluconate (Sigma Aldrich, #P1847), 20 KCl (Sigma Aldrich, #P5405), 10 HEPES free acid (OmniPur Merck Millipore, #5310), 0.2 EGTA (OmniPur Merck Millipore, #4100), ATP and GTP, then backfilled with 100 µM Gramicidin. GABAR-mediated currents were evoked using a bipolar stimulating electrode (CBARC75, FHC, USA) connected to a constant current stimulator (Digitimer, UK) and by holding the cell at different membrane potentials ranging from -100 to +40 mV in the presence of AMPAR and NMDAR blockers, 10 µM 6-Cyano-7-nitroquinoxaline-2,3-dione disodium (CNQX) (Tocris, #1045) and 100 µM (2R)-amino-5-phosphonovaleric acid (DL-AP5) (Tocris, #3693) respectively **Figure 2.7**. Whole-cell recordings were performed to measure giant depolarising potentials (GDPs) and tonic currents mediated by GABARs by holding the cell at -70 mV. In the case of GDP, K-Gluconate based internal solution (composition is the same as described earlier) was used, and 10 µM Bicuculline (Bic) was bath applied after recording 10-minute of baseline. Tonic currents were measured using CsCl based internal solution containing (mM): 120 CsCl (Sigma Aldrich, #289329), 10 HEPES free acid, 10 EGTA, 4 $MgCl_2$ (Sigma Aldrich, #M8266), 5 Lidocaine N-ethyl bromide (Sigma Aldrich, #5783), ATP and GTP. To isolate

GABAR-mediated currents, we bath applied AP-5 (50 µM) and CNQX (10 µM) for 10-minute followed by NO-711 hydrochloride (potent and selective GABA uptake inhibitor, GAT-1 antagonist) (20 µM) (Sigma Aldrich, #N142) for 10-minute to increase the ambient GABA and then tonic currents were blocked by Bicuculline (20 µM). Cells were held at -70 mV throughout the recording, and an increase in holding current after the application of Bicuculline was calculated and plotted against current amplitude in the presence or absence of Bicuculline. Cells showing a holding current of <-30 pA were discarded from the analysis except for the cells in which CsCl was used as an internal solution.

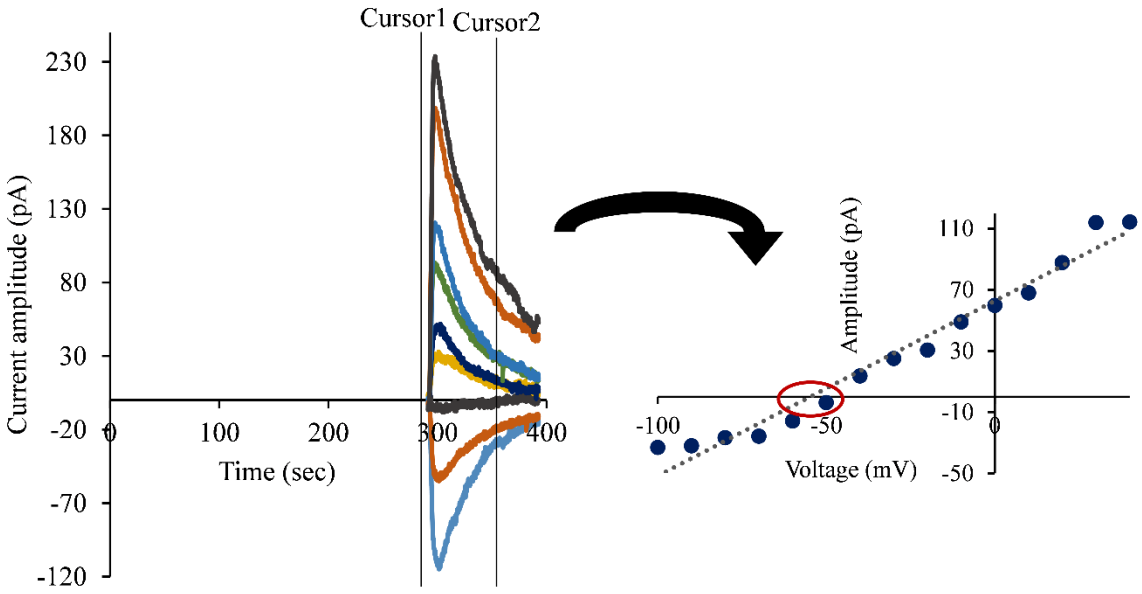

Figure 2.7 A schematic diagram representing the measurement of chloride reversal potential mediated by GABAR.

Neuron was voltage-clamped at different membrane potentials ranging from -100 to +40 mV in the presence of AMPAR and NMDAR blockers and corresponding positive going and negative going current amplitudes were obtained. Cursor1 and cursor2 were placed to capture the peak amplitude of current obtained with different voltages in Clampfit 10.7. Obtained current amplitude was plotted against voltage in Excel as a scatter plot. X-intercept highlighted in the red circle was taken as reversal potential for that neuron and stored for future compiled analysis.

2.6 Behavioural Studies:

For 6BIO treated mice, 5 mg/kg of 6BIO (stock was prepared in DMSO) in saline, and for vehicle mice, DMSO in saline was administered intraperitoneally to all the mice according to

body weight (measured daily). The side of injection was changed every 10 days for each mouse to avoid any injury or inflammation due to injections for an extended period.

For all mice giving time of injection was in a fixed range and continued till the end of the behaviour experiments for every day. On the day of the behaviour experiment, there was a time gap of 2-3-hour in between the injections and the behaviour. All four experimental groups of mice of three different age groups were kept in the soundproof behaviour room for at least 20-minute before the start of the behaviour experiments. The light intensity was checked every day and maintained at 90-110 LUX for all the experiments performed. Open field test, Novel object recognition, social isolation, and flurothyl-based seizure, behaviour experiments were done for WT, and *Syngap1*$^{+/-}$ mice (Vehicle and 6BIO treated) as anxiety, hyperactivity, memory recognition, sociability issues, and epilepsies are the most critical symptoms of individuals affected with *SYNGAP1*$^{+/-}$ mutation. The experimental groups were designed based on the injection regime illustrated in **Figure 2.8**.

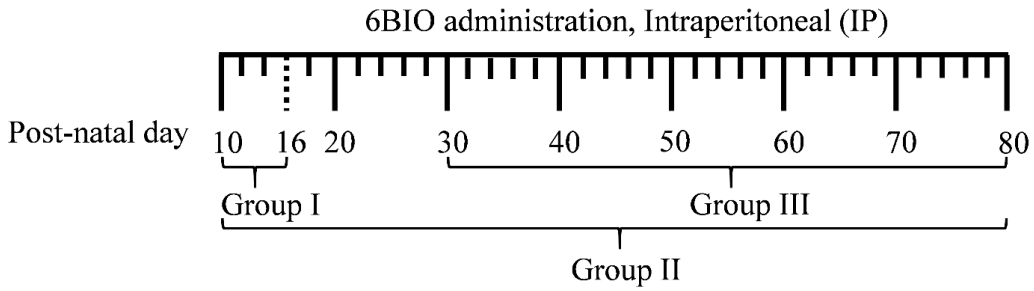

Figure 2.8 Injection regime for 6BIO treated mice

6BIO was IP treated for three age groups of mice (WT, *Syngap1*$^{+/-}$). Group, I include age P10-16 corresponding to the critical period of development, Group II include age P10-80 corresponding to the critical period of development as well as young adults, and Group III consists of P30-80 young adults of mice.

2.6.1 Open-Field test (OFT)

Open-Field test was performed to assess the locomotor activity (hyper/hypo) and anxiety behaviour of the mice. Total distance travelled would reveal the activity, and the number of entries in the centre would reveal the anxious state of mice. Less number of entries in the centre suggest mice have the sensation of fear or getting caught by prey, thus travelling more in the periphery as the wall 'protects" the mice similar to the behaviour of the mice in the

wild, hence increased anxiety. OFT was done in a wooden box 52×50×45 cm custom made in JNCASR using plywood, and the internal surface was coated with the odourless white polish. During testing, mice were left at the periphery in the corner of the box and allowed to explore the arena for 15-minute and then returned to their home cage. Before introducing other mice, the arena was cleaned with 70 % ethanol and air-dried for 5-minute. Mice that were immobile and failed to explore the box were not considered for the analysis. SMART v3.0.04 (Panlab Harvard Apparatus #DCBA5-E83) and a video camera (SONY #SSC-G118) was used to record the activity of the mice. An anti-vibration filter was always kept on in the software while recording the activity of the mice. Offline analysis for total distance travelled and the number of entries to the centre was done using SMART v3.0.04 (Panlab Harvard Apparatus #DCBA5-E83). The trajectory of the mouse and arena is shown in **Figure 2.9.**

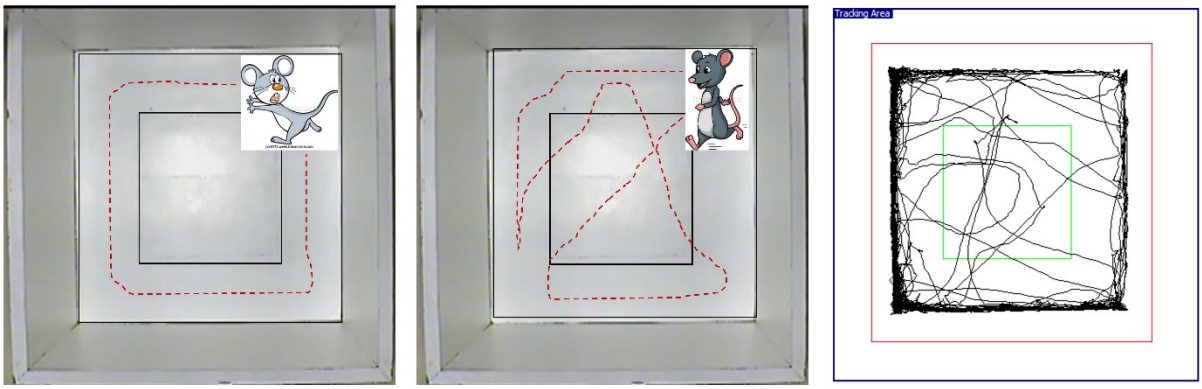

Figure 2.9 Representation of open field arena and trajectory of a mouse in the arena

The red dotted lines on the left image show the potential trajectory of the normal mice, whereas the middle figure illustrates the same of a mutant mouse. The representative image on the right image elucidates the trajectory of an actual mutant mouse, demonstrating the less anxious state of that mouse.

2.6.2 Novel object recognition (NOR)

The NOR was performed in a wooden box 35×35×35 cm custom made in JNCASR to study the recognition memory. Inside the box was painted with white, odourless polish. Two familiar (white coloured bottles) and two different (one blue coloured cone-shaped bottle and one rectangular green coloured bottle) novel objects were used for testing NOR in mice. All the objects were filled with sand and sealed. On Day-1, mice were familiarised with the arena without the objects for 5-minute. Day-2 and Day-3 sessions included habituation with two

familiar objects placed diagonally to each other, and mice explored it for 10-minute. The day-4 session involved a recognition memory test at 24 hours where the mice explored the novel object and a familiar object placed diagonally for 10-minute. For all the experimental sessions, the same diagonal pattern to position the objects were chosen and mice were placed in the corner diagonally opposite to where the object was kept, and mice were allowed to explore the objects. For each day of the experiment, after every mouse, the arena was cleaned with 70 % ethanol and air-dried for 5-minute. The discrimination index (DI) for novel object recognition test (NOR) [(time spent with novel object - time spent with familiar object)/(time spent with novel object + time spent with familiar object)] X 100, was evaluated as a measure of object recognition (either novel or familiar). DI values above 25 correlated with recognition of memory, and below 25 correlated with lack of memory. The time of interaction of the mice (sniffing/touch) to familiar and novel objects was calculated manually. The duration of time when mice climbed over the objects was not considered for analysis. The whole paradigm was recorded using Handycam (SONY #HDR-CX405). The objects and the arena are shown in **Figure 2.10**.

Figure 2.10 Representation of novel object recognition test arena

The arena and the objects chosen for the novel object recognition test kept diagonally during the procedure are depicted in this representative photo before the start of the actual experiment. Note the difference in the object used in the middle and right image.

2.6.3 Social Interaction and social preference (SI and SP)

SI and SP were performed in a transparent three-chamber plexiglass box 40.6×21×35 cm custom made in JNCASR to study the social responses of mice. The plastic doors to cover the entrances between the extreme chambers was black and mounted temporarily when required in between session with the help of double-sided tape. In the first session of the experiment,

the mouse was habituated in a three-chambered glass box for 5-minute to explore the arena. In the second session, the chambers were closed with doors, and the mouse was placed in mid-chamber and allowed to explore for 5-minute. In the third session, two steel mesh jars were kept in either chamber of the plexiglass box, in which one of the jars had a mouse of the same gender and age, and one was empty. The test mouse was introduced into the middle chamber, the doors were removed, and the mouse explored the entire arena for 10-minute. The social interaction was measured by the time spent between the mouse in the jar and the empty jar. In the last session, the mouse of the same gender and age was introduced into the empty mesh jar (Stranger 2), along with a familiar mouse (Stranger 1) in another jar and the test mouse was allowed to explore and interact with both the mice placed beneath the mesh jars. Social preference was calculated by the time spent between familiar (Stranger 1) and unfamiliar mouse (Stranger 2). The time mouse spent climbing over the mesh jar was not taken into consideration in the analysis. SI and SP were recorded from the top using a video camera (SONY #SSC-G118) and from the front using Handycam (SONY #HDR-CX405). The setup and arena are shown in **Figure 2.11.**

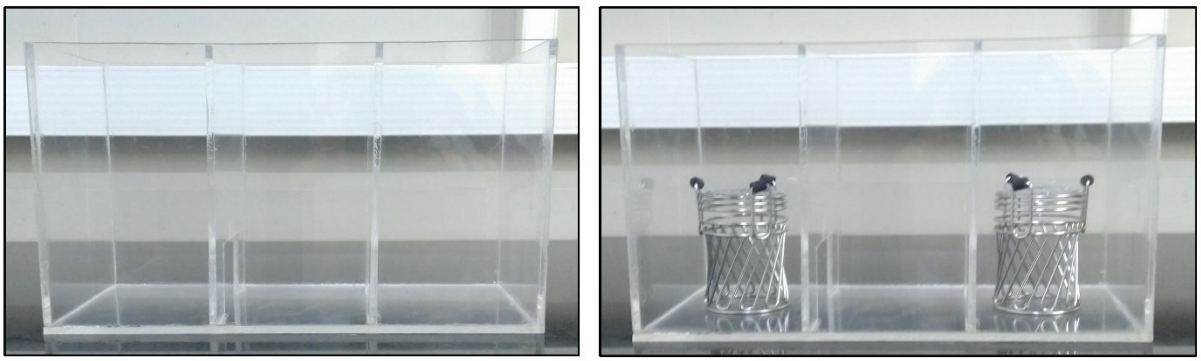

Three chamber used for social interaction and preference

Three chamber with steel mesh in which mice were kept

Figure 2.11 Representation of social isolation and preference chamber

Three-chambered box containing steel mess jars in which social isolation and preference were performed. The test mouse was placed in the middle chamber.

2.6.4 Flurothyl-induced seizure

A cylindrical transparent box was taken, and a narrow tube was inserted in the bottom such that it can reach the Whatman filter paper without obstructing the movement of mice in the box. After the mouse was placed inside the box, the lid was covered tightly. Seizures were induced using 10 % flurothyl (Sigma Aldrich #287571) (halogenated volatile ether, antagonises $GABA_A$ receptor, thus make neurons more excitable, causing epileptic seizure in

mice when inhaled) and 95 % ethanol (Merck #K46475383 511) (highly volatile and easily miscible in the ether without reacting with it) as solvent at the rate of 200 µl/minute using a Syringe pump (New era pump system #NE-1000). The whole procedure was performed in the hood. The analysis was done manually by counting the time of tonic-clonic seizure (Samoriski and Applegate 1997, Kadiyala, Papandrea et al. 2014) (muscle stiffening and rhythmic jerky movement at a higher pace). Less time for the tonic-clonic suggests a lower threshold of seizure, hence, increase susceptibility to seizures. The activity of mice was recorded from the front using Handycam (SONY #HDR-CX405).

2.7 Statistics:

All graphs were plotted, and statistical analysis was performed in Microsoft Excel (2019) and Prism GraphPad (version 8.3). Data are presented as Mean±Standard Error of Mean (SEM) except for box and whisker plots. Unpaired Student's *t*-test assessed the genotype difference for a given age group while Two-way ANOVA followed by *post-hoc* to determine genotype difference across other age groups unless otherwise mentioned.

Chapter- 3 Results

3.1 GABA dysfunction during development in *Syngap1*$^{+/-}$ mice

3.1.1 Introduction:

One of the major characteristics of neurodevelopmental disorders such as ASD/ID is excitatory/inhibitory (E/I) imbalance resulting in the altered critical period of development. In the central nervous system, glutamate and GABA are considered major excitatory and inhibitory neurotransmitter, respectively (Petroff 2002). GABA is shown to have a dual role during development (Ben-Ari 2002). In the early stages of development, because of increased expression of NKCC1, chloride influx occurs, and binding of GABA to receptors makes neurons excitatory. Whereas, in the later stages of development, increased KCC2 expression leads to chloride efflux and GABA activity results in the inhibitory state of neurons (Ben-Ari 2002). Chloride cotransporters, NKCC1 and KCC2, have been characterised over 20 decades as the most important regulator of reversal potential and homeostasis of Cl^-, and the state of neurons in the brain. For example, in addition to regulating AMPA receptor trafficking to the post-synapses, KCC2 regulates dendritic spine formation with BDNF in specific regions of the brain. The fact that *SYNGAP1* regulates AMPA receptor trafficking to the post-synapse could be considered as a common route to one of the hypotheses to study KCC2 in regulating neuronal function during development.

SYNGAP1-mediated ID is categorised as a rare form of ASD/ID among neurodevelopmental disorders (Jeyabalan and Clement 2016, Mignot, von Stulpnagel et al. 2016, Agarwal, Johnston et al. 2019, Verma, Paul et al. 2019, Gamache, Araki et al. 2020). Expression of chloride cotransporters, switch of GABA reversal potential from excitatory to inhibitory, and change from silent synapses to functional synapses, along with the occurrence of giant depolarisation potential, are considered as major milestones in the critical period of development, which are compromised in several models of ASD/ID (Duarte, Armstrong et al. 2013, Deidda, Allegra et al. 2015, Banerjee, Rikhye et al. 2016). As discussed in the introduction, *Syngap1*$^{+/-}$ has altered the critical period of development in the hippocampal and cortical circuits of the brain (Clement, Aceti et al. 2012, Clement, Ozkan et al. 2013). Thus, chloride cotransporters could be one of the most important causal candidates to

investigate in *Syngap1*$^{+/-}$ mice, given their involvement in AMPAR trafficking, the reversal potential of chloride, and the critical period of development.

3.1.2 Methods:

We measured the network activity of neurons in acute brain slices of mice at P8 and P14 by determining giant depolarisation potentials (GDPs). Whole-cell voltage-clamp at -70 mV was performed to determine the GDPs from dentate gyrus granular cells (DGGCs), and spontaneous activity was recorded, followed by application of Bicuculline (10 μM) after 10-minute. GABAR-mediated tonic currents were recorded from DGGCs by voltage clamping cells at -70 mV. We bath applied DL-AP5 (50 μM) and CNQX (10 μM) followed by NO-711 hydrochloride (20 μM) to increase the ambient tonic GABAR-mediated currents, and then tonic currents were blocked by Bicuculline (20 μM). An increase in holding current after the application of bicuculline was calculated and plotted against current amplitude in the presence or absence of bicuculline. GABA reversal potential (E_{Cl^-}) from the DGGCs was elicited by stimulating the medial perforant pathway (MPP) in the presence of NMDAR and AMPAR blockers DL-AP5 (100 μM) and CNQX, respectively. Responses were recorded by voltage clamping the cells between -100 mV to +40 mV. The measured responses were plotted as current and voltage relationship (I-V) and E_{Cl^-} was determined when the current direction reverses to positive. Altered functional aspects in *Syngap1*$^{+/-}$ mice encouraged us to check the expression of chloride cotransporters. Immunoblotting was performed to check the expression of NKCC1 and KCC2 during the development. KCC2 samples were prepared with 3 % β-mercaptoethanol and electrophoresed in 3-8 % tris-acetate gel, unlike NKCC1, which was done in 8 % SDS-PAGE with 1 % β-mercaptoethanol. Immunohistochemistry was also performed to validate the expression of the same. Briefly, after perfusion of mice with 4 % paraformaldehyde, the brain was immersed in 30 % sucrose solution and allowed it to settle at the bottom before froze until further use. Cryosectioning was performed to get 30 μm of sections that were subjected to antigen retrieval for immunostaining. Images were obtained using the confocal microscope. Gene expression analysis was done by reverse-transcriptase polymerase chain reaction (RT-PCR). RNA was isolated by the Trizol method followed by cDNA synthesis and RT-PCR for different developmental stages of mice. Relative mRNA levels were used to plot the graph.

3.1.3 Results:

3.1.3.1 Diminished network activity and inhibition at two weeks in *Syngap1*$^{+/-}$

Elucidating the role of the GABAergic system in the pathophysiology of *Synagp1*$^{+/-}$ could act as a therapeutic candidate, as illustrated in Braat and Kooy (Braat and Kooy 2015). To understand GABA-mediated dysfunction at the neuronal circuit level, giant depolarisation potentials (GDPs) were measured from dentate gyrus granular cells (DGGCs). GDPs are early network-driven synaptic potentials that occur due to recurrent excitatory connections between pyramidal neurons, mediated by GABA and presynaptically controlled by NMDA receptors, as Bicuculline blocked GDPs, but the application of NMDAR antagonist decreased amplitude and frequency of GDPs (Ben-Ari, Cherubini et al. 1989, Sipila, Huttu et al. 2005, Griguoli and Cherubini 2017). A significant change in GDP between genotypes in the absence of 10 μm bicuculline was not observed. However, a decrease in the number of GDPs was observed at P8-9 (**Figure 3.1 A** and **B**) and P14-15 (**Figure 3.1 C** and **D**) in the presence of bicuculline in *Syngap1*$^{+/-}$. It suggests a compensatory mechanism to balance increased excitatory activity observed in *Syngap1*$^{+/-}$ mice. The observed decrease in GDPs in the presence of Bicuculline at P8-9 indicated that it is mediated by GABA, resulting in an overall reduction in neuronal circuit activity. This reduction in GDP in Bicuculline further suggests that GABA is still excitatory, which can contribute to increased intrinsic excitability in *Syngap1*$^{+/-}$ mice observed in P8-9 (Clement, Aceti et al. 2012). Similarly, at P14-15, decreased GDPs in the presence of Bicuculline was observed, suggesting that GABA is still excitatory, which may fail to compensate for increased AMPAR/NMDAR ratio and mEPSC amplitude in *Syngap1*$^{+/-}$mice observed in P14-15. Thus, overall providing a compensatory mechanism for *Syngap1*$^{+/-}$mice to survive. Additionally, it suggests, perhaps, that GABA is still excitatory instead of compensating for the increased AMPAR, hence, leading to altered mIPSC in *Syngap1*$^{+/-}$ (Clement, Aceti et al. 2012, Ozkan, Creson et al. 2014).

Disrupted neuronal network activity led us to investigate whether GABAR-mediated inhibition in *Syngap1*$^{+/-}$mice is comparable to WT levels as disruption in GABAR-mediated tonic inhibition is reported in several models of neurodevelopmental disorders (Brickley and Mody 2012, Egawa and Fukuda 2013). Synaptic $GABA_A$Rs mediate phasic (γ2 subunit), which is fast inhibitory postsynaptic potentials, whereas, extrasynaptic $GABA_A$Rs mediate

tonic (α, δ subunits) inhibition which is persistent inhibitory conductance that together controls network excitability and oscillations thereby, regulate information processing in the brain (Farrant and Nusser 2005, Brickley and Mody 2012, Egawa and Fukuda 2013). As GABA concentration increases, interneurons become less excitable and phasic inhibition of cells attain "off" mode, whereas tonic inhibition of neurons increases. Generation of tonic currents requires a specific $GABA_ARs$ subunit combination, specifically $\alpha5GABA_ARs$ in CA1 and CA3 pyramidal cells (Caraiscos, Elliott et al. 2004) and δ-subunit in dentate-gyrus (Nusser and Mody 2002). The significant level of tonic currents in the hippocampus are mediated by extrasynaptic $GABA_ARs$ are highly sensitive to GABA and mediated by action potential-dependent vesicular GABA release (Glykys and Mody 2007). The vesicular release of GABA in the synaptic cleft can diffuse to some distance over perisynaptic regions where, with high affinity, it can bind to $GABA_ARs$ and result in tonic inhibition. GABA transporter-1 (GAT1) ($2Na^+$: $1Cl^-$: 1GABA) is one of the major transporters responsible for the uptake of GABA, thereby blocking GAT-1, which can allow measurement of tonic current resulting in an increased ambient concentration of GABA. The whole-cell patch-clamp recordings were performed to measure GABAR-mediated tonic currents at P14-15 based on the earlier findings and published results (Clement, Aceti et al. 2012, Clement, Ozkan et al. 2013). Upon application of glutamate receptor blockers, NO-711 and Bicuculline, there was a significant level of inhibition of downward deflecting currents (phasic) as well as the tonic current was observed, which resulted in the outward shift of the holding current (current traces in **Figure 3.1 F**). Additionally, GABAR-mediated inhibition was observed in WT but reduced in *Syngap1*$^{+/-}$ (**Figure 3.1 E** and **F**). The decreased GABAR-mediated inhibition would result in increased excitability and altered sensory processing, which we observe in *Syngap1*$^{+/-}$mice. Overall, these results imply diminished inhibition as a result of disrupted GABAR-mediated activity that contributes to the increase in excitation during development in *Syngap1*$^{+/-}$ (Clement, Aceti et al. 2012, Clement, Ozkan et al. 2013, Ozkan, Creson et al. 2014).

3.1.3.2 Disrupted GABA polarity switch at two weeks in *Syngap1*$^{+/-}$ mutation:

Maintenance of E/I balance with the coordinated activities of excitatory and inhibitory circuits is the fundamental requirement for normal brain responses towards any stimulus (Banerjee, Rikhye et al. 2016). GABA is considered as a major inhibitory neurotransmitter in the central nervous system and has a dual role (excitatory in early stages, inhibitory in adult

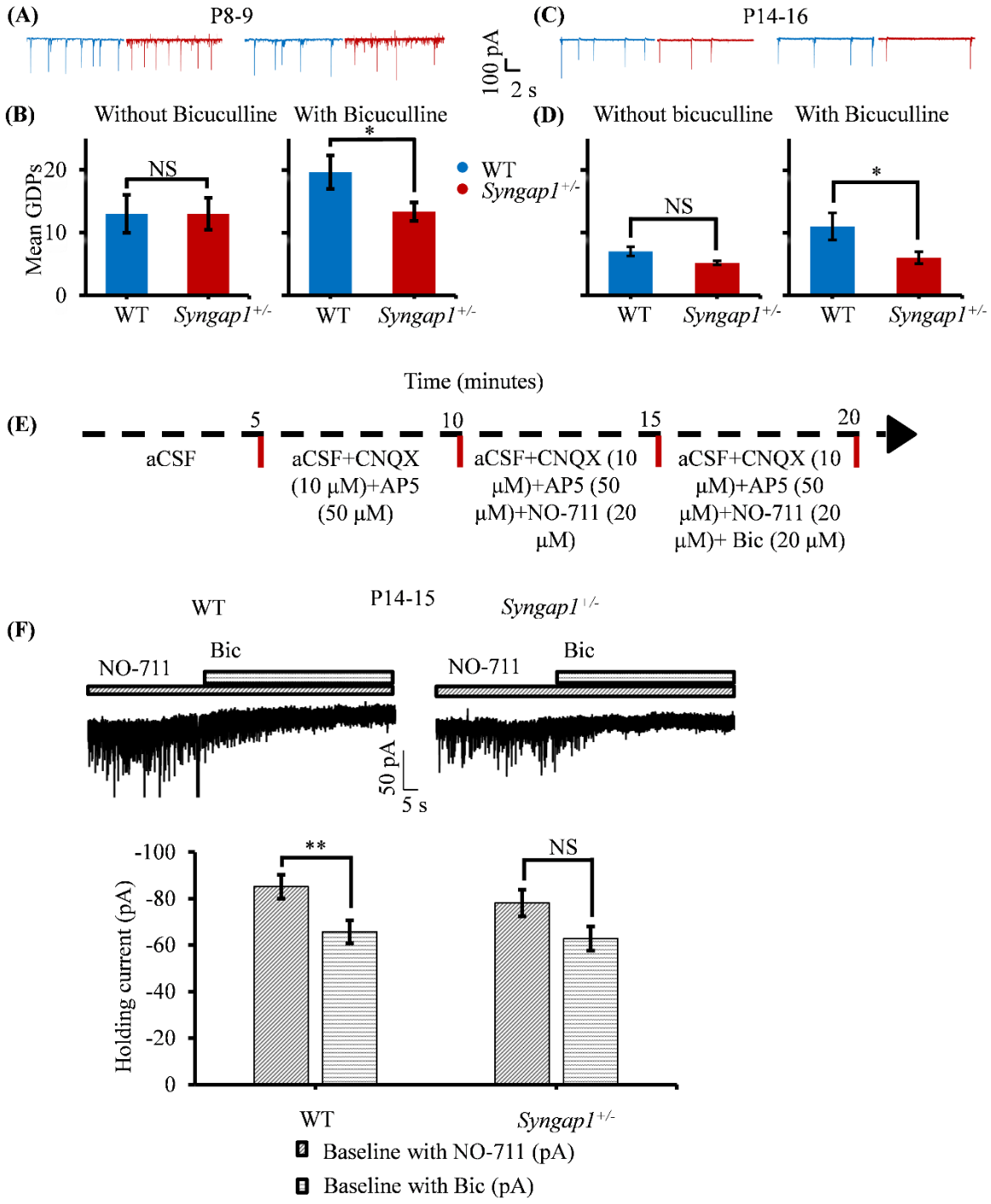

Figure 3.1 Developmental differences in neuronal network activity between genotypes and reduced GABA receptor-mediated tonic currents in *Syngap1*$^{+/-}$ mice at P14-15:

A) Representative traces of GDPs at a -70 mV holding potential with and without 10 µM Bicuculline at P8-9 are presented. **B)** Whereas without bicuculline, the values were similar between the two groups, a significant difference between WT and *Syngap1*$^{+/-}$ was observed in the experiments with the inhibition of GABA receptor-mediated currents (Without Bicuculline: WT, 13±3, N=7, n=6;

Syngap1$^{+/-}$, 13±3, N=6, n=11, NS: p>0.05. With Bicuculline: WT, 19±2, N=7, n=6; *Syngap1*$^{+/-}$, 13±2, N=6, n=9, *p<0.05). **C** and **D)** Experiments in neurons at P14-16-day-old mice revealed a significant difference between the two groups during the application of bicuculline. (Without Bicuculline: WT, 7±0.7, N=7, n=15; *Syngap1*$^{+/-}$, 5±0.3, N=6, n=17, NS: p>0.05. With Bicuculline: WT, 6±1, N=7, n=6; *Syngap1*$^{+/-}$, 3±0.8, N=6, n=17, *p<0.05). Data presented as mean ± SEM. N: number of mice, n: number of cells. **E)** Experimental paradigm depicting the procedure used to measure E_{Cl^-} from granule cells. **F)** *Top,* Representative traces of tonic currents from P14-15-day-old WT and *Syngap1*$^{+/-}$ mice. *Below*, the bar graph summarises the level of GABAR mediated tonic currents before and after the application of bicuculline. The GABAR mediated tonic currents were induced by NO-711 application. A significant reduction of the holding current by bicuculline was only observed in the DGGC of WT mice and not in *Syngap1*$^{+/-}$ mice (WT, 85±5.12, 65±4.89, N=4, n=9, Baseline with NO-711 to Baseline with Bicuculline, **p<0.01; *Syngap1*$^{+/-}$, 78±5.3, 62±5.14, N=5, n=12, Baseline with NO-711 to Baseline with Bicuculline, NS: p>0.05). Data presented as mean ± SEM, Unpaired *t*-test, N: number of mice, n: number of cells

stages) during the development, which is cardinal for the optimal critical period of plasticity in the brain (Ben-Ari 2002, Petroff 2002). The dual role of GABA is carried out by two Cl^- cotransporters in the brain. The primary role of NKCC1 and KCC2 is to maintain and regulate E_{Cl^-} and E_{GABA} with a secondary role of maintaining cell volume of Cl^-. In the early stages of development, when synapses are silent, the excitatory activity of neurons is mediated by GABA as the efflux of Cl^- occurs during activity, but the influx of Cl^- occurs through NKCC1 at rest. Chloride influx at rest renders the neuron's equilibrium potential more negative. Thus, when GABAR activation allows chloride to leave the neuron and makes it more depolarizing and excitatory. In adult stages, when functional synapses are present, Cl^- efflux occurs through KCC2, which makes cell equilibrium potential more positive, so when GABAR is activated, it allows chloride to enter the cell and makes it more hyperpolarising and inhibitory (Ben-Ari 2002, Ben-Ari, Gaiarsa et al. 2007, Blaesse, Airaksinen et al. 2009, Ben-Ari 2014).

Studies have shown altered GABA polarity switch and imbalanced E/I in various ASD/ID models, which exert a long-lasting effect on the development and function of neurons and the critical period of plasticity (Ozkan, Creson et al. 2014, Deidda, Allegra et al. 2015, Banerjee, Rikhye et al. 2016). Considering GABA as a major candidate for optimal neuronal development and function, we investigated whether the aberrant trophic role of GABA contributes to the GABA-mediated circuit dysfunctions. Chloride gradient is the major

determinant of $E_{GABA,}$ which decreases intracellular Cl^- during the development, thus, making E_{GABA} more negative or towards resting membrane potential, thereby hyperpolarising neurons (Owens, Boyce et al. 1996).

Using the Gramicidin-perforated patch-clamp, GABA reversal potential (E_{Cl^-} or E_{GABA}) was measured from the outer granular cell layer of the dentate gyrus of WT and *Syngap1*$^{+/-}$ from P4-5, P7, P8, P14-15, P21-23, and P≥90. GABA-mediated responses were elicited by stimulating medial perforant pathway (MPP) in the presence of NMDAR and AMPAR blockers, AP-5 (100 μM) and CNQX (10 μM) respectively. Responses were recorded by voltage clamping the cell between -100 mV to +40 mV (10 mV increments). The measured responses were plotted as current and voltage relationship (I-V) (**Figure 3.2 A** and **B**), and E_{Cl^-} was determined when the current direction reverses to positive. E_{Cl^-} was found to be more depolarised at P14-15 (**Figure 3.2 C**), suggesting neurons are still excitatory in *Syngap1*$^{+/-}$. The latter could be correlated to increased AMPAR/NMDAR ratio and increased mEPSC amplitude and frequency in postsynapses at P14-16 suggests more excitation at P14-16 in *Syngap1*$^{+/-}$ mice. (Clement, Aceti et al. 2012).

The depolarization observed in 2-week-old *Syngap1*$^{+/-}$ mice, perhaps, are due to disinhibition of GABA during early stages of development that may result from impaired compensation of GABAR-mediated currents, thereby leading to altered E/I as observed in *Syngap1*$^{+/-}$ mice (Clement, Aceti et al. 2012, Ozkan, Creson et al. 2014). Together, increased AMPAR/NMDAR, mEPSC, mIPSC, positive E_{GABA}, and decreased giant depolarisation potentials, possibly, indicating disrupted neuronal circuit activity at P14-16 perhaps as a compensatory mechanism to balance the E/I for the *Syngap1*$^{+/-}$ mice to survive. Additionally, all the factors mentioned above despite providing the compensatory mechanism for survival has serious implication on overall neuronal circuits, which may lead to the altered critical period of plasticity, impaired physiological, behavioural, and cognitive functions observed in *Syngap1*$^{+/-}$ mice.

3.1.3.3 Altered expression of NKCC1 and KCC2 during development in *Syngap1*$^{+/-}$ mice:

Spatiotemporal regulation of expression of NKCC1 and KCC2, two core candidates responsible for the maintenance of chloride homeostasis in the brain, orchestrates GABAergic polarity switch during the development, which parallels the formation of

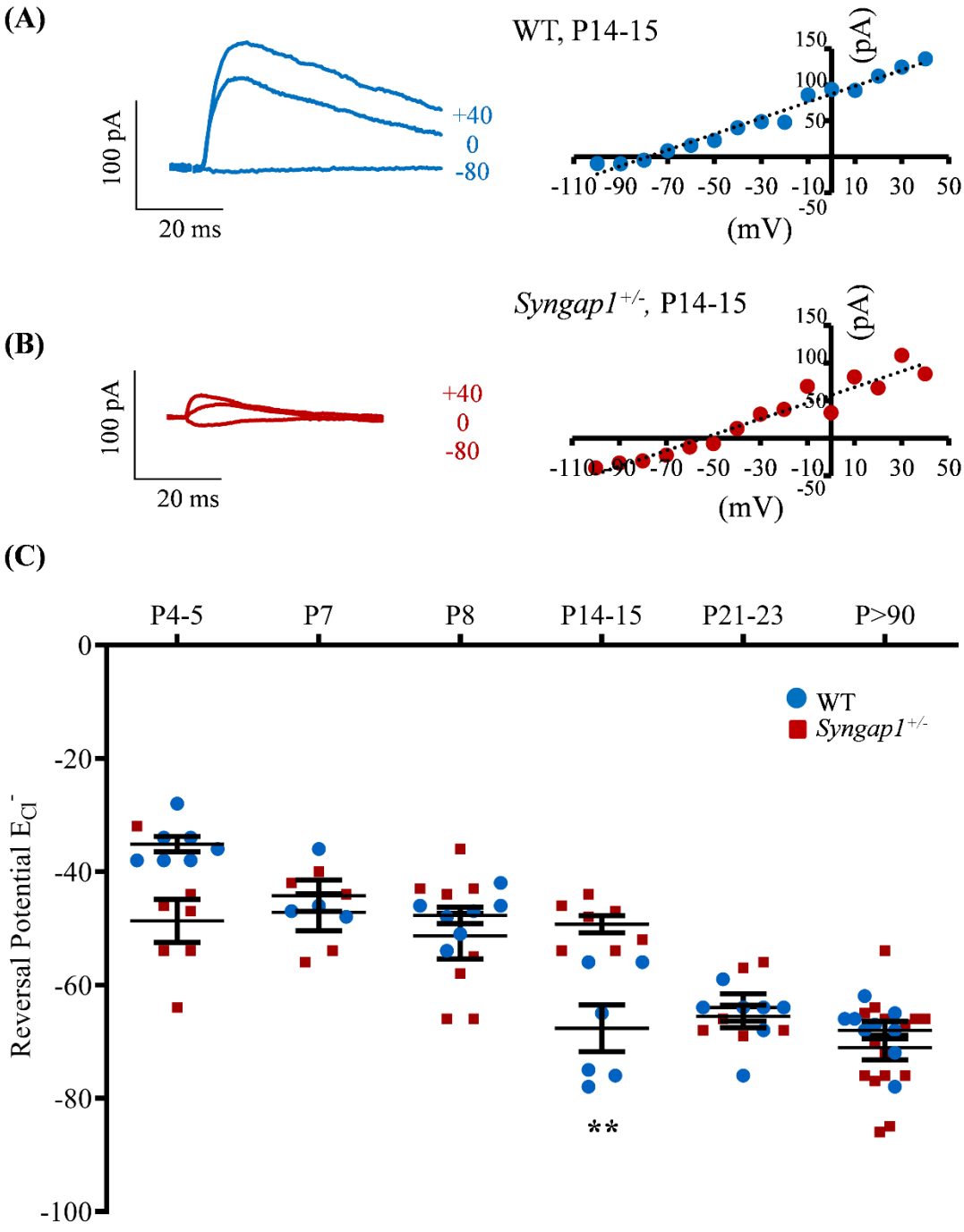

Figure 3.2 Neurons of *Syngap1*$^{+/-}$ mice show a shift in chloride reversal potential (E_{Cl^-}) at P14-15: A) *Left*, Evoked representative Cl^- mediated current traces at the indicated holding potentials of a Gramicidin-based perforated voltage-clamp experiment. *Right*, The graph to the right summarises the relationship of holding potential (mV) to current amplitude for one representative experiment and depicts the trend as a linear fit curve. The experiments were conducted at P14-15 in WT mice. B) Same as A but in P14-15 *Syngap1*$^{+/-}$. C) The graph summarises the reversal potentials of GABA receptor-mediated Cl^- current (E_{Cl^-}) in WT as well as *Syngap1*$^{+/-}$ at the indicated postnatal ages. P4-5:

WT: N=6, n=7, 35±1.37; *Syngap1*$^{+/-}$: N=4, n=7, 48±3, (NS: p>0.05); P7: WT: N= 3, n= 4, 44±2.78; *Syngap1*$^{+/-}$ N=3, n=5, 47±3,(NS: p>0.05); P8: WT N=5, n=6, 46±1; *Syngap1*$^{+/-}$: N=4, n=8, 51±4.04, NS: p>0.05; P14-15: WT: N=3, n=7; *Syngap1*$^{+/-}$: N=4, n=6, (**p<0.01); P21-23 WT, N=4, n=6, 65±2; *Syngap1*$^{+/-}$: N=3, n=7, 64±2, (NS: p>0.05); P≥90: WT: N=7, n=15, 68±1.53; *Syngap1*$^{+/-}$, N=5, n=9, 71±2.18, (NS: p>0.05). F (5, 76) = 6.83, p<0.0001 for the interaction. Data are presented as single data points and means ± SEM. N: number of mice, n: number of cells. Two-way ANOVA, Tukey's multiple comparisons test.

glutamatergic synapse development (Rivera, Voipio et al. 1999, Blaesse, Airaksinen et al. 2009). Given the function of chloride cotransporters are disrupted in *Syngap1*$^{+/-}$ mice during development, there is a possible alteration in the expression of NKCC1 and KCC2. Previous studies demonstrated the altered expression of NKCC1 and KCC2 during development in patients as well as various ASD/ID models (Duarte, Armstrong et al. 2013, Deidda, Allegra et al. 2015, Banerjee, Rikhye et al. 2016). Therefore, we investigated whether altered switchover of NKCC1 and KCC2 in *Syngap1*$^{+/-}$ is the consequence of altered network activity mediated by GABA and disrupted E_{Cl^-} during development. Immunoblot assays demonstrated that the expression level of NKCC1 and KCC2 during different stages of development. **Figure 3.3 A** and **B** demonstrates a significant increase in NKCC1 expression between Wild Type (WT) and *Syngap1*$^{+/-}$ in P8 (Hippocampus), depicting alteration in NKCC1 expression levels in *Syngap1*$^{+/-}$. Further, we had observed an increase in KCC2 expression at P8 but was decreased in P14, and the WT level matches *Syngap1*$^{+/-}$ from P21-23 onwards (**Figure 3.3 C** and **D**). Overall, these results suggest an irregular expression of NKCC1 and KCC2 during the early developmental stages in *Syngap1*$^{+/-}$ that could potentially interrupt the Cl^- accumulation inside the neuron, thereby affecting the synaptic maturation and function.

Information concerning protein or mRNA expression can potentially shed more light on the molecular mechanism underlying the disease caused during neuronal development. Any change in the expression of the protein is not necessarily accompanied by altered mRNA levels or vice versa (Ozkan, Creson et al. 2014, Miguez, Garcia-Diaz Barriga et al. 2015). The next question was to investigate the transcript levels of Cl^- co-transporters and related mRNAs during development in *Syngap1*$^{+/-}$. qPCR was performed for mRNAs *Nkcc1*, *Kcc2*, *Bdnf* and other potential genes linked to Cl^- co-transporters and observed no change in the transcript levels except increased relative *Bdnf* mRNA levels (**Figure 3.4**) at P14-15

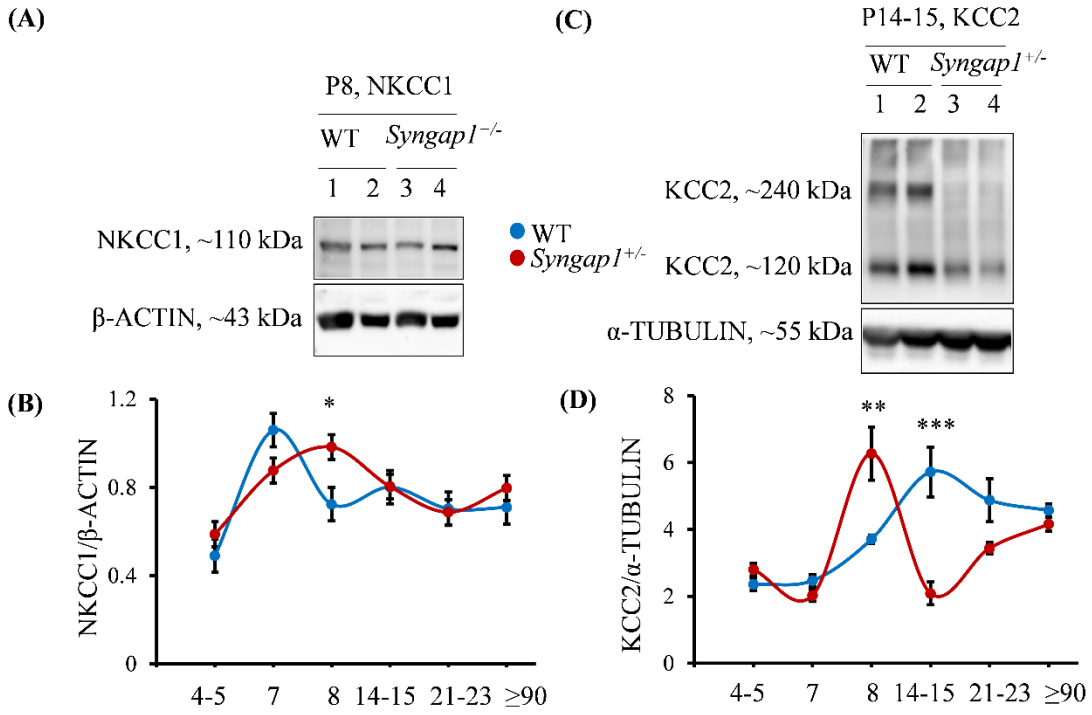

Figure 3.3 Age-dependent expression levels of NKCC1 and KCC2 Cl^- co-transporters in WT and *Syngap1*$^{+/-}$ mice:

A) *Top*, Representative NKCC1 immunoblots at P8 are depicted. B) *Bottom*, line graph summarizes NKCC1 expression levels at different postnatal ages for WT as well as *Syngap1*$^{+/-}$. P4-5 (WT) N=7, 0.48±0.1, (*Syngap1*$^{+/-}$) N=11, 0.58 ±0.03 (p: 0.1320); P7 (WT) N=7, 1 ±0.1, (*Syngap1*$^{+/-}$) N=8, 0.87 ±0.1228 (p>0.05); P8 (WT) N=6, 0.72±0.05, (*Syngap1*$^{+/-}$) N=6, 0.98±0.09 (*p<0.05); P14-15 (WT) N=13, 0.8±0.05, (*Syngap1*$^{+/-}$) N=10, 0.8±0.07 (p>0.05); P21-23 (WT) N=7, 0.7±0.03, (*Syngap1*$^{+/-}$) N=7, 0.68±0.06 (p>0.05); =>P90 (WT) N=10, 0.7±0.07, (*Syngap1*$^{+/-}$) N=10, 0.79±0.08 (p>0.05). F (5, 90) = 1.48, p=0.2027 for the interaction. C) *Top*, Representative P14-15 immunoblots for KCC2 are shown. D) *Bottom*, line graph summarizes KCC2 expression level during development in WT as well as *Syngap1*$^{+/-}$. (P4-5 (WT) N=9, 2.3±0.18, (*Syngap1*$^{+/-}$) N=9, 2.8±0.18 (p>0.05); P7 (WT) N=8, 2.4±0.17, (*Syngap1*$^{+/-}$) N=8, 2±0.17 (p>0.05); P8 (WT) N=5, 3.7±0.12, (*Syngap1*$^{+/-}$) N=6, 6.2±0.79 (**p<0.01); P14-15 (WT) N=7, 5.717±0.7434, (*Syngap1*$^{+/-}$) N=8, 2±0.3 (***p<0.001); P21-23 (WT) N=7, 4.872±0.6442, (*Syngap1*$^{+/-}$) N=7, 3.4±0.1 (p> 0.05); =>P90 (WT) N=10, 2.3±0.2, (*Syngap1*$^{+/-}$) N=10, 2.8±0.2 (p>0.05). F (5, 82) = 14.46, p<0.0001 for the interaction. Data are presented as mean ± SEM. N: number of mice. Two-way ANOVA, Tukey's multiple comparisons test. Data are presented as mean ± SEM.

Syngap1$^{+/-}$, which was very exciting as the development of the GABAergic system is highly dependent on BDNF (Porcher, Medina et al. 2018). BDNF is shown to downregulate KCC2

in TRKB (tropomyosin related kinase B) dependant manner when exogenously applied in slices or cells and altered the chloride extrusion capacity of KCC2 (Rivera, Li et al. 2002, Ludwig, Uvarov et al. 2011, Puskarjov, Ahmad et al. 2015). BDNF is a potent regulator of KCC2 expression and function that was able to block the increase in spine density induced by KCC2 in cortical neurons (Awad, Amegandjin et al. 2018). Based on the result from this thesis-related study in which altered KCC2 expression levels are observed and Clement et al shown (Clement, Aceti et al. 2012) more mature dendritic spine in *Syngap1*$^{+/-}$ mice at P14-15, BDNF might be contributing towards a compensatory mechanism which further needs to be explored. The extrusion of Cl^- via KCC2 is regulated by the development-based oligomerisation of KCC2, and disruption to this process can be detrimental to synapse development (Blaesse, Guillemin et al. 2006, Mahadevan, Pressey et al. 2014). Therefore, to investigate whether abnormal KCC2 oligomers form early during development in *Syngap1*$^{+/-}$, immunohistochemistry was done from different age groups.

As a control for each age group, SYNGAP1 was also stained, which was visualised by green colour in representative images, which showed a decrease in fluorescence for *Syngap1*$^{+/-}$ as compared to WT for the same age group, further conforming to reduced levels of SYNGAP1 in *Syngap1*$^{+/-}$ mice. An increase in the expression of KCC2 in P8, but a decrease as observed in P14 (**Figure 3.5**), in concurrence with the immunoblot results. These results indicate an uncharacteristic pattern of oligomerisation of KCC2 that may influence the GABA polarity switch during development and that can be detrimental to synapse maturation and function in *Syngap1*$^{+/-}$.

Incoherence with previous studies where Cl^- cotransporters protein expression levels were found to be altered poses as a candidate target for therapeutics in ASD/ID models. Thus, our result suggests a possible alteration of NKCC1 and KCC2 translationally during the development in *Syngap1*$^{+/-}$ mice which could potentially contribute to altered E_{Cl^-}. The results obtained thus far shows aberrant neuronal network activity, GABAR-mediated tonic inhibition, GABA polarity switch as well as protein expression of NKCC1 and KCC2, suggesting dysfunctional GABAergic system as one of the primary underlying cause for the physiological, emotional, and cognitive deficits observed in *Syngap1*$^{+/-}$ mice and correspondingly a potential therapeutic target.

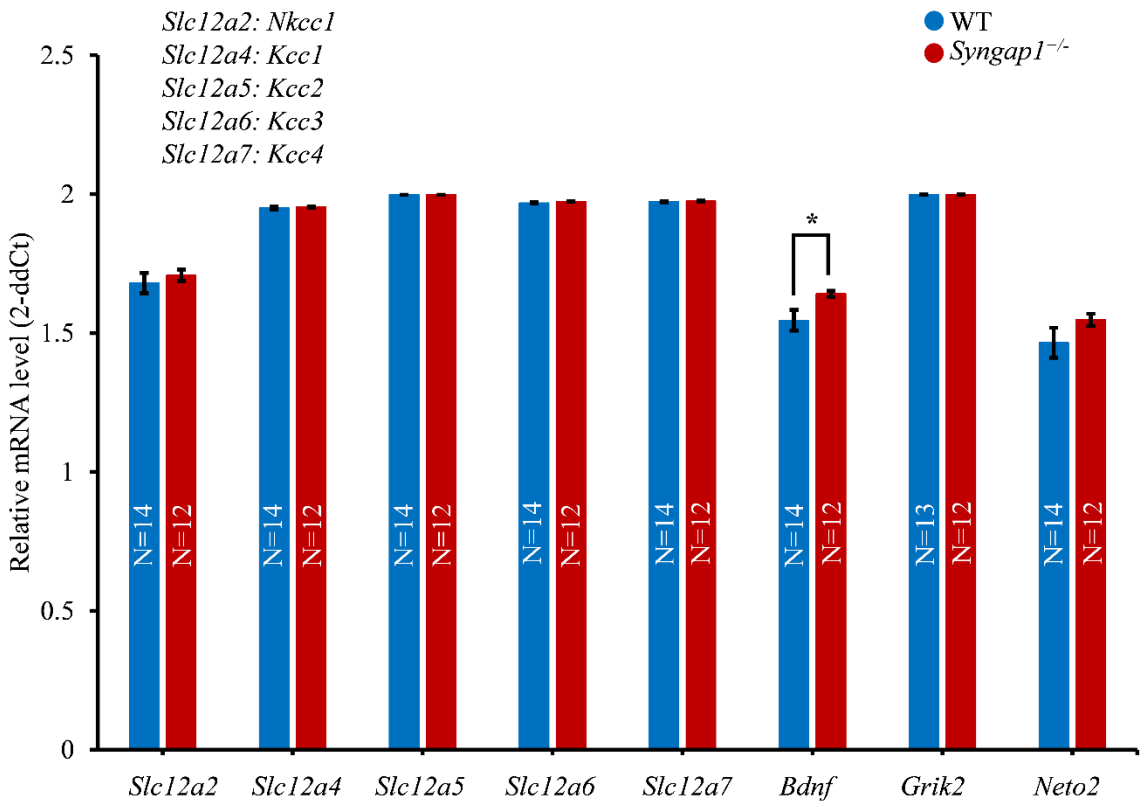

Figure 3.4 Transcript (mRNA) profile of *Nkcc1* and *Kcc2* Cl^- co-transporters and other relevant proteins at P14-15:

Relative mRNA level (2-ddCt) is represented as bar graph quantification of mRNA levels of *Nkcc1* (WT, 1.68±0.036, *Syngap1*$^{+/-}$ 1.70±0.021, p>0.5), *Kcc1* (WT, 1.94±0.004, *Syngap1*$^{+/-}$, 1.95±0.001, p>0.05), *Kcc2* (WT, 1.99±0.0002, *Syngap1*$^{+/-}$ 1.99±0.0002, p>0.05), *Kcc3* (WT, 1.96±0.002, *Syngap1*$^{+/-}$ 1.97±0.0009, p>0.05), *Kcc4* (WT, 1.97±0.001, *Syngap1*$^{+/-}$ 1.97±0.001, p>0.05), *Bdnf* (WT, 1.54±0.037, *Syngap1*$^{+/-}$ 1.64±0.011, p<0.05), *Grik2* (WT, 1.99±0.0002, *Syngap1*$^{+/-}$ 1.99±0.0002, p>0.05) and *Neto2* (WT, 1.46±0.054, *Syngap1*$^{+/-}$ 1.54±0.022, p>0.05) proteins during development in *Syngap1*$^{+/-}$ as well as WT in hippocampus samples. *p>0.05. Bars present mean value and error bars indicate SEM. N: number of mice.

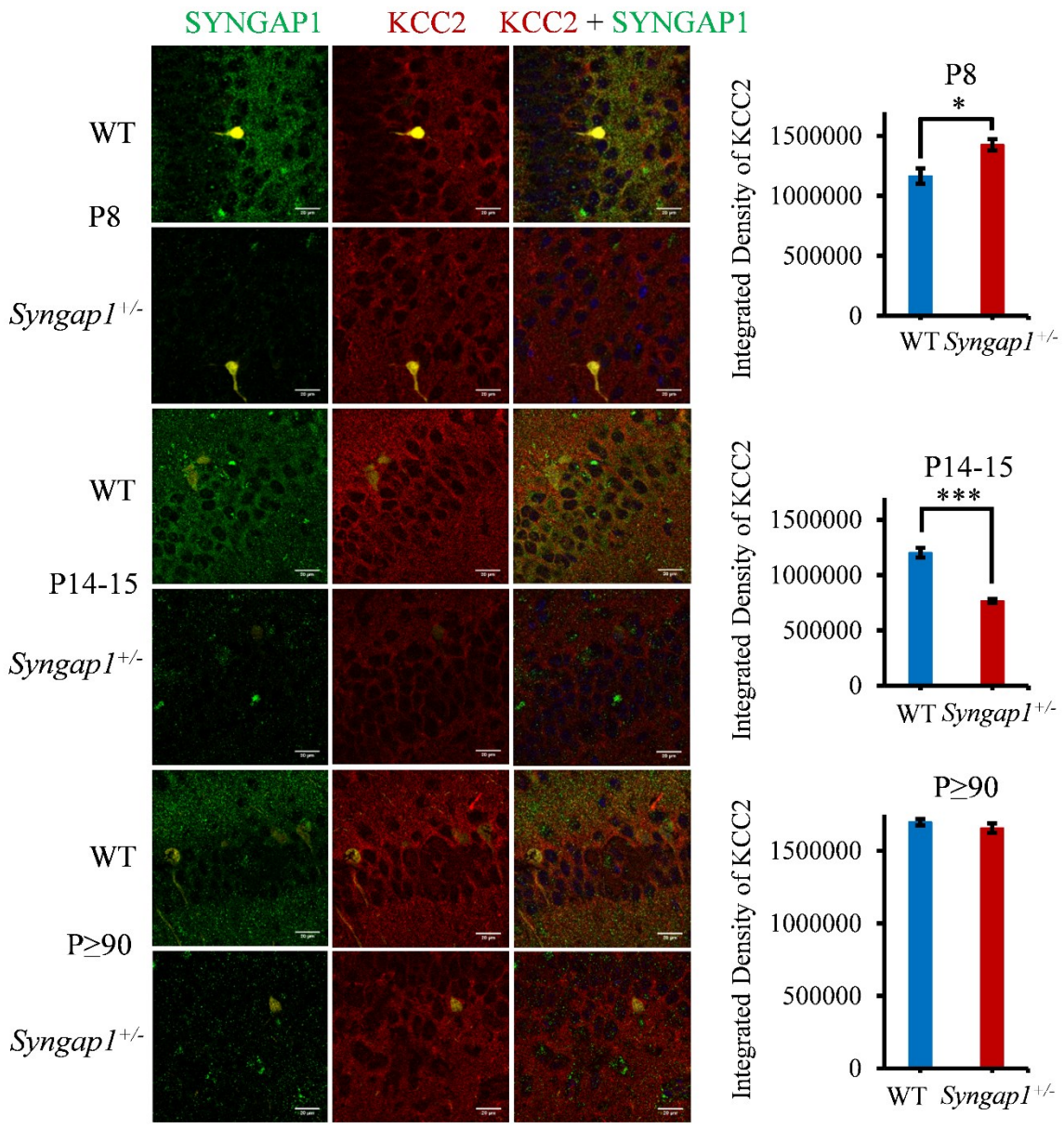

Figure 3.5 Age-dependent expression levels of KCC2 in WT and *Syngap1*$^{+/-}$ mice:

Representative immunofluorescence images depicting SYNGAP1 and KCC2 localisation and expression pattern in hippocampus region in WT and *Syngap1*$^{+/-}$ mice at P8, 14-15 and ≥90. Blue colour represents the Hoescht staining of the nucleus, green coloured puncta are of SYNGAP1 protein, and KCC2 puncta surrounding soma and dendrites are presented in red. A bar graph representing the integrated density of WT and *Syngap1*$^{+/-}$ in the individual age group is shown in front of the respective panel of P8, 14-15 and ≥90. P8 (WT) n=4, 1165283±64324, (*Syngap1*$^{+/-}$) n=5, 1426211±47106 (*p<0.05); P14-15 (WT) n=7, 1202925±43917, (*Syngap1*$^{+/-}$) n=6, 766779±18128 (***p<0.001); P≥90 (WT) n=6, 1697380±22155, (*Syngap1*$^{+/-}$) n=8, 1656486±32631 (p>0.05). Scale bar = 20 µm. Data are presented as mean ± SEM. Unpaired *t*-test, n: number of sections.

3.2 6BIO corrects physiological as well as behavioural deficits in *Syngap1*$^{+/-}$-mediated intellectual disability

3.2.1 Introduction:

The results, thus far, demonstrate that *Syngap1*$^{+/-}$ mutation results in the altered network activity, inhibition, and GABA polarity switch. These can result in E/I imbalance and eventually disrupt the critical period of development, synaptic plasticity, and cognition. The disrupted GABAergic system is one of the hallmarks of ID/ASD and positions itself as a vital candidate therapeutic target to correct phenotypes (Cellot and Cherubini 2014, Braat and Kooy 2015). $GABA_A$ receptor heterogeneity and well-established pharmacological properties provide an excellent opportunity for therapy in ASD/ID.

Due to the co-morbidity of ASD/ID with epilepsy, anxiety, attention, insomnia, and cognition, to date, most of the pharmacological interventions are based on alleviating individual symptoms in various models such as Dravet syndrome, Fragile-X syndrome, Rett syndrome, and animal models of idiopathic autism. Most of the commercially available drugs used to ameliorate symptoms of neurodevelopmental disorders (ASD/ID: Fragile-X, Rett) or neuropsychiatric disorders (Schizophrenia, Bipolar, Anxiety, Depression disorders) such as Lithium, statins, which are based on the inhibition of GSK3-β that is implicated in most of these disorders, and thus, as the primary or secondary target of these drugs (Jaworski, Banach-Kasper et al. 2019). GSK3-β has been shown as an essential regulator for synaptic plasticity (Peineau, Taghibiglou et al. 2007, Liu, Xie et al. 2017). However, finding potent therapeutics that can target GSK-3β and restore phenotypes, mainly when administered after a critical period of development, has been elusive.

As mentioned earlier, there are many commercially available drugs prescribed to treat ID/ASD patients to alleviate symptoms rather than to correct the phenotypes, particularly after neuronal connections are established (hard-wired). The opportunity, therefore, exists to develop a therapeutically viable drug, in this case, a GSK-3β inhibitor. Small molecules such as 6BIO is a potent negative regulator of GSK3-β by crossing the blood-brain barrier and neuroprotective in an MPTP-based mouse model of Parkinson's disease (Meijer, Skaltsounis et al. 2003, Polychronopoulos, Magiatis et al. 2004, Vougogiannopoulou and Skaltsounis 2012, Suresh, Chavalmane et al. 2017). Accordingly, we sought to test whether

administration of 6BIO corrects synaptic plasticity, E_{GABA}, and behavioural dysfunctions in *Syngap1*$^{+/-}$ mice.

3.2.2 Methods:

Considering *Syngap1*$^{+/-}$ mutation displays disrupted critical period of development (critical period), we selected three different age groups (strategies) for 6BIO injections to determine the developmental time point that is most efficient in correcting the deficits; Group I: P10-16 (critical period), Group II: P10-80 (listed critical period and adulthood), and Group III: P30-80 (adulthood) (**Figure 3.6 A**). P10-16 will address whether targeting the critical period alone would be sufficient to correct the phenotype with lasting effects in adulthood. P10-80 would answer whether the drug should be administered from the critical period and continue into adulthood. P30-80, the most crucial aspect of the drug discovery, which remains a challenge, would imply whether administration of the drug after a critical period of development corrects synaptic dysfunction and behavioural deficits, which remains a challenge to date. We evaluated the effect of 6BIO on three different behavioural paradigms that are the core characteristics of neurodevelopmental disorder: 1) Open field test, 2) Novel object recognition and, 3) Social interaction and preference, and 4) Seizure threshold.

The open field has an open square box arena explored, which determines the anxious state and activity of the test mice. Novel object recognition evaluates the recognition memory of the mice, where mice have to explore the square box having objects in it. Day1 is the exploration of the empty arena, Day2 and 3 has the familiar objects in the same diagonal and Day4 has one familiar object replaced by one novel object. Mice spending more time with novel object suggest recognition memory of mice for familiar object and novelty for the novel object. Social interaction was performed in three chamber box where two off-centre chambers would contain mice in a steel mesh jar (stranger1) and an empty jar and test mice were allowed to explore. Time spent more with mice in the jar would suggest a socially active mouse. Social preference was performed in three chamber box where both off-centre chambers would contain mice in a steel mesh jar (stranger1 and stranger 2), and test mice were allowed to explore. As a mouse is a curious mammal, time spent more with stranger 2 would suggest a mouse able to prefer or being curious to accept social novelty.

ASD/ID is often co-morbid with epilepsy. *Syngap1*$^{+/-}$ mice has a lower threshold for seizure (Clement, Aceti et al. 2012), hence more prone to get seizures which we observe in the

individuals suffering from ASD/ID (could be one of the reasons for their sleeplessness). The flurothyl-based seizure was used to test whether 6BIO could increase the seizure threshold in *Syngap1*$^{+/-}$ mice in adulthood, past the critical period of development.

3.2.3 Results:

3.2.3.1 6BIO corrects behavioural deficits in *Syngap1*$^{+/-}$ mutation:

The *SYNGAP1*-mediated ID appears to be equally prevalent for all ethnic groups, and among males and females, of incidence reported 1-4/10,000 individuals (less than 1% of all ID cases). Currently, there is no cure or specific treatment for individuals with *SYNGAP1* mutations. However, most strategic therapies target the symptoms such as seizures, hypotonia, sleeplessness, mania, and euphoria. Cholesterol-lowering statins, such as lovastatin or lithium has been proven to ameliorates deficits in global behaviour and cognitive behaviour in a 31-year-old patient along with ASD/ID models (Liu, Huang et al. 2012, Osterweil, Chuang et al. 2013, Siegel, Beresford et al. 2014, Asiminas, Jackson et al. 2019, Cook, Masaki et al. 2019, Muscas, Louros et al. 2019).

Up until now, in animal models of *Syngap1*$^{+/-}$, no study has shown the correction of physiological, behavioural, and cognitive upon therapeutic intervention in the adult stage of development which to date remains the most challenging question. In adult stages, when most neuronal connectional would be hard-wired with less scope of plasticity hence, it becomes difficult to rewire the neuronal connections to correct deficits without secondary issues in *Syngap1*$^{+/-}$. Most cases of individuals suffering from *SYNGAP1*-related ID are diagnosed in 2-3-years of age when many neuronal connections had already been established for most milestones of childhood (past critical period). Therefore, re-establishing neuronal connections in adult stages has become imperative to correct the deficits observed in *Syngap1*$^{+/-}$. 6BIO has opened a new therapeutic option by addressing the mentioned gap in the treatment of ID/ASD.

Open field test (OFT) evaluates hypo- or hyper-activity (total distance travelled) and the level of anxiety (number of entries to the centre) in mice. It was observed upon treatment of 6BIO, *Syngap1*$^{+/-}$ mice showed correction of hyperactivity (total distance) as compared to *Syngap1*$^{+/-}$ vehicle mice in P16 (P10-80 age group), where behaviour was performed at P16

(**Figure 3.6 B**). For the same age group, when the behaviour was performed at P42, the partial correction was observed (**Figure 3.6 D**), suggesting that the dose given might not be sufficient to sustain the changes induced by 6BIO as the brain matures. Similarly, when tested at P80 (P10-16 age group), partial correction of hyperactivity was observed in *Syngap1*$^{+/-}$ (**Figure 3.6 F**). This result suggests that injections only during the critical period may not be sufficient to correct locomotor activity. Furthermore, 6BIO did not correct locomotor activity when administered at P30-80 (**Figure 3.6 H**), suggesting that the drug is most effective in correcting the phenotype when administered only during the critical period of development.

When the effect of 6BIO on anxiety level was investigated, phenotypes in *Syngap1*$^{+/-}$ mice were corrected for behaviour performed at P16 (**Figure 3.6 C**; P10-80 age group), where behaviour was performed at P80 (**Figure 3.6 G;** P10-16 age group) and a partial correction for P42 (P10-80 age group; **Figure 3.6 E**), and P30-80 (**Figure 3.6 I**) age group, suggesting that anxiety was corrected when 6BIO was administered even after the critical period of development. Overall, the OFT results suggest that 6BIO will be effective to correct locomotor activity when treated only in the critical period of development but given the partial correction of phenotypes in adult stages (P30-80), open up the possibility of giving a high dosage to correct the phenotype in adult stages, which is yet to be explored.

Based on freezing behaviour observed in contextual fear conditioning paradigm upon delivery of conditioned stimulus (CS) (white noise), which was paired with an unconditioned stimulus (US) (foot shock) in previous trials, *Syngap1*$^{+/-}$ mice showed less percentage of freezing suggesting impaired memory (Nakajima, Takao et al. 2019). A characteristic feature of ID/ASD is impaired learning and memory recollection. Since 6BIO is a GSK-3β inhibitor and a regulator of memory and plasticity, its effect on *Syngap1*$^{+/-}$ mice for behaviour involved in the memory test was evaluated. To investigate the effect of 6BIO, a novel object recognition test (NOR; Familiar vs novel object) was performed. The behaviour was carried out for all age groups at P80 (P10-16: **Figure 3.7 A**; P10-80 **Figure 3.7 B**; P30-80 **Figure 3.7 C**), and DI was calculated. Remarkably, it was found that 6BIO substantially corrected memory deficits in *Syngap1*$^{+/-}$ mice. These results are encouraging as 6BIO, especially when administered after a critical period of development, corrected the memory deficits.

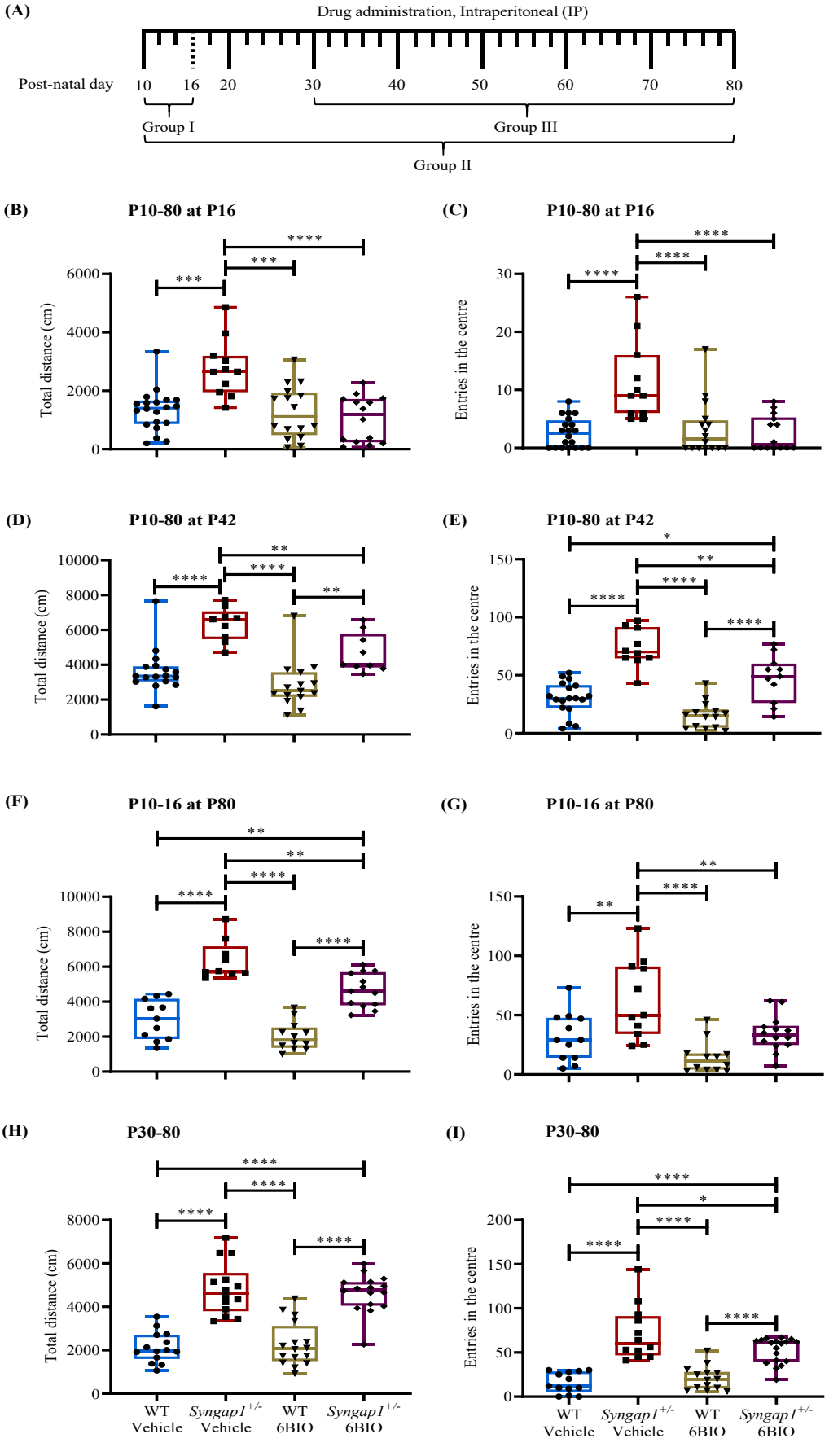
(A)
Drug administration, Intraperitoneal (IP)
Post-natal day
10
16
20
30
40
50
60
70
80
Group I
Group III
Group II
(B)
P10-80 at P16
Total distance (cm)
(C)
P10-80 at P16
Entries in the centre
(D)
P10-80 at P42
Total distance (cm)
(E)
P10-80 at P42
Entries in the centre
(F)
P10-16 at P80
Total distance (cm)
(G)
P10-16 at P80
Entries in the centre
(H)
P30-80
Total distance (cm)
(I)
P30-80
Entries in the centre
WT Vehicle
Syngap1+/- Vehicle
WT 6BIO
Syngap1+/- 6BIO

Figure 3.6 6BIO corrects hyperactivity and anxiety deficits in *Syngap1*$^{+/-}$

A) Chart depicting the regime for 6BIO intraperitoneal injection (5 mg/kg) and categorisation of age groups. **B)** Total distance travelled by the mice in open field chamber was grouped and shown as individual data points for P10-80 where behaviour was done at P16 WT–Vehicle: N=20; *Syngap1*$^{+/-}$–Vehicle: N=11; WT–6BIO: N=16; *Syngap1*$^{+/-}$–6BIO: N=14, $F_{(1, 57)} = 14.83$, p=0.0003, **C)** P10-80 where behaviour was done at P42, WT–Vehicle: N=17; *Syngap1*$^{+/-}$–Vehicle: N=9; WT–6BIO: N=15; *Syngap1*$^{+/-}$–6BIO: N=9, $F_{(1, 44)} = 4.752$, p=0.0347, and **D)** P30-80, WT–Vehicle: N=14; *Syngap1*$^{+/-}$–Vehicle: N=14; WT–6BIO: N=16; *Syngap1*$^{+/-}$–6BIO: N=16, $F_{(1, 56)} = 0.4686$, p=0.4965. **E)** Number of entries in the centre as a measure of anxiety was grouped and shown as individual data points for P10-80 where behaviour was done at P16, WT–Vehicle: N=20; *Syngap1*$^{+/-}$–Vehicle: N=11; WT–6BIO: N=16; *Syngap1*$^{+/-}$–6BIO: N=14, $F_{(1, 57)} = 18.01$, p<0.0001, **F)** P10-80 where behaviour was done at P42, WT–Vehicle: N=18; *Syngap1*$^{+/-}$–Vehicle: N=10; WT–6BIO: N=15; *Syngap1*$^{+/-}$–6BIO: N=11, $F_{(1, 50)} = 2.194$, p=0.1449, and **G)** P30-80, WT–Vehicle: N=13; *Syngap1*$^{+/-}$–Vehicle: N=12; WT–6BIO: N=15; *Syngap1*$^{+/-}$–6BIO: N=18, $F_{(1, 54)} = 6.002$, p=0.0176. Mice were injected from P10-16 and behaviour was performed at P80 where mice were allowed to explore the open field chamber for 15-minute. Total distance travelled **H)**. WT–Vehicle: N=11; *Syngap1*$^{+/-}$–Vehicle: N=9; WT–6BIO: N=12; *Syngap1*$^{+/-}$–6BIO: N=13, $F_{(1, 41)} = 1.676$, p=0.2027, and number of entries. **I)** WT–Vehicle: N=12; *Syngap1*$^{+/-}$–Vehicle: N=11; WT–6BIO: N=12; *Syngap1*$^{+/-}$–6BIO: N=14, $F_{(1, 45)} = 0.8829$, P=0.3524, Two-way ANOVA, Tukey's multiple comparisons test, was plotted as grouped data with individual values on graph

A major trait of ID/ASD is the lack of ability to be social with others, to express emotions verbally or non-verbally, difficulty in understanding social norms, communication impairment, and restrictive and repetitive behaviour, which all encompasses social behaviour. A case study from India and abroad listed a large array of behavioural deficits (Vlaskamp, Shaw et al. 2019, Verma, Mandora et al. 2020), which makes life almost unimaginable to consider oneself without being able to communicate or emotionally express, which restrains ASD/ID individuals from performing the everyday task and taking care of themselves, which makes correcting social deficits imperative.

Similar to NOR, social isolation test involving social interaction (SI) and social preference (SP) was performed for all age groups at P80 (P10-16: **Figure 3.7 D** and **G**; P10-80: **Figure 3.7 E** and **H**; P30-80: **Figure 3.7 F** and **I**). Results unveil that the time spent with stranger-1 as compared to the empty jar for 6BIO treated *Syngap1*$^{+/-}$ mice were comparable to WT

levels in all age groups, suggesting 6BIO can correct social interaction deficits observed in *SYNGAP1*-related ID which can be corroborated to a child preferring inanimate objects than interacting with a child of a similar age. The results further demonstrated that social preference for 6BIO treated *Syngap1*$^{+/-}$ mice in P10-80 and P30-80 age group were corrected, but not in P10-16, where behaviour was performed at P80. It could be due to a different time point for critical period regulation of the SYNGAP1 function for different types of behaviours, which needs to be explored. One reason could be the maturation of cortical circuits associated with different behaviours varies for different regions of the brain (Aceti, Creson et al. 2015, Chakraborty, Vijay Kumar et al. 2021). Overall, the results suggest that 6BIO is effective in correcting the SI and SP deficits when administered after a critical period of development in *Syngap1*$^{+/-}$ mice. Though it is a long shot, these results are encouraging as 6BIO establishes itself as a substantial therapeutic option to treat *SYNGAP1*-related ID.

Another primary attribute of ID/ASD is epileptic seizures which are observed in patients with *SYNGAP1* haploinsufficiency (Hamdan, Gauthier et al. 2009, Hamdan, Daoud et al. 2011) and reduced threshold to fluoroethyl in *Syngap1*$^{+/-}$ mice (Clement, Aceti et al. 2012). Sleeplessness, irritability and attention deficits could be the consequence of epileptic seizures, which may contribute to cognitive and social deficits observed in children suffering from *SYNGAP1*-related ID. The epileptic seizure could be a result of less inhibition or cases where GABA function is impaired, both of which are observed in *Syngap1*$^{+/-}$ mice, as discussed earlier. Therefore, the next question was to study whether 6BIO restores the seizure threshold to WT levels in P30-80 *Syngap1*$^{+/-}$ mice. Indeed, 6BIO increased seizure threshold for the tonic-clonic grade of seizure in *Syngap1*$^{+/-}$ mice to WT levels (**Figure 3.8**). Thus, 6BIO administration after the critical period of development is effective in correcting seizure threshold, which can reduce the epileptic seizure episodes, or none, observed in *SYNGAP1* patients. The results of all the behaviour experiments are summarised in **Table 4.1**.

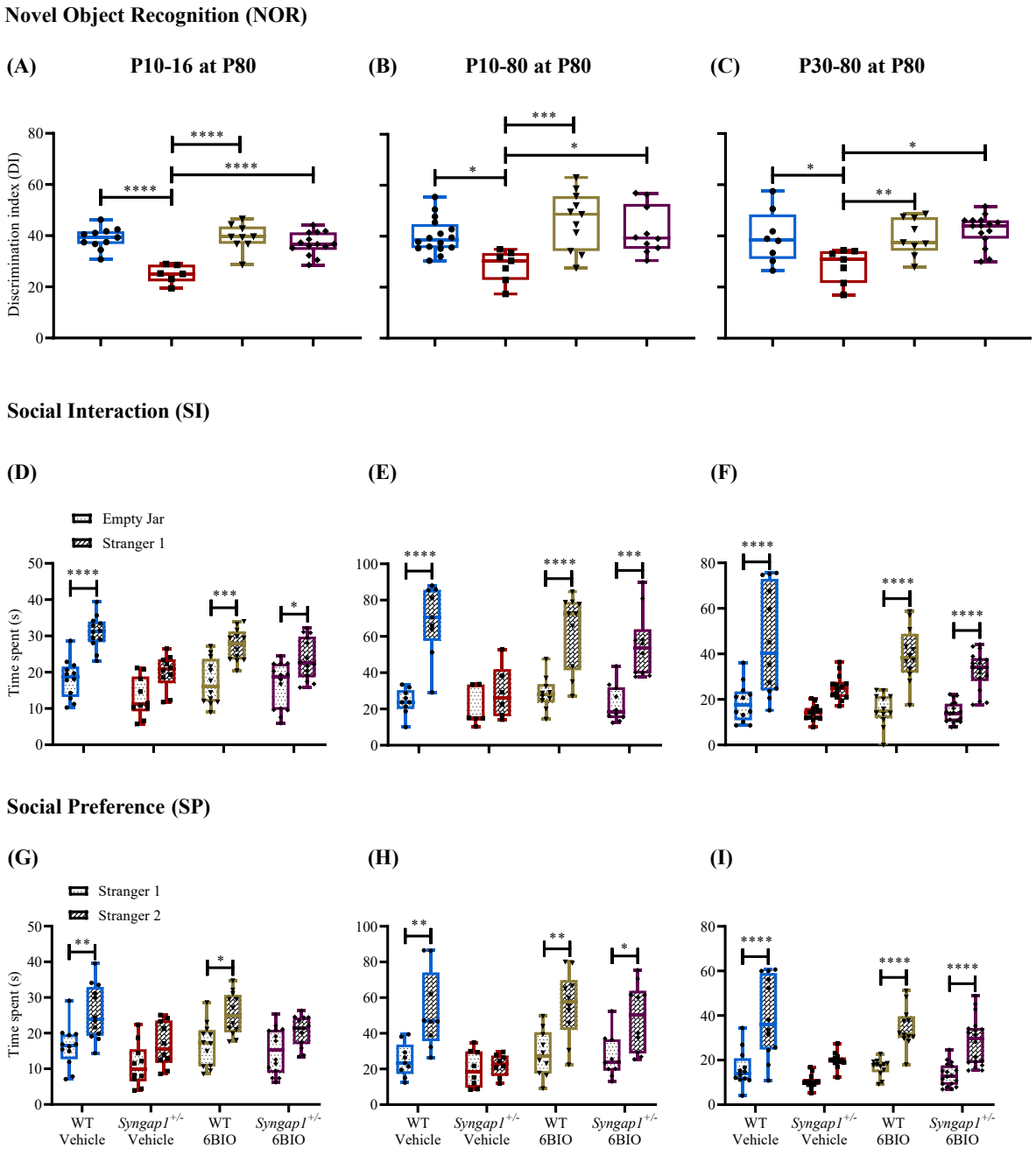

Figure 3.7 6BIO corrects memory recognition and sociability deficits in *Syngap1*$^{+/-}$ particularly in the post-critical period of development:

A) Discrimination index was plotted as the measure of recognition memory and plotted as individual data points for P10-16 where behavior was done at P80, WT–Vehicle: N=11; *Syngap1*$^{+/-}$–Vehicle: N=6; WT–6BIO: N=9; *Syngap1*$^{+/-}$–6BIO: N=14, $F_{(1, 36)} = 14.76$, p=0.0005, **B)** P10-80 where behavior was done at P80, WT–Vehicle: N=16; *Syngap1*$^{+/-}$–Vehicle: N=7; WT–6BIO: N=11; *Syngap1*$^{+/-}$–6BIO: N=10, $F_{(1, 40)} = 1.982$, p=0.1669, and **C)** P30-80 where behavior was done at P80, WT–

Vehicle: N=8; *Syngap1*$^{+/-}$–Vehicle: N=7; WT–6BIO: N=9; *Syngap1*$^{+/-}$–6BIO: N=15, $F_{(1, 35)} = 7.687$, p=0.0089. Social interaction and preference was evaluated as time spent with stranger1 as compared to empty jar, and time spent with stanger2 as compared to stranger1 respectively for **D)** P10-16 where behavior was done at P80, WT–Vehicle: N=12; *Syngap1*$^{+/-}$–Vehicle: N=10; WT–6BIO: N=12; *Syngap1*$^{+/-}$–6BIO: N=14, $F_{(3, 88)} = 1.481$, p=0.2252, **G)** WT–Vehicle: N=12; *Syngap1*$^{+/-}$–Vehicle: N=10; WT–6BIO: N=12; *Syngap1*$^{+/-}$–6BIO: N=14, $F_{(3, 88)} = 0.6549$, p=0.5820, **E)** P10-80 where behavior was done at P80, WT–Vehicle: N=9; *Syngap1*$^{+/-}$–Vehicle: N=6; WT–6BIO: N=10; *Syngap1*$^{+/-}$–6BIO: N=10, $F_{(3, 62)} = 3.722$, p=0.0158, **H)** WT–Vehicle: N=9; *Syngap1*$^{+/-}$–Vehicle: N=8; WT–6BIO: N=10; *Syngap1*$^{+/-}$–6BIO: N=10, $F_{(3, 66)} = 2.692$, p=0.0532, and **F)** P30-80 where behavior was done at P80, N=12; *Syngap1*$^{+/-}$–Vehicle: N=14; WT–6BIO: N=12; *Syngap1*$^{+/-}$–6BIO: N=18, $F_{(3, 104)} = 2.909$, p=0.0381, **I)**, WT–Vehicle: N=12; *Syngap1*$^{+/-}$–Vehicle: N=13; WT–6BIO: N=12; *Syngap1*$^{+/-}$–6BIO: N=18, $F_{(3, 102)} = 2.616$, p=0.0551. Two-way ANOVA, Tukey's multiple comparisons test.

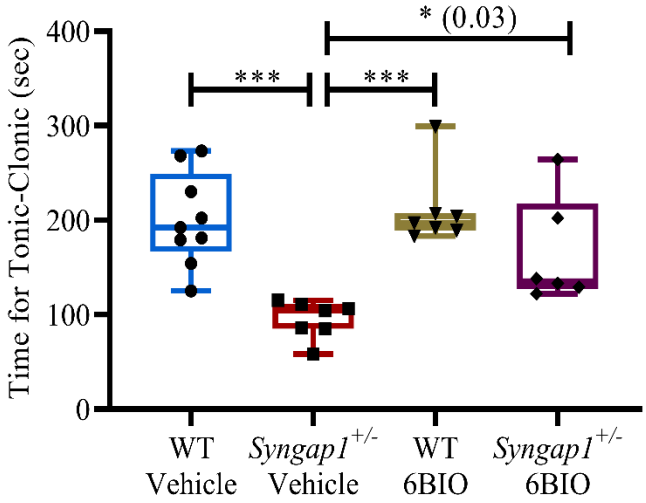

Figure 3.8 6BIO ameliorates seizure threshold in *Syngap1*$^{+/-}$ mice after the critical period of development:

Mice were injected 6BIO from P30-80; thereafter, fluoroethyl-based seizure threshold was evaluated and plotted as grouped data showing individual points for tonic-clonic seizure. 6BIO increased the threshold for tonic-clonic, similar to WT levels, in *Syngap1*$^{+/-}$. $F_{(1,25)}=3.354$, p=0.0790, WT–Vehicle: N=9; *Syngap1*$^{+/-}$–Vehicle: N=7; WT–6BIO: N=7; *Syngap1*$^{+/-}$–6BIO: N=6.

3.2.3.2 6BIO induces a hyperpolarising shift in E_{GABA} and restores LTP in *Syngap1*$^{+/-}$ mutation:

As described earlier, one of the major findings was depolarised neurons observed at P14-15 in *Syngap1*$^{+/-}$ mice, which would have resulted by impaired function of chloride cotransporters responsible for maintaining chloride homeostasis in the brain. Depolarised neurons at P14-15 indicate neurons to be excitatory instead of inhibitory, which is normally observed in age-matched WT mice. Based on the encouraging results of 6BIO restoring the phenotypes, it is necessary to determine whether 6BIO rescues synaptic function, which is fundamental in correcting behaviour in *Syngap1*$^{+/-}$ mice. LTP, a cellular correlate of memory, is disrupted in *Syngap1*$^{+/-}$ mice (Ozkan, Creson et al. 2014). Thus, LTP and E_{Cl^-} was performed to investigate the effect of 6BIO in restoring synaptic function. Based on results obtained earlier in Figure 3.7, we treated mice with 6BIO from P10 to P16, but E_{GABA} was measured at P16, and LTP was measured at P60 as we observed reduced LTP in adults but no change in E_{GABA} in adults.

A gramicidin-perforated patch clamp was performed to measure the E_{GABA}. The results demonstrate that the reversal membrane potential was restored in 6BIO treated *Syngap1*$^{+/-}$ mice (**Figure 3.9**), suggesting that 6BIO ameliorates E_{Cl^-} and thereby rectified increased excitation observed in *Syngap1*$^{+/-}$. Similarly, the next challenge was to investigate whether 6BIO can restore LTP deficits observed in *Syngap1*$^{+/-}$ mice to WT level given that 6BIO is a GSK-3β inhibitor, a potent regulator of memory and plasticity. Remarkably, LTP was rescued in 6BIO treated *Syngap1*$^{+/-}$ mice, particularly after the critical period of development (P10-80: **Figure 3.10 A**; P30-80: **Figure 3.10 B**), correlating with our behaviour results described earlier. Overall, these results suggest small molecules such as 6BIO interventions, particularly after the critical period of development, can correct physiological and behavioural deficits in *Syngap1*$^{+/-}$ mice, indicating an opportunity for novel therapeutics to treat neurodevelopmental disorders, especially for rare disorders such as *SYNGAP1*-related ID.

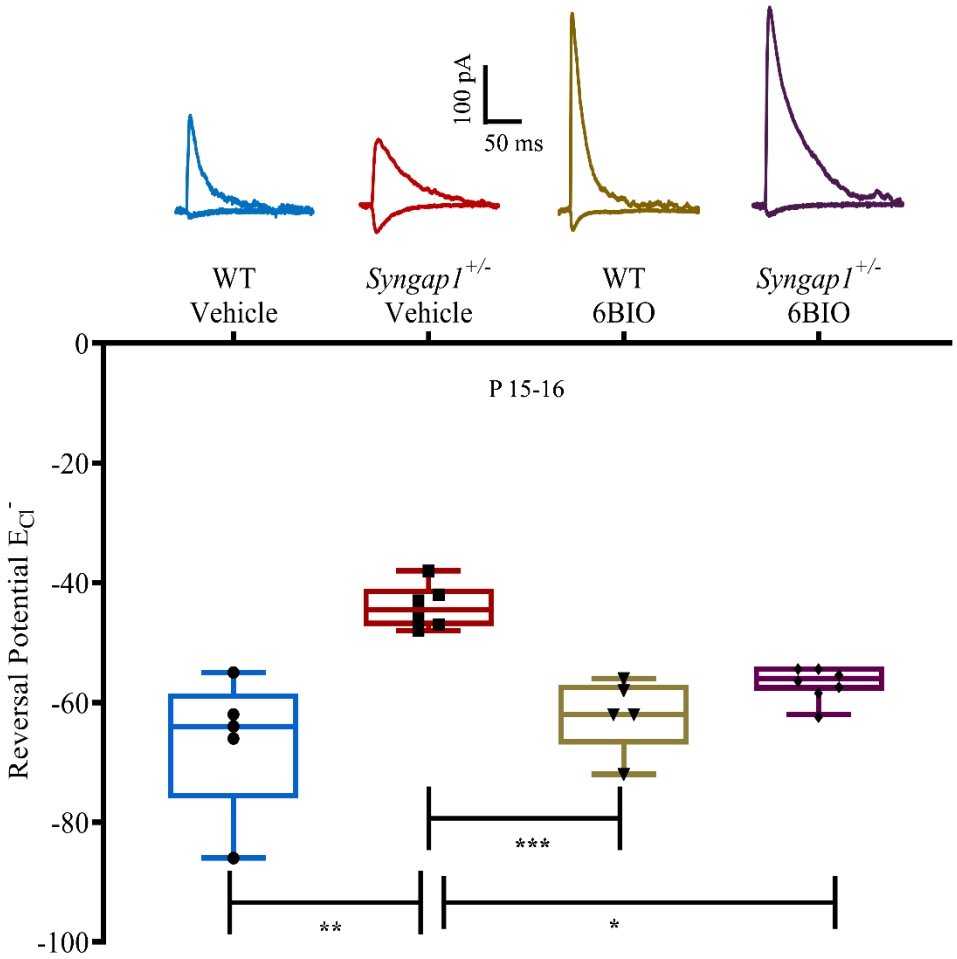

Figure 3.9 6BIO hyperpolarises GABA reversal potential at P15-16 in *Syngap1*$^{+/-}$ mice in the critical period of development:

Grouped data for E_{GABA} estimated from I-V curve from individual WT (Vehicle and 6BIO treated) and *Syngap1*$^{+/-}$ mice (Vehicle and 6BIO treated). WT-Vehicle: N=5, n=5; *Syngap1*$^{+/-}$-Vehicle: N=4, n=6; WT-6BIO: N=3, n=5; *Syngap1*$^{+/-}$-6BIO: N=3, n=7; $F_{(1,19)}$=9.761, p=0.0056. Two-way ANOVA, Tukey's multiple comparisons test.

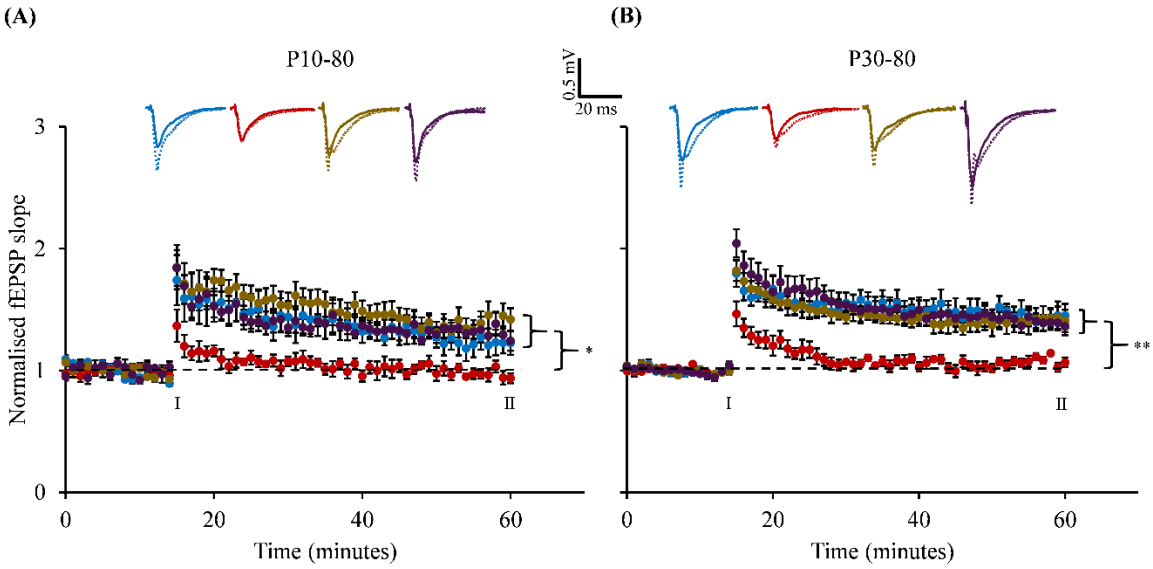

Figure 3.10 6BIO corrects LTP deficits post-critical period of development in *Syngap1*$^{+/-}$ mice: **A)** For Group II, where injections were done from P10-80, WT-Vehicle: N=4, n=8; *Syngap1*$^{+/-}$-Vehicle: N=4, n=7; WT-6BIO: N=4, n=8; *Syngap1*$^{+/-}$-6BIO: N=4, n=6, $F_{(1,25)}$=2.047, p=0.1649 and **B)** Group III, where injections were done from P30-80, WT-Vehicle: N=3, n=6; *Syngap1*$^{+/-}$-Vehicle: N=4, n=6; WT-6BIO: N=5, n=9; *Syngap1*$^{+/-}$-6BIO: N=5, n=9, $F_{(1,26)}$=4.731, p=0.0389, slope of fEPSP was normalised to mean value of 15-minute baseline period and 45-minute post-LTP recordings were performed. Example traces are the average of those recorded in 1-2 min around the time point indicted (I and II). Two-way ANOVA, Tukey's multiple comparisons test.

Chapter- 4 Discussion

Constructing a functional neuronal circuit requires synchronised currents mediated by glutamatergic principal cells and GABAergic interneurons and progressive alterations in molecular components of neurons. The developing brain undergoes several changes for orchestrated output. Any genetic mutations or environmental insults to the developmentally regulated brain activity leads to disruption of brain function over time. ID/ASD is a prime example of neurodevelopmental disorder (NDD) in which alteration of excitation/inhibition is observed. GABAergic system, which is critical for normal neuronal circuit function, is found to be disturbed in many NDDs (Ramamoorthi and Lin 2011, Ozkan, Creson et al. 2014, Rudolph and Mohler 2014, Braat and Kooy 2015). There is a unique opportunity that exists to use GABAR as a key candidate for therapeutic intervention in NDDs.

4.1 GABA-mediated dysfunction at the circuit as well as neuronal levels:

Syngap1 expression peaks around [post-natal day (P)] P7-14 in different regions of the brain, which coincides with the timeline of robust synaptogenesis (McMohan 2012, Porter 2005), consistent with involvement in activity-dependent processes such as LTP, AMPA receptor trafficking (Komiyama et al., 2002; Kim et al., 2003, Yang et al, 2011, Araki Y et al, 2015). SYNGAP1 regulates small GTPases such as RAP, RAS, RAB, which in turn regulates axon outgrowth, dendritic morphology by AMPAR trafficking, which suggests the role of SYNGAP1 in neuronal maturation, distinct from its role at the synapse (Zhu et al, 2002, Krapivinsky et al, 2004, Tomoda et al, 2004, Carlisle et al, 2008, Aceti et al, 2015). Conditional removal of *Syngap1* from forebrain excitatory synapses were sufficient to cause behavioural deficits and several secondary developmental consequences at the circuit level. This developmental dysregulation in cortical circuits leads to reduced critical period plasticity and altered long-range circuit connectivity (Ozkan, 2014, Aceti, 2015).

Systems neuroscience approaches based on distributed neuronal circuits, and brain organizations have recently taken a lot of attention from researchers. *In-vivo* studies where pre-mature expression of KCC2 was mimicked by in-utero electroporation resulted in gross impairment of morphological and functional maturation of neonatal cortical neurons (Laura Cancedda et al, 2007). These dramatic effects could impair the formation and function of neuronal circuits of the mature brain and thus the information processing and overall

behaviour of an individual. Factors affecting the action of early depolarizing GABA are likely to have a profound consequence on the structural and functional development of the mature brain leading to brain disorders such as Autism spectrum disorder.

Based on our results, we consider abnormal activation of neurons to occur upon GABAR activation during developmental stages due to increased NKCC1 levels at P8 and a concomitant increase in KCC2 levels at P8 in *Syngap1*$^{+/-}$ contributing to the increased intrinsic excitability (Clement, Aceti et al. 2012, Kaila, Price et al. 2014), similar to what is reported in Fragile-X- and Rett syndrome (Banerjee, Rikhye et al. 2016), Hinz, Torrella Barrufet et al. (2019). Increased KCC2 expression levels at P8 may further contribute to the intrinsic excitability, as demonstrated by an intriguing interaction with the Na^+-K^+-ATPase pump (Ikeda, Onimaru et al. 2004). Further, disrupted KCC2 expression may compensate for the increase in AMPAR/NMDAR ratio at P14-15, causing increased excitability of the neurons at the developmental stage, which is linked with synaptogenesis through KCC2 interactions with cytoskeletons such as 4.1, and ANKYRIN to regulate AMPAR clustering at the postsynapse (Ikeda, Onimaru et al. 2004, Glykys and Mody 2007, Chamma, Chevy et al. 2012, Clement, Aceti et al. 2012, Chevy, Heubl et al. 2015, Llano, Smirnov et al. 2015).

Besides, the most potent regulators of KCC2 are trophic factors such as BDNF that influence dendritic spine formation and maturation during development (Ludwig, Uvarov et al. 2011, Awad, Amegandjin et al. 2018). Exogenous BDNF has been shown to downregulate KCC2 protein as well as mRNA expression in organotypic and acute hippocampal slices. Additionally, incubation of mature rat hippocampal slices in BDNF reduces the capacity of chloride extrusion, may suggest regulation of KCC2 expression by BDNF-mediated signalling mechanism, which has a profound action on chloride homeostasis (Rivera, Li et al. 2002). In contrast to developing embryonic neurons, BDNF induced an increase in KCC2 expression, suggesting a developmentally controlled regulation of KCC2 expression via BDNF. Further, KCC2 protein upregulation during development in the hippocampus took place even in the absence of BDNF expression *in vivo*, suggesting along with BDNF, other trophic factors aid parallelly for KCC2 expression regulation (Ludwig, Uvarov et al. 2011, Puskarjov, Ahmad et al. 2015). Site-specific *in utero* electroporation of KCC2 cDNA in the hippocampus and somatosensory cortex pyramidal neurons decrease spine density in CA1 neurons whilst increase in cortical neurons, in the region and BDNF dependent manner. Spine dynamics across the hippocampus is mainly mediated by transporter function, whereas,

in the cortex, BDNF plays an important role (Awad, Amegandjin et al. 2018). Consequently, we have observed an irregular expression of *Bdnf* mRNA at PND14-15 in *Syngap1*$^{+/-}$. We speculate that premature elevated expression of *Bdnf* mRNA, potentially caused by aberrant KCC2 expression, may lead to dysregulated GABAergic expression at the synapse resulting in the disarrayed critical period of development as observed in *Syngap1*$^{+/-}$ (Ludwig, Uvarov et al. 2011, Clement, Aceti et al. 2012, Eftekhari, Mehrabi et al. 2014), which needs to be explored to investigate the link between KCC2, SYNGAP1, and BDNF.

We propose that the irregular E_{GABA} and subsequent depolarisation could lead to the disinhibition of GABA. An increase in the mIPSC amplitude at P14-15 (Clement, Aceti et al. 2012) indicating elevated GABA receptor at the postsynapses, thus, compensating for the reduced expression of KCC2 at P14-15. Enhanced excitation through disinhibition is reflected by disrupted network activity mediated by GABA in P8-9 and P14-15, further corroborated by less tonic inhibition in 2-week-old *Syngap1*$^{+/-}$ mice. Less network activity in P14-15 indicates abnormality either in the compensatory effect of increased excitation due to disrupted GABA polarity switch or the decreased expression of KCC2 at the postsynapses in *Syngap1*$^{+/-}$.

4.2 Potent therapeutics for *SYNGAP1* patients with ASD/ID:

"We are all now connected by the internet, like neurons in the giant brain", Stephen Hawking. Keeping in mind today's technology and the artificial intelligence-oriented world, the slightest issue with the internet connection can pause the virtual moving world, which we might have experienced in our daily life too. Similarly, a minor issue in neuronal connections could put a pause to an independent life of an individual, which we have observed in neurodevelopmental disorders such as ASD/ID. With increasing incidence and prevalence of co-morbidities, increased usage of psychiatric drugs is prescribed within the population of ASD/ID.

Two FDA approved drugs, risperidone and aripiprazole, has been shown to alleviate behavioural deficits such as aggression and deliberate self-injuriousness with good efficacy in the ASD population. Antipsychotics, antidepressants, and psychostimulants such as methylphenidate (shown to be effective in reducing ADHD symptoms in about 40% of children with intellectual disability including ASD), dexamfetamine or atomoxetine are frequently used to treat ASD individuals (Masi, DeMayo et al. 2017, Lord, Elsabbagh et al.

2018, Sharma, Gonda et al. 2018). Benzodiazepines and other drugs are used to alleviate sleep disorder symptoms, whose trend has been observed to be increased with time (Broadstock, Doughty et al. 2007, Axmon, Kristensson et al. 2017). Though psychiatric drugs help in alleviating symptoms in ASD, individuals have experienced behavioural toxicity with tricyclic antidepressants, and social withdrawal and irritability with methylphenidate psychotropic medication (Broadstock, Doughty et al. 2007). They are more dependent on prescribed psychotropic medications than on non-psychotropic drugs and much more likely to be exposed to hazardous polypharmacy.

The reported side effects of antipsychotic drugs include significant weight gain and other metabolic effects such as hyperprolactinemia and diabetes mellitus and movement disorders such as tardive dyskinesia, tremor, and dystonia; life-threatening side effects such as rhabdomyolysis, neuroleptic malignant syndrome and seizures have also been reported (Broadstock, Doughty et al. 2007, Murray, Hsia et al. 2014). Briefly, for various comorbidities associated with ASD/ID, different drugs are provided to alleviate the symptoms. Therefore, an individual with ASD/ID might take an average of 15-18 medications based on symptoms. Marita Broadstock and colleagues have discussed the effectiveness of the medications, including risperidone, and yet concluded the need for more reliable strategies, including more placebo trials associated with drugs to the confident assessment of treatment effectiveness, which lacks in most of the compounds tested in ID/ASD (Broadstock, Doughty et al. 2007). Parents are advised to come forward and get tested for the Mullen scale and other initial tests to find out if their child has ASD/ID if delayed milestones/global developmental delay is observed for their children.

Due to various similar comorbidities and genetic forms of global developmental delay or ID, *SYNGAP1* NSID is often get confused by other psychiatric disorders. Hence, genetic sequencing-based confirmation can verify which gene is mutated that causes ID/ASD. Due to lack of awareness and high costs of tests, often treatments for individuals suffering from ASD/ID is either not performed or delayed. Since ASD/ID is a neurodevelopmental disorder and is tightly associated with the critical period of development and plasticity, there is a need to make effective strategies that could enable the remapping of the neuronal connections after this time point.

The advent of exploring the cortical critical period of plasticity started with milestone studies performed using visual and thalamocortical regions of the brain as a model to understand how the occlusion of sensory input impairs the formation, maturation, and elimination of neuronal connections (Hubel 1957, Hubel and Wiesel 1963, Wiesel and Hubel 1963, Wiesel and Hubel 1963, Hubel and Wiesel 1965, Wiesel and Hubel 1965, Wiesel and Hubel 1965, Constantine-Paton 2008). A major factor that regulates the critical period of plasticity during development is the expression of GABA in the neuron. Demonstration of the existence of inhibitory threshold using gene disruption method to prevent the increase of GABA indicated the possibility to use GABA to open critical period of plasticity and, hence, a potential target for therapeutics (Fagiolini and Hensch 2000, Braat and Kooy 2015).

Alteration in the timing of sensitive periods could underlie various neurodevelopmental disorders, including ASD, ID and Schizophrenia (Bavelier, Levi et al. 2010, Baroncelli, Braschi et al. 2011). In all these disorders, one of the common features observed is an imbalance of E/I ratio, which can serve as a key factor to understand the major cause of these disorders, and how manipulating critical period of development, particularly targeting GABAR, would help to resolve the assisted defects. It has been known for decades that maturation of inhibitory cortical circuits in the brain parallels the opening of the critical period of development (Hensch, Fagiolini et al. 1998, Hanover, Huang et al. 1999, Kanold, Kim et al. 2009, Kanold and Luhmann 2010, Southwell, Froemke et al. 2010, Le Magueresse and Monyer 2013, Toyoizumi, Miyamoto et al. 2013).

Using GAD KO mice (Glutamate decarboxylase (GAD): catalyse the decarboxylation reaction of glutamate (excitatory) to GABA (inhibitory in adults), indirectly helping in GABA synthesis) has shown how inhibitory signalling regulates the critical period of development. Gating of the critical period of plasticity is dependent on optimal inhibition during the development, which in turn determines the fate of inhibitory circuits in the brain (Hensch 2005, Duarte, Armstrong et al. 2013, Hubener and Bonhoeffer 2014, Ozkan, Creson et al. 2014, Verma, Paul et al. 2019). Selective pharmacological modulations in GABAergic circuits during development have shown promising results in rescuing several physiological and behavioural deficits in ID/ASD models (Braat and Kooy 2015, Deidda, Allegra et al. 2015, Banerjee, Rikhye et al. 2016, Vlaskamp, Shaw et al. 2019), thus, a key candidate target for the therapeutic intervention.

Restoring the protein level of SYNGAP1 in adult stages reinstated synaptic function (LTP) but not behaviour, suggesting that these neurons are hard-wired during development (Ozkan, Creson et al. 2014). Nevertheless, genetic restoration of *Syngap1* in the adult stages has restored some of the phenotypes, implying that not all deficits related to *Syngap1*$^{+/-}$ can be ascribed to neuronal circuit damage caused by aberrant neurodevelopment (Creson, Rojas et al. 2019). A significant caveat evaluating the efficacy of drugs in pre-clinical models is either the lack of investigation on the effectiveness of drugs after the critical period of development (during hard-wiring) or the inability of the drug to restore the synaptic function after the critical period of development (after hard-wiring) (Vlaskamp, Shaw et al. 2019, McCamphill, Stoppel et al. 2020). Thus, concise therapeutics to correct deficiencies observed in *Syngap1*$^{+/-}$ -mediated ID/ASD is unfounded and provides the platform to find a candidate target for therapeutics that can restore phenotypes after the neurodevelopment period.

It has been recently shown that 6-bromoindirubin-3`-oxime (6BIO) is neuroprotective in an MPTP-based mouse model of Parkinson's disease, suggesting the potency to cross the blood-brain barrier and inhibit GSK-3β in neurons (Suresh, Chavalmane et al. 2017). In a preliminary study, mice were administered 50mg/kg of 6BIO by oral gavage, and pharmacokinetic parameters of 6BIO were determined in blood plasma. The mean maximum concentration (C_{max}) was 118.2 ± 58.7 ng/ml, the half-life time ($t_{1/2}$) was 0.72±0.09-hour as the plasma concentration of 6BIO decreased rapidly and was eliminated from plasma. The low bioavailability could be attributed to the low solubility of 6BIO. The rapid decline of plasma concentrations of 6BIO, however, suggests its rapid distribution to other tissues. This could further assist in the clearance and metabolism mechanism of 6BIO when administered for preclinical and clinical studies (Tchoumtchoua, Halabalaki et al. 2019).

In an *in-silico* study, Absorption, distribution, metabolism, excretion and toxicity (ADMET) parameters and docking for 6BIO was studied. From docking parameters, the binding energy is derived, which represents the docking affinity of a receptor to its ligand. Low binding energy suggests better binding. The binding energy of 6BIO was -9.2 kcal/mol. The computational blood-brain barrier permeability of 6BIO was pretty high. Caco-2 and HIA value, which denotes intestinal absorption, was also high. MDCK component, which predicts the renal clearance, was close to the control group. The PBP, which predicts the molecule stay in the system and its clearance, was best and close to control groups. 6BIO was tested negative for AMES test for mutagenesis and carcinogenicity. $LD_{50,}$ which is a measure for

lethal dose required to cause the death of 50% of the test population of the organism, was highest for 6BIO, which suggest a very high dose would be considered as lethal (Nisha, Kumar et al. 2016).

Activation of NMDAR leads to phosphorylation of CaMKII, thus SYNGAP1 phosphorylation, which activates RAS and RAC GTPases. Increased RAS activity would activate ERK, which further helps in AMPAR trafficking to post synapse (Carlisle, Manzerra et al. 2008, Araki, Zeng et al. 2015). NMDAR-mediated inhibition of ERK leads to activation of Rheb, which in turn activates mTOR leading to AMPAR trafficking to post synapse (Wang, Held et al. 2013). SYNGAP1 via RAC1 and LIMK leads to ACTIN polymerization, which ultimately leads to synaptic plasticity (Carlisle, Manzerra et al. 2008, Araki, Zeng et al. 2015). BDNF via MEK/ERK1/2 pathway regulates transcription of the *Kcc2* gene (Medina, Friedel et al. 2014). BDNF via PI3K/AKT pathway is involved in plasticity. PI3K/AKT pathway also regulates phosphorylation of GSK-3β and, in turn, helps in neuronal function and plasticity (Kitagishi, Kobayashi et al. 2012). KCC2 with βPIX and via RAC1, LIMK, and COFILIN regulates AMPAR trafficking to post-synapse (Chevy, Heubl et al. 2015). All these above-mentioned pathways have their identity, and their ultimate function is synaptic plasticity. Hence, PI3K/AKT, MEK/ERK1/2 and mTOR could serve as the targets for GSK-3β in *SYNGAP1*-related ASD/ID. However, more studies are required to ascertain the molecular mechanisms involved in the action of 6BIO via GSK-3β inhibition in *SYNGAP1*-related ASD/ID.

KCC2 expression was shown to be decreased in cerebrospinal fluid of Rett syndrome patients, highlighting the possibility of involvement of KCC2 in its pathophysiology (Duarte, Armstrong et al. 2013). 6BIO, along with KCC2 expression-enhancing compounds (KEECs), was shown to increase expression of KCC2 in neurons and rescue electrophysiological and morphological abnormalities of *RTT* neurons (Tang, Drotar et al. 2019). This opens up the possibility of the use of 6BIO as a therapeutic agent in neurological disorders involving dysregulation of KCC2. Our study has also shown dysregulation of KCC2 during development in *Syngap1*$^{+/-}$ mice.

6BIO was intraperitoneally (IP) treated for three age groups of mice (WT, *Syngap1*$^{+/-}$). Group, I include age P10-16 corresponding to the critical period of development, Group II include age P10-80 corresponding to the critical period of development as well as young

adults, and Group III include age P30-80 corresponding to young adults of mice. 6BIO administration in P30-80 (group III) has substantially restored functional (LTP, E_{GABA} (P16)) and behavioural deficits (sociability, memory, and anxiety) in *Syngap1*$^{+/-}$ mice. However, hyperactivity was not corrected after the neurodevelopmental period suggesting that the target period is during the critical period of development. It appears that social isolation, social preference, and seizure threshold were not impacted by the hard-wiring of the neuronal circuit during development as it is corrected in all three strategies, except in group I for SP. Primarily, we demonstrate that administration of 6BIO corrected memory deficits in all therapeutic strategies, particularly after the neurodevelopmental period. All the behaviour result is compiled in **Table 4.1** presented as a summary.

These results are extremely encouraging as the administration of 6BIO after the neurodevelopmental period amended not only most of the phenotypes evaluated but also the synaptic functions. These results further emphasize the regime for therapeutic intervention should target the developmental period to protect the brain from hard-wired circuit damage and to maximise the correction of phenotype. Our results suggest a general mechanism involving GABAergic signalling prevailing in several neurodevelopmental disorders that can be corrected by 6BIO. In conclusion, our study supports the possibility that cognitive, emotional, and social symptoms that result from hard-wired neuronal circuit damage during development may still be corrected by late pharmacological intervention in adulthood.

4.3 Model and Summary:

Based on our results, we propose a model that demonstrates the potential link between impaired expression of Cl^- co-transporters, particularly KCC2, and that of AMPAR expression (based on other studies) and synaptic function. Our model proposes that because of a pleiotropic effect of *Syngap1*$^{+/-}$, KCC2 is incapable of extruding Cl^- from neurons at P14-16. This altered function of KCC2 may lead to impaired GABA polarity switch, E_{Cl^-} that may disrupt intrinsic properties of the cell at P14-15 in *Syngap1*$^{+/-}$. Besides, altered KCC2 expression affects GABA activity that might result in GABAergic disinhibition leading to increased excitable neurons at P14-15 in *Syngap1*$^{+/-}$. Thus, our study suggests a potentially important neuronal developmental disruption in maintaining Cl^- homeostasis due to altered polarity switch of GABA, resulting in a pleiotropic effect on synapse function and development, which can be corrected by administration of 6BIO in *Syngap1*$^{+/-}$ mice (**Table 4.1**).

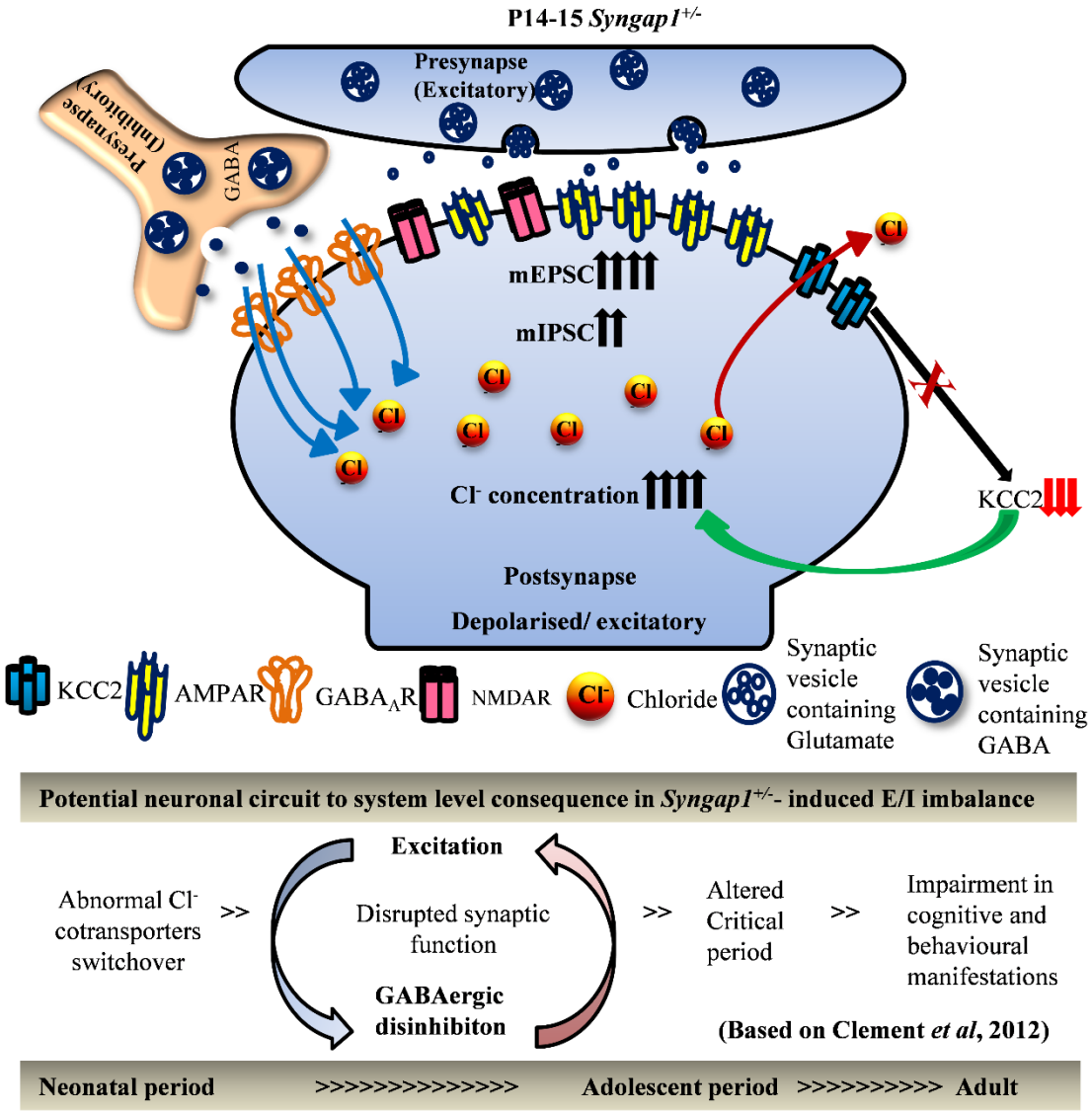

Figure 4.1 Model illustrates the potential impact of altered expression and function of Cl^- co-transporters on synaptic function in *Syngap1*$^{+/-}$

The model demonstrates the potential link between impaired expression of Cl^- co-transporters, particularly KCC2, and to that of AMPAR expression (based on other studies) and synaptic function. Our model proposes that as a result of a pleiotropic effect of *Syngap1*$^{+/-}$, KCC2 is incapable of extruding Cl^- from neurons at P14-16. This altered function of KCC2 may lead to impaired GABA polarity switch, E_{Cl-} that may disrupt intrinsic properties of the cell at P14-15 in *Syngap1*$^{+/-}$. Besides, altered KCC2 expression affects GABA activity that might result in GABAergic disinhibition leading to increased excitable neurons at P14-15 in *Syngap1*$^{+/-}$. Thus, our study suggests a potentially important neuronal developmental disruption in maintaining Cl^- homeostasis due to altered polarity switch of GABA, resulting in a pleiotropic effect on synapse function and development, which can be corrected by administration of 6BIO in *Syngap1*$^{+/-}$.

Table 4.1 Summary of the behaviour experiments performed where *Syngap1*$^{+/-}$ mice were administered with 6BIO:

Administration of 6BIO restores synaptic and behavioural deficits observed in *Syngap1*$^{+/-}$ mice summarised in the tabular format.

Experiment/Injection regime	P10-16 (Recording or behaviour was done at P16)	P10-16 (Behaviour was done at P80)	P10-80 (Behaviour or recording was done at P42/80)	P30-80 (Behaviour or recording was done at P80)
Open Field test (Motor)	Corrected	Partially corrected	Partially corrected	Not corrected
Open Field test (Anxiety)	Corrected	Corrected	Partially corrected	Partially corrected
Novel object recognition	-	Corrected	Corrected	Corrected
Social Interaction	-	Corrected	Corrected	Corrected
Social preference	-	Not corrected	Corrected	Corrected
Seizure threshold	-	-	-	Corrected
Long term potentiation	-	-	Corrected	Corrected
E_{GABA}, Cl^- reversal potential	Corrected	-	-	-

Future directions:

- Restoring SYNGAP1 levels in postnatal stages in *Syngap1*$^{+/-}$ mice have shown a positive hope for the future but is associated with their limitations (Creson, Rojas et al. 2019). Thus, there is a need to explore other proteins which are indirectly associated with SYNGAP1 but have a vital role in neuronal function and survival like SYNGAP1. Braat and Kooy have shown the GABA receptor (function is regulated by KCC2 and NKCC1) as a promising therapeutic candidate for ASD/ID in future (Braat and Kooy 2015). We have observed decreased protein expression levels of KCC2 in *Syngap1*$^{+/-}$ mice and no change in mRNA levels at P14-15. This could be either due to some molecule in signalling pathway inhibiting signal which facilitates the surface expression of KCC2 or distorted oligomerization of KCC2 by which it is becoming non-functional. In either case, there is a need for evaluating protein expression levels by native gel which would give exact oligomeric and monomeric expression levels of KCC2. Additionally, surface expression of KCC2 by tagging and extracting plasma membrane would tell us whether trafficking of KCC2 is fine because it's related to AMPAR trafficking too which is found to be dysregulated in *Syngap1*$^{+/-}$ mice. Once, we will answer these questions we could check if the application of the KCC2 agonist could restore the pathophysiological and behavioural deficits observed in *Syngap1*$^{+/-}$ mice. After checking *in-vitro*, if promising results are observed, then the study could be proceeded by re-expression of KCC2b in *Syngap1*$^{+/-}$ mice by Cre-lox recombination system and checking of phenotypes and function.

- The compound 6BIO was not water-soluble and was injected intraperitoneally into mice every day which may not be a good option to treat children with ASD/ID. There is a need for the water-soluble and oral derivative of 6BIO which could ease the application.

- 6BIO a GSK-3β inhibitor was used to check the therapeutic efficacy to restore synaptic, cognitive, and behavioural deficits in *Syngap1*$^{+/-}$ mice. We decided on one paradigm of 6BIO injection and performed a battery of functional and behavioural experiments. The signalling pathway involved in the mechanism of action of 6BIO was not explored. There is a need to check expression levels of pGSK-3β and total GSK-3β in *Syngap1*$^{+/-}$

mice. Additionally, KCC2 expression levels could also be checked at P14-15 after the 6BIO application. SYNGAP1 via ERK helps in AMPAR trafficking and via RAC1 and LIMK, ACTIN polymerization, which ultimately leads to synaptic plasticity. BDNF via MEK/ERK1/2 pathway regulates transcription of the *Kcc2* gene. KCC2 with βPIX and via RAC1, LIMK, and COFILIN regulates AMPAR trafficking to post-synapse. BDNF via PI3K/AKT pathway is involved in plasticity. PI3K/AKT pathway also regulates phosphorylation of GSK-3β and in turn, helps in neuronal function and plasticity. All these above-mentioned pathways have their identity, and their ultimate function is synaptic plasticity. There is a need to connect these pathways to understand the function and regulation of 6BIO in *Syngap1*$^{+/-}$ mice.

- We have used 5mg/kg of 6BIO for all the age groups considered for the study. When 6BIO was administered from P10-16 (critical period of development only) and behaviour was performed at P16, anxiety and hyperactivity was corrected, but when the same behaviour was tested at P80, hyperactivity was partially corrected. When 6BIO was administered from P10-80 anxiety and hyperactivity was partially corrected. In the social preference case, 6BIO corrected the deficit when administrated from P10-80, but not when administered from P10-16 (critical period). If 6BIO administration in the critical period only is not able to correct the deficit then how same deficit is getting corrected when administered from the critical period to adulthood or vice versa for locomotion and anxiety test? We could increase the dosage in adulthood and check if that is helping. Addressing this question would help in determining the optimum dosage for 6BIO with increased efficiency.

- A filopodium to higher-order spine structure transition is often associated with functional remapping of sensory circuits in response to experiences. In the current study, we know that administration of 6BIO corrected several behaviours in the critical period as well as adolescent stages of development in *Syngap1*$^{+/-}$ mice. Based on the reversal potential data, it is evident that the reversal potential of chloride from depolarized to a hyperpolarized state is closer to the resting membrane potential. However, to answer whether the observed changes are occurring through the remapping of synaptic connections is yet to be explored. Whisker trimming experiments would be able to reliably demonstrate remapping on the administration of 6BIO in *Syngap1*$^{+/-}$ mice or

simple Golgi-cox staining of sections from the vehicle and 6BIO treated groups. It could give the comparative idea of remapping of synaptic connection based on the percentage of type of spine structure present as done by Aceti et al (Aceti, Creson et al. 2015).

- The mouse model used to study the current study is made in such a way (discussed in materials and methods of the study) that it fulfils face and construct validity. In preclinical studies, scientists have tried to put forth the mechanisms and drugs which can alleviate the symptoms yet not correct ID/ASD, especially when administered in adulthood. One reason could be the use of a mouse model which is not humanised. The humanised mouse model of *SYNGAP1* haploinsufficiency may provide us with a better understanding of the basic mechanism and targeted drug delivery for the concerned disorder.

- Advancement in technology has provided various model systems (rodents, primates, invertebrates, etc.) to study basic science, diseases, and disorders. Even though the results from the study would be fascinating but, the common question that prevails to date is how accurately data from these models can correlate to humans (as the model to study is different than human, hence different biology)? Induced pluripotent stem cells (iPSCs) has provided the opportunity for the generation of personalized human cells including neurons, thus easing the task of modelling neurological disorders which could be directly correlated to humans (Pinto, Pagnamenta et al. 2010, Marchese, Valvo et al. 2016). Up until now, the information provided on *SYNGAP1* mediated ASD/ID are from *Syngap1*$^{+/-}$ mice or cell culture-based models, hence provide a dire need to develop a model which can be directly correlated to human in a more affirmative way avoiding ethical and religious concerns. Recently, a study from Gavin Rumbaugh's group has shown how *SYNGAP1* loss of function impacts the development and function of human neurons in the hiPSC system (Llamosas, Arora et al. 2020). Thus, these human iPSCs provide a platform to test 6BIO before rodent or clinical trials. This may enable more accurate efficacy of 6BIO or any other potential drug.

References:

1. Abdala, A. P., M. Dutschmann, J. M. Bissonnette and J. F. Paton (2010). "Correction of respiratory disorders in a mouse model of Rett syndrome." Proceedings of the National Academy of Sciences: 201012104.
2. Aceti, M., T. K. Creson, T. Vaissiere, C. Rojas, W. C. Huang, Y. X. Wang, R. S. Petralia, D. T. Page, C. A. Miller and G. Rumbaugh (2015). "Syngap1 haploinsufficiency damages a postnatal critical period of pyramidal cell structural maturation linked to cortical circuit assembly." Biol Psychiatry **77**(9): 805-815.
3. Agarwal, M., M. V. Johnston and C. E. Stafstrom (2019). "SYNGAP1 mutations: Clinical, genetic, and pathophysiological features." Int J Dev Neurosci **78**: 65-76.
4. Amaral, D. G. and M. P. Witter (1989). "The three-dimensional organization of the hippocampal formation: a review of anatomical data." Neuroscience **31**(3): 571-591.
5. Anazi, S., S. Maddirevula, V. Salpietro, Y. T. Asi, S. Alsahli, A. Alhashem, H. E. Shamseldin, F. AlZahrani, N. Patel, N. Ibrahim, F. M. Abdulwahab, M. Hashem, N. Alhashmi, F. Al Murshedi, A. Al Kindy, A. Alshaer, A. Rumayyan, S. Al Tala, W. Kurdi, A. Alsaman, A. Alasmari, S. Banu, T. Sultan, M. M. Saleh, H. Alkuraya, M. A. Salih, H. Aldhalaan, T. Ben-Omran, F. Al Musafri, R. Ali, J. Suleiman, B. Tabarki, A. W. El-Hattab, C. Bupp, M. Alfadhel, N. Al Tassan, D. Monies, S. T. Arold, M. Abouelhoda, T. Lashley, H. Houlden, E. Faqeih and F. S. Alkuraya (2017). "Expanding the genetic heterogeneity of intellectual disability." Hum Genet **136**(11-12): 1419-1429.
6. Andersen, P., T. V. Bliss, T. Lomo, L. I. Olsen and K. K. Skrede (1969). "Lamellar organization of hippocampal excitatory pathways." Acta Physiol Scand **76**(1): 4A-5A.
7. Araki, Y., M. Zeng, M. Zhang and R. L. Huganir (2015). "Rapid dispersion of SynGAP from synaptic spines triggers AMPA receptor insertion and spine enlargement during LTP." Neuron **85**(1): 173-189.
8. Asiminas, A., A. D. Jackson, S. R. Louros, S. M. Till, T. Spano, O. Dando, M. F. Bear, S. Chattarji, G. E. Hardingham, E. K. Osterweil, D. J. A. Wyllie, E. R. Wood

and P. C. Kind (2019). "Sustained correction of associative learning deficits after brief, early treatment in a rat model of Fragile X Syndrome." Sci Transl Med **11**(494).

9. Awad, P. N., C. A. Amegandjin, J. Szczurkowska, J. N. Carrico, A. S. Fernandes do Nascimento, E. Baho, B. Chattopadhyaya, L. Cancedda, L. Carmant and G. Di Cristo (2018). "KCC2 Regulates Dendritic Spine Formation in a Brain-Region Specific and BDNF Dependent Manner." Cereb Cortex **28**(11): 4049-4062.
10. Axmon, A., J. Kristensson, G. Ahlstrom and P. Midlov (2017). "Use of antipsychotics, benzodiazepine derivatives, and dementia medication among older people with intellectual disability and/or autism spectrum disorder and dementia." Res Dev Disabil **62**: 50-57.
11. Azevedo, F. A., L. R. Carvalho, L. T. Grinberg, J. M. Farfel, R. E. Ferretti, R. E. Leite, W. Jacob Filho, R. Lent and S. Herculano-Houzel (2009). "Equal numbers of neuronal and nonneuronal cells make the human brain an isometrically scaled-up primate brain." J Comp Neurol **513**(5): 532-541.
12. Baldi, R., C. Varga and G. Tamas (2010). "Differential distribution of KCC2 along the axo-somato-dendritic axis of hippocampal principal cells." Eur J Neurosci **32**(8): 1319-1325.
13. Banerjee, A., R. V. Rikhye, V. Breton-Provencher, X. Tang, C. Li, K. Li, C. A. Runyan, Z. Fu, R. Jaenisch and M. Sur (2016). "Jointly reduced inhibition and excitation underlies circuit-wide changes in cortical processing in Rett syndrome." Proc Natl Acad Sci U S A **113**(46): E7287-E7296.
14. Barnes, S. A., L. S. Wijetunge, A. D. Jackson, D. Katsanevaki, E. K. Osterweil, N. H. Komiyama, S. G. Grant, M. F. Bear, U. V. Nagerl, P. C. Kind and D. J. Wyllie (2015). "Convergence of Hippocampal Pathophysiology in Syngap+/- and Fmr1-/y Mice." J Neurosci **35**(45): 15073-15081.
15. Baroncelli, L., C. Braschi, M. Spolidoro, T. Begenisic, L. Maffei and A. Sale (2011). "Brain plasticity and disease: a matter of inhibition." Neural Plast **2011**: 286073.
16. Bartho, P., C. Curto, A. Luczak, S. L. Marguet and K. D. Harris (2009). "Population coding of tone stimuli in auditory cortex: dynamic rate vector analysis." Eur J Neurosci **30**(9): 1767-1778.
17. Bavelier, D., D. M. Levi, R. W. Li, Y. Dan and T. K. Hensch (2010). "Removing brakes on adult brain plasticity: from molecular to behavioral interventions." J Neurosci **30**(45): 14964-14971.

18. Bear, M. F., K. M. Huber and S. T. Warren (2004). "The mGluR theory of fragile X mental retardation." Trends Neurosci **27**(7): 370-377.
19. Ben-Ari, Y. (2002). "Excitatory actions of gaba during development: the nature of the nurture." Nat Rev Neurosci **3**(9): 728-739.
20. Ben-Ari, Y. (2014). "The GABA excitatory/inhibitory developmental sequence: a personal journey." Neuroscience **279**: 187-219.
21. Ben-Ari, Y., E. Cherubini, R. Corradetti and J. L. Gaiarsa (1989). "Giant synaptic potentials in immature rat CA3 hippocampal neurones." J Physiol **416**: 303-325.
22. Ben-Ari, Y., J. L. Gaiarsa, R. Tyzio and R. Khazipov (2007). "GABA: a pioneer transmitter that excites immature neurons and generates primitive oscillations." Physiol Rev **87**(4): 1215-1284.
23. Ben-Ari, Y., I. Khalilov, K. T. Kahle and E. Cherubini (2012). "The GABA excitatory/inhibitory shift in brain maturation and neurological disorders." Neuroscientist **18**(5): 467-486.
24. Berry-Kravis, E. M., L. Lindemann, A. E. Jonch, G. Apostol, M. F. Bear, R. L. Carpenter, J. N. Crawley, A. Curie, V. Des Portes, F. Hossain, F. Gasparini, B. Gomez-Mancilla, D. Hessl, E. Loth, S. H. Scharf, P. P. Wang, F. Von Raison, R. Hagerman, W. Spooren and S. Jacquemont (2018). "Drug development for neurodevelopmental disorders: lessons learned from fragile X syndrome." Nat Rev Drug Discov **17**(4): 280-299.
25. Berryer, M. H., B. Chattopadhyaya, P. Xing, I. Riebe, C. Bosoi, N. Sanon, J. Antoine-Bertrand, M. Levesque, M. Avoli, F. F. Hamdan, L. Carmant, N. Lamarche-Vane, J. C. Lacaille, J. L. Michaud and G. Di Cristo (2016). "Decrease of SYNGAP1 in GABAergic cells impairs inhibitory synapse connectivity, synaptic inhibition and cognitive function." Nat Commun **7**: 13340.
26. Berryer, M. H., F. F. Hamdan, L. L. Klitten, R. S. Moller, L. Carmant, J. Schwartzentruber, L. Patry, S. Dobrzeniecka, D. Rochefort, M. Neugnot-Cerioli, J. C. Lacaille, Z. Niu, C. M. Eng, Y. Yang, S. Palardy, C. Belhumeur, G. A. Rouleau, N. Tommerup, L. Immken, M. H. Beauchamp, G. S. Patel, J. Majewski, M. A. Tarnopolsky, K. Scheffzek, H. Hjalgrim, J. L. Michaud and G. Di Cristo (2013). "Mutations in SYNGAP1 cause intellectual disability, autism, and a specific form of epilepsy by inducing haploinsufficiency." Hum Mutat **34**(2): 385-394.
27. Beurel, E. and R. S. Jope (2008). "Differential regulation of STAT family members by glycogen synthase kinase-3." J Biol Chem **283**(32): 21934-21944.

28. Blaesse, P., M. S. Airaksinen, C. Rivera and K. Kaila (2009). "Cation-chloride cotransporters and neuronal function." Neuron **61**(6): 820-838.
29. Blaesse, P., I. Guillemin, J. Schindler, M. Schweizer, E. Delpire, L. Khiroug, E. Friauf and H. G. Nothwang (2006). "Oligomerization of KCC2 correlates with development of inhibitory neurotransmission." J Neurosci **26**(41): 10407-10419.
30. Bliss, T. V. and G. L. Collingridge (1993). "A synaptic model of memory: long-term potentiation in the hippocampus." Nature **361**(6407): 31-39.
31. Bliss, T. V. and T. Lomo (1973). "Long-lasting potentiation of synaptic transmission in the dentate area of the anaesthetized rabbit following stimulation of the perforant path." J Physiol **232**(2): 331-356.
32. Blue, M. E., W. E. Kaufmann, J. Bressler, C. Eyring, C. O'driscoll, S. Naidu and M. V. Johnston (2011). "Temporal and regional alterations in NMDA receptor expression in Mecp2-null mice." The Anatomical Record **294**(10): 1624-1634.
33. Boda, B., A. Dubos and D. Muller (2010). "Signaling mechanisms regulating synapse formation and function in mental retardation." Curr Opin Neurobiol **20**(4): 519-527.
34. Booth, C. A., J. T. Brown and A. D. Randall (2014). "Neurophysiological modification of CA1 pyramidal neurons in a transgenic mouse expressing a truncated form of disrupted-in-schizophrenia 1." Eur J Neurosci **39**(7): 1074-1090.
35. Bozdagi, O., T. Sakurai, D. Papapetrou, X. Wang, D. L. Dickstein, N. Takahashi, Y. Kajiwara, M. Yang, A. M. Katz, M. L. Scattoni, M. J. Harris, R. Saxena, J. L. Silverman, J. N. Crawley, Q. Zhou, P. R. Hof and J. D. Buxbaum (2010). "Haploinsufficiency of the autism-associated Shank3 gene leads to deficits in synaptic function, social interaction, and social communication." Mol Autism **1**(1): 15.
36. Braat, S. and R. F. Kooy (2015). "The GABAA Receptor as a Therapeutic Target for Neurodevelopmental Disorders." Neuron **86**(5): 1119-1130.
37. Brickley, S. G. and I. Mody (2012). "Extrasynaptic GABA(A) receptors: their function in the CNS and implications for disease." Neuron **73**(1): 23-34.
38. Broadstock, M., C. Doughty and M. Eggleston (2007). "Systematic review of the effectiveness of pharmacological treatments for adolescents and adults with autism spectrum disorder." Autism **11**(4): 335-348.
39. Caraiscos, V. B., E. M. Elliott, K. E. You-Ten, V. Y. Cheng, D. Belelli, J. G. Newell, M. F. Jackson, J. J. Lambert, T. W. Rosahl, K. A. Wafford, J. F. MacDonald and B. A. Orser (2004). "Tonic inhibition in mouse hippocampal CA1 pyramidal neurons is

mediated by alpha5 subunit-containing gamma-aminobutyric acid type A receptors." Proc Natl Acad Sci U S A **101**(10): 3662-3667.

40. Carlisle, H. J., P. Manzerra, E. Marcora and M. B. Kennedy (2008). "SynGAP regulates steady-state and activity-dependent phosphorylation of cofilin." J Neurosci **28**(50): 13673-13683.
41. Carouge, D., L. Host, D. Aunis, J. Zwiller and P. Anglard (2010). "CDKL5 is a brain MeCP2 target gene regulated by DNA methylation." Neurobiology of disease **38**(3): 414-424.
42. Carvill, G. L., S. B. Heavin, S. C. Yendle, J. M. McMahon, B. J. O'Roak, J. Cook, A. Khan, M. O. Dorschner, M. Weaver, S. Calvert, S. Malone, G. Wallace, T. Stanley, A. M. Bye, A. Bleasel, K. B. Howell, S. Kivity, M. T. Mackay, V. Rodriguez-Casero, R. Webster, A. Korczyn, Z. Afawi, N. Zelnick, T. Lerman-Sagie, D. Lev, R. S. Moller, D. Gill, D. M. Andrade, J. L. Freeman, L. G. Sadleir, J. Shendure, S. F. Berkovic, I. E. Scheffer and H. C. Mefford (2013). "Targeted resequencing in epileptic encephalopathies identifies de novo mutations in CHD2 and SYNGAP1." Nat Genet **45**(7): 825-830.
43. Casula, S., B. E. Shmukler, S. Wilhelm, A. K. Stuart-Tilley, W. Su, M. N. Chernova, C. Brugnara and S. L. Alper (2001). "A dominant negative mutant of the KCC1 K-Cl cotransporter: both N- and C-terminal cytoplasmic domains are required for K-Cl cotransport activity." J Biol Chem **276**(45): 41870-41878.
44. Cellot, G. and E. Cherubini (2014). "GABAergic signaling as therapeutic target for autism spectrum disorders." Front Pediatr **2**: 70.
45. Chakraborty, R., M. J. Vijay Kumar and J. P. Clement (2021). "Critical aspects of neurodevelopment." Neurobiol Learn Mem **180**: 107415.
46. Chamma, I., Q. Chevy, J. C. Poncer and S. Levi (2012). "Role of the neuronal K-Cl co-transporter KCC2 in inhibitory and excitatory neurotransmission." Front Cell Neurosci **6**: 5.
47. Chechlacz, M. and J. G. Gleeson (2003). "Is mental retardation a defect of synapse structure and function?" Pediatr Neurol **29**(1): 11-17.
48. Chelly, J., M. Khelfaoui, F. Francis, B. Cherif and T. Bienvenu (2006). "Genetics and pathophysiology of mental retardation." Eur J Hum Genet **14**(6): 701-713.
49. Chen, H. J., M. Rojas-Soto, A. Oguni and M. B. Kennedy (1998). "A synaptic Ras-GTPase activating protein (p135 SynGAP) inhibited by CaM kinase II." Neuron **20**(5): 895-904.

50. Chevy, Q., M. Heubl, M. Goutierre, S. Backer, I. Moutkine, E. Eugene, E. Bloch-Gallego, S. Levi and J. C. Poncer (2015). "KCC2 Gates Activity-Driven AMPA Receptor Traffic through Cofilin Phosphorylation." J Neurosci **35**(48): 15772-15786.
51. Chilian, B., H. Abdollahpour, T. Bierhals, I. Haltrich, G. Fekete, I. Nagel, G. Rosenberger and K. Kutsche (2013). "Dysfunction of SHANK2 and CHRNA7 in a patient with intellectual disability and language impairment supports genetic epistasis of the two loci." Clin Genet **84**(6): 560-565.
52. Clement, J. P., M. Aceti, T. K. Creson, E. D. Ozkan, Y. Shi, N. J. Reish, A. G. Almonte, B. H. Miller, B. J. Wiltgen, C. A. Miller, X. Xu and G. Rumbaugh (2012). "Pathogenic SYNGAP1 mutations impair cognitive development by disrupting maturation of dendritic spine synapses." Cell **151**(4): 709-723.
53. Clement, J. P., E. D. Ozkan, M. Aceti, C. A. Miller and G. Rumbaugh (2013). "SYNGAP1 links the maturation rate of excitatory synapses to the duration of critical-period synaptic plasticity." J Neurosci **33**(25): 10447-10452.
54. Constantine-Paton, M. (2008). "Pioneers of cortical plasticity: six classic papers by Wiesel and Hubel." J Neurophysiol **99**(6): 2741-2744.
55. Cook, E. H., J. T. Masaki, S. J. Guter and F. Najjar (2019). "Lovastatin Treatment of a Patient with a De Novo SYNGAP1 Protein Truncating Variant." J Child Adolesc Psychopharmacol **29**(4): 321-322.
56. Creson, T. K., C. Rojas, E. Hwaun, T. Vaissiere, M. Kilinc, A. Jimenez-Gomez, J. L. Holder, Jr., J. Tang, L. L. Colgin, C. A. Miller and G. Rumbaugh (2019). "Re-expression of SynGAP protein in adulthood improves translatable measures of brain function and behavior." Elife **8**.
57. Culbert, A. A., M. J. Brown, S. Frame, T. Hagen, D. A. Cross, B. Bax and A. D. Reith (2001). "GSK-3 inhibition by adenoviral FRAT1 overexpression is neuroprotective and induces Tau dephosphorylation and beta-catenin stabilisation without elevation of glycogen synthase activity." FEBS Lett **507**(3): 288-294.
58. Dahlhaus, R. (2018). "Of Men and Mice: Modeling the Fragile X Syndrome." Front Mol Neurosci **11**: 41.
59. Deidda, G., M. Allegra, C. Cerri, S. Naskar, G. Bony, G. Zunino, Y. Bozzi, M. Caleo and L. Cancedda (2015). "Early depolarizing GABA controls critical-period plasticity in the rat visual cortex." Nat Neurosci **18**(1): 87-96.

60. Delpire, E., J. Lu, R. England, C. Dull and T. Thorne (1999). "Deafness and imbalance associated with inactivation of the secretory Na-K-2Cl co-transporter." Nat Genet **22**(2): 192-195.
61. Delpire, E. and D. B. Mount (2002). "Human and murine phenotypes associated with defects in cation-chloride cotransport." Annu Rev Physiol **64**: 803-843.
62. Dickstein, D. L., C. M. Weaver, J. I. Luebke and P. R. Hof (2013). "Dendritic spine changes associated with normal aging." Neuroscience **251**: 21-32.
63. Dixon, M. J., J. Gazzard, S. S. Chaudhry, N. Sampson, B. A. Schulte and K. P. Steel (1999). "Mutation of the Na-K-Cl co-transporter gene Slc12a2 results in deafness in mice." Hum Mol Genet **8**(8): 1579-1584.
64. Doble, B. W. and J. R. Woodgett (2003). "GSK-3: tricks of the trade for a multi-tasking kinase." J Cell Sci **116**(Pt 7): 1175-1186.
65. Duarte, S. T., J. Armstrong, A. Roche, C. Ortez, A. Perez, M. O'Callaghan Mdel, A. Pereira, F. Sanmarti, A. Ormazabal, R. Artuch, M. Pineda and A. Garcia-Cazorla (2013). "Abnormal expression of cerebrospinal fluid cation chloride cotransporters in patients with Rett syndrome." PLoS One **8**(7): e68851.
66. Dzhala, V. I., D. M. Talos, D. A. Sdrulla, A. C. Brumback, G. C. Mathews, T. A. Benke, E. Delpire, F. E. Jensen and K. J. Staley (2005). "NKCC1 transporter facilitates seizures in the developing brain." Nat Med **11**(11): 1205-1213.
67. Eftekhari, S., S. Mehrabi, M. Soleimani, G. Hassanzadeh, A. Shahrokhi, H. Mostafavi, P. Hayat, M. Barati, H. Mehdizadeh, R. Rahmanzadeh, M. R. Hadjighassem and M. T. Joghataei (2014). "BDNF modifies hippocampal KCC2 and NKCC1 expression in a temporal lobe epilepsy model." Acta Neurobiol Exp (Wars) **74**(3): 276-287.
68. Egawa, K. and A. Fukuda (2013). "Pathophysiological power of improper tonic GABA(A) conductances in mature and immature models." Front Neural Circuits **7**: 170.
69. El-Khoury, R., N. Panayotis, V. Matagne, A. Ghata, L. Villard and J.-C. Roux (2014). "GABA and glutamate pathways are spatially and developmentally affected in the brain of Mecp2-deficient mice." PLoS One **9**(3): e92169.
70. Ellison, J. W., J. A. Rosenfeld and L. G. Shaffer (2013). "Genetic basis of intellectual disability." Annu Rev Med **64**: 441-450.
71. Etherton, M., C. Foldy, M. Sharma, K. Tabuchi, X. Liu, M. Shamloo, R. C. Malenka and T. C. Sudhof (2011). "Autism-linked neuroligin-3 R451C mutation differentially

alters hippocampal and cortical synaptic function." Proc Natl Acad Sci U S A **108**(33): 13764-13769.

72. Evans, R. L., K. Park, R. J. Turner, G. E. Watson, H. V. Nguyen, M. R. Dennett, A. R. Hand, M. Flagella, G. E. Shull and J. E. Melvin (2000). "Severe impairment of salivation in Na+/K+/2Cl- cotransporter (NKCC1)-deficient mice." J Biol Chem **275**(35): 26720-26726.
73. Fagiolini, M. and T. K. Hensch (2000). "Inhibitory threshold for critical-period activation in primary visual cortex." Nature **404**(6774): 183-186.
74. Farrant, M. and Z. Nusser (2005). "Variations on an inhibitory theme: phasic and tonic activation of GABA(A) receptors." Nat Rev Neurosci **6**(3): 215-229.
75. Feng, G., R. H. Mellor, M. Bernstein, C. Keller-Peck, Q. T. Nguyen, M. Wallace, J. M. Nerbonne, J. W. Lichtman and J. R. Sanes (2000). "Imaging neuronal subsets in transgenic mice expressing multiple spectral variants of GFP." Neuron **28**(1): 41-51.
76. Flagella, M., L. L. Clarke, M. L. Miller, L. C. Erway, R. A. Giannella, A. Andringa, L. R. Gawenis, J. Kramer, J. J. Duffy, T. Doetschman, J. N. Lorenz, E. N. Yamoah, E. L. Cardell and G. E. Shull (1999). "Mice lacking the basolateral Na-K-2Cl cotransporter have impaired epithelial chloride secretion and are profoundly deaf." J Biol Chem **274**(38): 26946-26955.
77. Foldy, C., R. C. Malenka and T. C. Sudhof (2013). "Autism-associated neuroligin-3 mutations commonly disrupt tonic endocannabinoid signaling." Neuron **78**(3): 498-509.
78. Gaiarsa, J. L., O. Caillard and Y. Ben-Ari (2002). "Long-term plasticity at GABAergic and glycinergic synapses: mechanisms and functional significance." Trends Neurosci **25**(11): 564-570.
79. Gamache, T. R., Y. Araki and R. L. Huganir (2020). "Twenty Years of SynGAP Research: From Synapses to Cognition." J Neurosci **40**(8): 1596-1605.
80. Gamba, G. (2005). "Molecular physiology and pathophysiology of electroneutral cation-chloride cotransporters." Physiol Rev **85**(2): 423-493.
81. Gamba, G. and P. A. Friedman (2009). "Thick ascending limb: the Na(+):K (+):2Cl (-) co-transporter, NKCC2, and the calcium-sensing receptor, CaSR." Pflugers Arch **458**(1): 61-76.
82. Gaudissard, J., M. Ginger, M. Premoli, M. Memo, A. Frick and S. Pietropaolo (2017). "Behavioral abnormalities in the Fmr1-KO2 mouse model of fragile X syndrome: The relevance of early life phases." Autism Research **10**(10): 1584-1596.

83. Gauvain, G., I. Chamma, Q. Chevy, C. Cabezas, T. Irinopoulou, N. Bodrug, M. Carnaud, S. Levi and J. C. Poncer (2011). "The neuronal K-Cl cotransporter KCC2 influences postsynaptic AMPA receptor content and lateral diffusion in dendritic spines." Proc Natl Acad Sci U S A **108**(37): 15474-15479.
84. Glykys, J. and I. Mody (2007). "The main source of ambient GABA responsible for tonic inhibition in the mouse hippocampus." J Physiol **582**(Pt 3): 1163-1178.
85. Griguoli, M. and E. Cherubini (2017). "Early Correlated Network Activity in the Hippocampus: Its Putative Role in Shaping Neuronal Circuits." Front Cell Neurosci **11**: 255.
86. Grubb, B. R., E. Lee, A. J. Pace, B. H. Koller and R. C. Boucher (2000). "Intestinal ion transport in NKCC1-deficient mice." Am J Physiol Gastrointest Liver Physiol **279**(4): G707-718.
87. Gulyas, A. I., A. Sik, J. A. Payne, K. Kaila and T. F. Freund (2001). "The KCl cotransporter, KCC2, is highly expressed in the vicinity of excitatory synapses in the rat hippocampus." Eur J Neurosci **13**(12): 2205-2217.
88. Guo, W., A. M. Allan, R. Zong, L. Zhang, E. B. Johnson, E. G. Schaller, A. C. Murthy, S. L. Goggin, A. J. Eisch and B. A. Oostra (2011). "Ablation of Fmrp in adult neural stem cells disrupts hippocampus-dependent learning." Nature medicine **17**(5): 559.
89. Guo, X., P. J. Hamilton, N. J. Reish, J. D. Sweatt, C. A. Miller and G. Rumbaugh (2009). "Reduced expression of the NMDA receptor-interacting protein SynGAP causes behavioral abnormalities that model symptoms of Schizophrenia." Neuropsychopharmacology **34**(7): 1659-1672.
90. Guy, J., B. Hendrich, M. Holmes, J. E. Martin and A. Bird (2001). "A mouse Mecp2-null mutation causes neurological symptoms that mimic Rett syndrome." Nat Genet **27**(3): 322-326.
91. Haas, M. and B. Forbush, 3rd (2000). "The Na-K-Cl cotransporter of secretory epithelia." Annu Rev Physiol **62**: 515-534.
92. Hamdan, F. F., H. Daoud, A. Piton, J. Gauthier, S. Dobrzeniecka, M. O. Krebs, R. Joober, J. C. Lacaille, A. Nadeau, J. M. Milunsky, Z. Wang, L. Carmant, L. Mottron, M. H. Beauchamp, G. A. Rouleau and J. L. Michaud (2011). "De novo SYNGAP1 mutations in nonsyndromic intellectual disability and autism." Biol Psychiatry **69**(9): 898-901.

93. Hamdan, F. F., J. Gauthier, D. Spiegelman, A. Noreau, Y. Yang, S. Pellerin, S. Dobrzeniecka, M. Cote, E. Perreau-Linck, L. Carmant, G. D'Anjou, E. Fombonne, A. M. Addington, J. L. Rapoport, L. E. Delisi, M. O. Krebs, F. Mouaffak, R. Joober, L. Mottron, P. Drapeau, C. Marineau, R. G. Lafreniere, J. C. Lacaille, G. A. Rouleau, J. L. Michaud and G. Synapse to Disease (2009). "Mutations in SYNGAP1 in autosomal nonsyndromic mental retardation." N Engl J Med **360**(6): 599-605.
94. Hanover, J. L., Z. J. Huang, S. Tonegawa and M. P. Stryker (1999). "Brain-derived neurotrophic factor overexpression induces precocious critical period in mouse visual cortex." J Neurosci **19**(22): RC40.
95. Hebert, S. C., D. B. Mount and G. Gamba (2004). "Molecular physiology of cation-coupled Cl- cotransport: the SLC12 family." Pflugers Arch **447**(5): 580-593.
96. Hensch, T. K. (2005). "Critical period plasticity in local cortical circuits." Nat Rev Neurosci **6**(11): 877-888.
97. Hensch, T. K., M. Fagiolini, N. Mataga, M. P. Stryker, S. Baekkeskov and S. F. Kash (1998). "Local GABA circuit control of experience-dependent plasticity in developing visual cortex." Science **282**(5393): 1504-1508.
98. Hinz, L., J. Torrella Barrufet and V. M. Heine (2019). "KCC2 expression levels are reduced in post mortem brain tissue of Rett syndrome patients." Acta Neuropathol Commun **7**(1): 196.
99. Hoessel, R., S. Leclerc, J. A. Endicott, M. E. Nobel, A. Lawrie, P. Tunnah, M. Leost, E. Damiens, D. Marie, D. Marko, E. Niederberger, W. Tang, G. Eisenbrand and L. Meijer (1999). "Indirubin, the active constituent of a Chinese antileukaemia medicine, inhibits cyclin-dependent kinases." Nat Cell Biol **1**(1): 60-67.
100. Huang, Z. J., A. Kirkwood, T. Pizzorusso, V. Porciatti, B. Morales, M. F. Bear, L. Maffei and S. Tonegawa (1999). "BDNF regulates the maturation of inhibition and the critical period of plasticity in mouse visual cortex." Cell **98**(6): 739-755.
101. Hubel, D. H. (1957). "Tungsten Microelectrode for Recording from Single Units." Science **125**(3247): 549-550.
102. Hubel, D. H. and T. N. Wiesel (1963). "Receptive Fields of Cells in Striate Cortex of Very Young, Visually Inexperienced Kittens." J Neurophysiol **26**: 994-1002.
103. Hubel, D. H. and T. N. Wiesel (1965). "Binocular interaction in striate cortex of kittens reared with artificial squint." J Neurophysiol **28**(6): 1041-1059.

104. Hubener, M. and T. Bonhoeffer (2014). "Neuronal plasticity: beyond the critical period." Cell **159**(4): 727-737.

105. Hyde, T. M., B. K. Lipska, T. Ali, S. V. Mathew, A. J. Law, O. E. Metitiri, R. E. Straub, T. Ye, C. Colantuoni, M. M. Herman, L. B. Bigelow, D. R. Weinberger and J. E. Kleinman (2011). "Expression of GABA signaling molecules KCC2, NKCC1, and GAD1 in cortical development and schizophrenia." J Neurosci **31**(30): 11088-11095.

106. Ikeda, K., H. Onimaru, J. Yamada, K. Inoue, S. Ueno, T. Onaka, H. Toyoda, A. Arata, T. O. Ishikawa, M. M. Taketo, A. Fukuda and K. Kawakami (2004). "Malfunction of respiratory-related neuronal activity in Na+, K+-ATPase alpha2 subunit-deficient mice is attributable to abnormal Cl- homeostasis in brainstem neurons." J Neurosci **24**(47): 10693-10701.

107. Jaworski, T., E. Banach-Kasper and K. Gralec (2019). "GSK-3beta at the Intersection of Neuronal Plasticity and Neurodegeneration." Neural Plast **2019**: 4209475.

108. Jeyabalan, N. and J. P. Clement (2016). "SYNGAP1: Mind the Gap." Front Cell Neurosci **10**: 32.

109. Kadiyala, S. B., D. Papandrea, B. J. Herron and R. J. Ferland (2014). "Segregation of seizure traits in C57 black mouse substrains using the repeated-flurothyl model." PLoS One **9**(3): e90506.

110. Kaila, K., T. J. Price, J. A. Payne, M. Puskarjov and J. Voipio (2014). "Cation-chloride cotransporters in neuronal development, plasticity and disease." Nat Rev Neurosci **15**(10): 637-654.

111. Kanold, P. O., Y. A. Kim, T. GrandPre and C. J. Shatz (2009). "Co-regulation of ocular dominance plasticity and NMDA receptor subunit expression in glutamic acid decarboxylase-65 knock-out mice." J Physiol **587**(Pt 12): 2857-2867.

112. Kanold, P. O. and H. J. Luhmann (2010). "The subplate and early cortical circuits." Annu Rev Neurosci **33**: 23-48.

113. Kaufman, L., M. Ayub and J. B. Vincent (2010). "The genetic basis of non-syndromic intellectual disability: a review." J Neurodev Disord **2**(4): 182-209.

114. Kepecs, A. and G. Fishell (2014). "Interneuron cell types are fit to function." Nature **505**(7483): 318-326.

115. Khirug, S., J. Yamada, R. Afzalov, J. Voipio, L. Khiroug and K. Kaila (2008). "GABAergic depolarization of the axon initial segment in cortical principal neurons is caused by the Na-K-2Cl cotransporter NKCC1." J Neurosci **28**(18): 4635-4639.

116. Kilinc, M., T. Creson, C. Rojas, M. Aceti, J. Ellegood, T. Vaissiere, J. P. Lerch and G. Rumbaugh (2018). "Species-conserved SYNGAP1 phenotypes associated with neurodevelopmental disorders." Mol Cell Neurosci **91**: 140-150.

117. Kim, J. H., H. K. Lee, K. Takamiya and R. L. Huganir (2003). "The role of synaptic GTPase-activating protein in neuronal development and synaptic plasticity." J Neurosci **23**(4): 1119-1124.

118. Kim, J. H., D. Liao, L. F. Lau and R. L. Huganir (1998). "SynGAP: a synaptic RasGAP that associates with the PSD-95/SAP90 protein family." Neuron **20**(4): 683-691.

119. Kimura, T., S. Yamashita, S. Nakao, J. M. Park, M. Murayama, T. Mizoroki, Y. Yoshiike, N. Sahara and A. Takashima (2008). "GSK-3beta is required for memory reconsolidation in adult brain." PLoS One **3**(10): e3540.

120. Kimura, Y., M. Akahira-Azuma, N. Harada, Y. Enomoto, Y. Tsurusaki and K. Kurosawa (2018). "Novel SYNGAP1 variant in a patient with intellectual disability and distinctive dysmorphisms." Congenit Anom (Kyoto) **58**(6): 188-190.

121. Kitagishi, Y., M. Kobayashi, K. Kikuta and S. Matsuda (2012). "Roles of PI3K/AKT/GSK3/mTOR Pathway in Cell Signaling of Mental Illnesses." Depress Res Treat **2012**: 752563.

122. Knockaert, M., M. Blondel, S. Bach, M. Leost, C. Elbi, G. L. Hager, S. R. Nagy, D. Han, M. Denison, M. Ffrench, X. P. Ryan, P. Magiatis, P. Polychronopoulos, P. Greengard, L. Skaltsounis and L. Meijer (2004). "Independent actions on cyclin-dependent kinases and aryl hydrocarbon receptor mediate the antiproliferative effects of indirubins." Oncogene **23**(25): 4400-4412.

123. Koekkoek, S., K. Yamaguchi, B. Milojkovic, B. Dortland, T. Ruigrok, R. Maex, W. De Graaf, A. E. Smit, F. VanderWerf and C. Bakker (2005). "Deletion of FMR1 in Purkinje cells enhances parallel fiber LTD, enlarges spines, and attenuates cerebellar eyelid conditioning in Fragile X syndrome." Neuron **47**(3): 339-352.

124. Komiyama, N. H., A. M. Watabe, H. J. Carlisle, K. Porter, P. Charlesworth, J. Monti, D. J. Strathdee, C. M. O'Carroll, S. J. Martin, R. G. Morris, T. J. O'Dell and S. G. Grant (2002). "SynGAP regulates ERK/MAPK signaling, synaptic plasticity, and

learning in the complex with postsynaptic density 95 and NMDA receptor." J Neurosci **22**(22): 9721-9732.

125. Kozlovsky, N., R. H. Belmaker and G. Agam (2000). "Low GSK-3beta immunoreactivity in postmortem frontal cortex of schizophrenic patients." Am J Psychiatry **157**(5): 831-833.

126. Kozlovsky, N., R. H. Belmaker and G. Agam (2001). "Low GSK-3 activity in frontal cortex of schizophrenic patients." Schizophr Res **52**(1-2): 101-105.

127. Krishnan, K., B.-S. Wang, J. Lu, L. Wang, A. Maffei, J. Cang and Z. J. Huang (2015). "MeCP2 regulates the timing of critical period plasticity that shapes functional connectivity in primary visual cortex." Proceedings of the National Academy of Sciences **112**(34): E4782-E4791.

128. Krupp, D. R., R. A. Barnard, Y. Duffourd, S. A. Evans, R. M. Mulqueen, R. Bernier, J. B. Riviere, E. Fombonne and B. J. O'Roak (2017). "Exonic Mosaic Mutations Contribute Risk for Autism Spectrum Disorder." Am J Hum Genet **101**(3): 369-390.

129. Laird, J. M., E. Garcia-Nicas, E. J. Delpire and F. Cervero (2004). "Presynaptic inhibition and spinal pain processing in mice: a possible role of the NKCC1 cation-chloride co-transporter in hyperalgesia." Neurosci Lett **361**(1-3): 200-203.

130. Laumonnier, F., P. C. Cuthbert and S. G. Grant (2007). "The role of neuronal complexes in human X-linked brain diseases." Am J Hum Genet **80**(2): 205-220.

131. Lawson-Yuen, A., D. Liu, L. Han, Z. I. Jiang, G. E. Tsai, A. C. Basu, J. Picker, J. Feng and J. T. Coyle (2007). "Ube3a mRNA and protein expression are not decreased in Mecp2R168X mutant mice." Brain research **1180**: 1-6.

132. Le Magueresse, C. and H. Monyer (2013). "GABAergic interneurons shape the functional maturation of the cortex." Neuron **77**(3): 388-405.

133. Leclerc, S., M. Garnier, R. Hoessel, D. Marko, J. A. Bibb, G. L. Snyder, P. Greengard, J. Biernat, Y. Z. Wu, E. M. Mandelkow, G. Eisenbrand and L. Meijer (2001). "Indirubins inhibit glycogen synthase kinase-3 beta and CDK5/p25, two protein kinases involved in abnormal tau phosphorylation in Alzheimer's disease. A property common to most cyclin-dependent kinase inhibitors?" J Biol Chem **276**(1): 251-260.

134. Levitt, P. (2003). "Structural and functional maturation of the developing primate brain." J Pediatr **143**(4 Suppl): S35-45.

135. Liu, E., A. J. Xie, Q. Zhou, M. Li, S. Zhang, S. Li, W. Wang, X. Wang, Q. Wang and J. Z. Wang (2017). "GSK-3beta deletion in dentate gyrus excitatory neuron impairs synaptic plasticity and memory." Sci Rep **7**(1): 5781.

136. Liu, Z. H., T. Huang and C. B. Smith (2012). "Lithium reverses increased rates of cerebral protein synthesis in a mouse model of fragile X syndrome." Neurobiol Dis **45**(3): 1145-1152.

137. Llamosas, N., V. Arora, R. Vij, M. Kilinc, L. Bijoch, C. Rojas, A. Reich, B. Sridharan, E. Willems, D. R. Piper, L. Scampavia, T. P. Spicer, C. A. Miller, J. L. Holder and G. Rumbaugh (2020). "SYNGAP1 Controls the Maturation of Dendrites, Synaptic Function, and Network Activity in Developing Human Neurons." J Neurosci **40**(41): 7980-7994.

138. Llano, O., S. Smirnov, S. Soni, A. Golubtsov, I. Guillemin, P. Hotulainen, I. Medina, H. G. Nothwang, C. Rivera and A. Ludwig (2015). "KCC2 regulates actin dynamics in dendritic spines via interaction with beta-PIX." J Cell Biol **209**(5): 671-686.

139. Lord, C., M. Elsabbagh, G. Baird and J. Veenstra-Vanderweele (2018). "Autism spectrum disorder." Lancet **392**(10146): 508-520.

140. Ludwig, A., P. Uvarov, S. Soni, J. Thomas-Crusells, M. S. Airaksinen and C. Rivera (2011). "Early growth response 4 mediates BDNF induction of potassium chloride cotransporter 2 transcription." J Neurosci **31**(2): 644-649.

141. Luikenhuis, S., E. Giacometti, C. F. Beard and R. Jaenisch (2004). "Expression of MeCP2 in postmitotic neurons rescues Rett syndrome in mice." Proceedings of the National Academy of Sciences **101**(16): 6033-6038.

142. Macnamara, E. F., A. E. Koehler, P. D'Souza, T. Estwick, P. Lee, G. Vezina, N. Undiagnosed Diseases, H. Fauni, S. R. Braddock, E. Torti, J. M. Holt, P. Sharma, M. C. V. Malicdan and C. J. Tifft (2019). "Kilquist syndrome: A novel syndromic hearing loss disorder caused by homozygous deletion of SLC12A2." Hum Mutat **40**(5): 532-538.

143. Mahadevan, V., J. C. Pressey, B. A. Acton, P. Uvarov, M. Y. Huang, J. Chevrier, A. Puchalski, C. M. Li, E. A. Ivakine, M. S. Airaksinen, E. Delpire, R. R. McInnes and M. A. Woodin (2014). "Kainate receptors coexist in a functional complex with KCC2 and regulate chloride homeostasis in hippocampal neurons." Cell Rep **7**(6): 1762-1770.

144. Marchese, M., G. Valvo, F. Moro, F. Sicca and F. M. Santorelli (2016). "Targeted Gene Resequencing (Astrochip) to Explore the Tripartite Synapse in Autism-Epilepsy Phenotype with Macrocephaly." Neuromolecular Med **18**(1): 69-80.

145. Masi, A., M. M. DeMayo, N. Glozier and A. J. Guastella (2017). "An Overview of Autism Spectrum Disorder, Heterogeneity and Treatment Options." Neurosci Bull **33**(2): 183-193.

146. Maya Vetencourt, J. F., A. Sale, A. Viegi, L. Baroncelli, R. De Pasquale, O. F. O'Leary, E. Castren and L. Maffei (2008). "The antidepressant fluoxetine restores plasticity in the adult visual cortex." Science **320**(5874): 385-388.

147. McCamphill, P. K., L. J. Stoppel, R. K. Senter, M. C. Lewis, A. J. Heynen, D. C. Stoppel, V. Sridhar, K. A. Collins, X. Shi, J. Q. Pan, J. Madison, J. R. Cottrell, K. M. Huber, E. M. Scolnick, E. B. Holson, F. F. Wagner and M. F. Bear (2020). "Selective inhibition of glycogen synthase kinase 3alpha corrects pathophysiology in a mouse model of fragile X syndrome." Sci Transl Med **12**(544).

148. Medina, I., P. Friedel, C. Rivera, K. T. Kahle, N. Kourdougli, P. Uvarov and C. Pellegrino (2014). "Current view on the functional regulation of the neuronal K(+)-Cl(-) cotransporter KCC2." Front Cell Neurosci **8**: 27.

149. Meijer, L., A. L. Skaltsounis, P. Magiatis, P. Polychronopoulos, M. Knockaert, M. Leost, X. P. Ryan, C. A. Vonica, A. Brivanlou, R. Dajani, C. Crovace, C. Tarricone, A. Musacchio, S. M. Roe, L. Pearl and P. Greengard (2003). "GSK-3-selective inhibitors derived from Tyrian purple indirubins." Chem Biol **10**(12): 1255-1266.

150. Merner, N. D., M. R. Chandler, C. Bourassa, B. Liang, A. R. Khanna, P. Dion, G. A. Rouleau and K. T. Kahle (2015). "Regulatory domain or CpG site variation in SLC12A5, encoding the chloride transporter KCC2, in human autism and schizophrenia." Front Cell Neurosci **9**: 386.

151. Mientjes, E., I. Nieuwenhuizen, L. Kirkpatrick, T. Zu, M. Hoogeveen-Westerveld, L. Severijnen, M. Rifé, R. Willemsen, D. Nelson and B. Oostra (2006). "The generation of a conditional Fmr1 knock out mouse model to study Fmrp function in vivo." Neurobiology of disease **21**(3): 549-555.

152. Mignot, C., C. von Stulpnagel, C. Nava, D. Ville, D. Sanlaville, G. Lesca, A. Rastetter, B. Gachet, Y. Marie, G. C. Korenke, I. Borggraefe, D. Hoffmann-Zacharska, E. Szczepanik, M. Rudzka-Dybala, U. Yis, H. Caglayan, A. Isapof, I. Marey, E. Panagiotakaki, C. Korff, E. Rossier, A. Riess, S. Beck-Woedl, A. Rauch, C.

Zweier, J. Hoyer, A. Reis, M. Mironov, M. Bobylova, K. Mukhin, L. Hernandez-Hernandez, B. Maher, S. Sisodiya, M. Kuhn, D. Glaeser, S. Weckhuysen, C. T. Myers, H. C. Mefford, K. Hortnagel, S. Biskup, E.-R. E. S. M. A. E. w. g. Euro, J. R. Lemke, D. Heron, G. Kluger and C. Depienne (2016). "Genetic and neurodevelopmental spectrum of SYNGAP1-associated intellectual disability and epilepsy." J Med Genet **53**(8): 511-522.

153. Miguez, A., G. Garcia-Diaz Barriga, V. Brito, M. Straccia, A. Giralt, S. Gines, J. M. Canals and J. Alberch (2015). "Fingolimod (FTY720) enhances hippocampal synaptic plasticity and memory in Huntington's disease by preventing p75NTR up-regulation and astrocyte-mediated inflammation." Hum Mol Genet **24**(17): 4958-4970.

154. Mines, M. A. and R. S. Jope (2011). "Glycogen synthase kinase-3: a promising therapeutic target for fragile x syndrome." Front Mol Neurosci **4**: 35.

155. Muhia, M., B. K. Yee, J. Feldon, F. Markopoulos and I. Knuesel (2010). "Disruption of hippocampus-regulated behavioural and cognitive processes by heterozygous constitutive deletion of SynGAP." Eur J Neurosci **31**(3): 529-543.

156. Murray, M. L., Y. Hsia, K. Glaser, E. Simonoff, D. G. Murphy, P. J. Asherson, H. Eklund and I. C. Wong (2014). "Pharmacological treatments prescribed to people with autism spectrum disorder (ASD) in primary health care." Psychopharmacology (Berl) **231**(6): 1011-1021.

157. Muscas, M., S. R. Louros and E. K. Osterweil (2019). "Lovastatin, not Simvastatin, Corrects Core Phenotypes in the Fragile X Mouse Model." eNeuro **6**(3).

158. Myrianthopoulos, V., P. Magiatis, Y. Ferandin, A. L. Skaltsounis, L. Meijer and E. Mikros (2007). "An integrated computational approach to the phenomenon of potent and selective inhibition of aurora kinases B and C by a series of 7-substituted indirubins." J Med Chem **50**(17): 4027-4037.

159. Nadri, C., B. K. Lipska, N. Kozlovsky, D. R. Weinberger, R. H. Belmaker and G. Agam (2003). "Glycogen synthase kinase (GSK)-3beta levels and activity in a neurodevelopmental rat model of schizophrenia." Brain Res Dev Brain Res **141**(1-2): 33-37.

160. Nakajima, R., K. Takao, S. Hattori, H. Shoji, N. H. Komiyama, S. G. N. Grant and T. Miyakawa (2019). "Comprehensive behavioral analysis of heterozygous Syngap1 knockout mice." Neuropsychopharmacol Rep **39**(3): 223-237.

161. Nisha, C. M., A. Kumar, A. Vimal, B. M. Bai, D. Pal and A. Kumar (2016). "Docking and ADMET prediction of few GSK-3 inhibitors divulges 6-bromoindirubin-3-oxime as a potential inhibitor." J Mol Graph Model **65**: 100-107.

162. Nusser, Z. and I. Mody (2002). "Selective modulation of tonic and phasic inhibitions in dentate gyrus granule cells." J Neurophysiol **87**(5): 2624-2628.

163. O'Brien, W. T., A. D. Harper, F. Jove, J. R. Woodgett, S. Maretto, S. Piccolo and P. S. Klein (2004). "Glycogen synthase kinase-3beta haploinsufficiency mimics the behavioral and molecular effects of lithium." J Neurosci **24**(30): 6791-6798.

164. Oostra, B., C. Bakker and E. Reyniers (1994). "FMR1 knockout mice: a model to study fragile X mental retardation." American Journal of Human Genetics **55**(CONF-941009--).

165. Osterweil, E. K., S. C. Chuang, A. A. Chubykin, M. Sidorov, R. Bianchi, R. K. Wong and M. F. Bear (2013). "Lovastatin corrects excess protein synthesis and prevents epileptogenesis in a mouse model of fragile X syndrome." Neuron **77**(2): 243-250.

166. Owens, D. F., L. H. Boyce, M. B. Davis and A. R. Kriegstein (1996). "Excitatory GABA responses in embryonic and neonatal cortical slices demonstrated by gramicidin perforated-patch recordings and calcium imaging." J Neurosci **16**(20): 6414-6423.

167. Ozkan, E. D., T. K. Creson, E. A. Kramar, C. Rojas, R. R. Seese, A. H. Babyan, Y. Shi, R. Lucero, X. Xu, J. L. Noebels, C. A. Miller, G. Lynch and G. Rumbaugh (2014). "Reduced cognition in Syngap1 mutants is caused by isolated damage within developing forebrain excitatory neurons." Neuron **82**(6): 1317-1333.

168. Pace, A. J., V. J. Madden, O. W. Henson, Jr., B. H. Koller and M. M. Henson (2001). "Ultrastructure of the inner ear of NKCC1-deficient mice." Hear Res **156**(1-2): 17-30.

169. Payne, J. A. (1997). "Functional characterization of the neuronal-specific K-Cl cotransporter: implications for [K+]o regulation." Am J Physiol **273**(5 Pt 1): C1516-1525.

170. Peça, J., C. Feliciano, J. T. Ting, W. Wang, M. F. Wells, T. N. Venkatraman, C. D. Lascola, Z. Fu and G. Feng (2011). "Shank3 mutant mice display autistic-like behaviours and striatal dysfunction." Nature **472**(7344): 437.

171. Peineau, S., C. Taghibiglou, C. Bradley, T. P. Wong, L. Liu, J. Lu, E. Lo, D. Wu, E. Saule, T. Bouschet, P. Matthews, J. T. Isaac, Z. A. Bortolotto, Y. T. Wang and

G. L. Collingridge (2007). "LTP inhibits LTD in the hippocampus via regulation of GSK3beta." Neuron **53**(5): 703-717.

172. Penzes, P., M. E. Cahill, K. A. Jones, J. E. VanLeeuwen and K. M. Woolfrey (2011). "Dendritic spine pathology in neuropsychiatric disorders." Nat Neurosci **14**(3): 285-293.

173. Petrini, E. M., J. Lu, L. Cognet, B. Lounis, M. D. Ehlers and D. Choquet (2009). "Endocytic trafficking and recycling maintain a pool of mobile surface AMPA receptors required for synaptic potentiation." Neuron **63**(1): 92-105.

174. Petroff, O. A. (2002). "GABA and glutamate in the human brain." Neuroscientist **8**(6): 562-573.

175. Pfeffer, C. K., V. Stein, D. J. Keating, H. Maier, I. Rinke, Y. Rudhard, M. Hentschke, G. M. Rune, T. J. Jentsch and C. A. Hubner (2009). "NKCC1-dependent GABAergic excitation drives synaptic network maturation during early hippocampal development." J Neurosci **29**(11): 3419-3430.

176. Pinto, D., A. T. Pagnamenta, L. Klei, R. Anney, D. Merico, R. Regan, J. Conroy, T. R. Magalhaes, C. Correia, B. S. Abrahams, J. Almeida, E. Bacchelli, G. D. Bader, A. J. Bailey, G. Baird, A. Battaglia, T. Berney, N. Bolshakova, S. Bolte, P. F. Bolton, T. Bourgeron, S. Brennan, J. Brian, S. E. Bryson, A. R. Carson, G. Casallo, J. Casey, B. H. Chung, L. Cochrane, C. Corsello, E. L. Crawford, A. Crossett, C. Cytrynbaum, G. Dawson, M. de Jonge, R. Delorme, I. Drmic, E. Duketis, F. Duque, A. Estes, P. Farrar, B. A. Fernandez, S. E. Folstein, E. Fombonne, C. M. Freitag, J. Gilbert, C. Gillberg, J. T. Glessner, J. Goldberg, A. Green, J. Green, S. J. Guter, H. Hakonarson, E. A. Heron, M. Hill, R. Holt, J. L. Howe, G. Hughes, V. Hus, R. Igliozzi, C. Kim, S. M. Klauck, A. Kolevzon, O. Korvatska, V. Kustanovich, C. M. Lajonchere, J. A. Lamb, M. Laskawiec, M. Leboyer, A. Le Couteur, B. L. Leventhal, A. C. Lionel, X. Q. Liu, C. Lord, L. Lotspeich, S. C. Lund, E. Maestrini, W. Mahoney, C. Mantoulan, C. R. Marshall, H. McConachie, C. J. McDougle, J. McGrath, W. M. McMahon, A. Merikangas, O. Migita, N. J. Minshew, G. K. Mirza, J. Munson, S. F. Nelson, C. Noakes, A. Noor, G. Nygren, G. Oliveira, K. Papanikolaou, J. R. Parr, B. Parrini, T. Paton, A. Pickles, M. Pilorge, J. Piven, C. P. Ponting, D. J. Posey, A. Poustka, F. Poustka, A. Prasad, J. Ragoussis, K. Renshaw, J. Rickaby, W. Roberts, K. Roeder, B. Roge, M. L. Rutter, L. J. Bierut, J. P. Rice, J. Salt, K. Sansom, D. Sato, R. Segurado, A. F. Sequeira, L. Senman, N. Shah, V. C. Sheffield, L. Soorya, I. Sousa, O. Stein, N. Sykes, V. Stoppioni, C. Strawbridge, R.

Tancredi, K. Tansey, B. Thiruvahindrapduram, A. P. Thompson, S. Thomson, A. Tryfon, J. Tsiantis, H. Van Engeland, J. B. Vincent, F. Volkmar, S. Wallace, K. Wang, Z. Wang, T. H. Wassink, C. Webber, R. Weksberg, K. Wing, K. Wittemeyer, S. Wood, J. Wu, B. L. Yaspan, D. Zurawiecki, L. Zwaigenbaum, J. D. Buxbaum, R. M. Cantor, E. H. Cook, H. Coon, M. L. Cuccaro, B. Devlin, S. Ennis, L. Gallagher, D. H. Geschwind, M. Gill, J. L. Haines, J. Hallmayer, J. Miller, A. P. Monaco, J. I. Nurnberger, Jr., A. D. Paterson, M. A. Pericak-Vance, G. D. Schellenberg, P. Szatmari, A. M. Vicente, V. J. Vieland, E. M. Wijsman, S. W. Scherer, J. S. Sutcliffe and C. Betancur (2010). "Functional impact of global rare copy number variation in autism spectrum disorders." Nature **466**(7304): 368-372.

177. Pizzarelli, R. and E. Cherubini (2013). "Developmental regulation of GABAergic signalling in the hippocampus of neuroligin 3 R451C knock-in mice: an animal model of Autism." Front Cell Neurosci **7**: 85.

178. Polychronopoulos, P., P. Magiatis, A. L. Skaltsounis, V. Myrianthopoulos, E. Mikros, A. Tarricone, A. Musacchio, S. M. Roe, L. Pearl, M. Leost, P. Greengard and L. Meijer (2004). "Structural basis for the synthesis of indirubins as potent and selective inhibitors of glycogen synthase kinase-3 and cyclin-dependent kinases." J Med Chem **47**(4): 935-946.

179. Porcher, C., I. Medina and J. L. Gaiarsa (2018). "Mechanism of BDNF Modulation in GABAergic Synaptic Transmission in Healthy and Disease Brains." Front Cell Neurosci **12**: 273.

180. Purpura, D. P. (1974). "Dendritic spine "dysgenesis" and mental retardation." Science **186**(4169): 1126-1128.

181. Puskarjov, M., F. Ahmad, S. Khirug, S. Sivakumaran, K. Kaila and P. Blaesse (2015). "BDNF is required for seizure-induced but not developmental up-regulation of KCC2 in the neonatal hippocampus." Neuropharmacology **88**: 103-109.

182. Qin, Y., Y. Zhu, J. P. Baumgart, R. L. Stornetta, K. Seidenman, V. Mack, L. van Aelst and J. J. Zhu (2005). "State-dependent Ras signaling and AMPA receptor trafficking." Genes Dev **19**(17): 2000-2015.

183. Ramamoorthi, K. and Y. Lin (2011). "The contribution of GABAergic dysfunction to neurodevelopmental disorders." Trends Mol Med **17**(8): 452-462.

184. Rivera, C., H. Li, J. Thomas-Crusells, H. Lahtinen, T. Viitanen, A. Nanobashvili, Z. Kokaia, M. S. Airaksinen, J. Voipio, K. Kaila and M. Saarma

(2002). "BDNF-induced TrkB activation down-regulates the K+-Cl- cotransporter KCC2 and impairs neuronal Cl- extrusion." J Cell Biol **159**(5): 747-752.

185. Rivera, C., J. Voipio and K. Kaila (2005). "Two developmental switches in GABAergic signalling: the K+-Cl- cotransporter KCC2 and carbonic anhydrase CAVII." J Physiol **562**(Pt 1): 27-36.

186. Rivera, C., J. Voipio, J. A. Payne, E. Ruusuvuori, H. Lahtinen, K. Lamsa, U. Pirvola, M. Saarma and K. Kaila (1999). "The K+/Cl- co-transporter KCC2 renders GABA hyperpolarizing during neuronal maturation." Nature **397**(6716): 251-255.

187. Ropers, H. H. and B. C. Hamel (2005). "X-linked mental retardation." Nat Rev Genet **6**(1): 46-57.

188. Rothwell, P. E., M. V. Fuccillo, S. Maxeiner, S. J. Hayton, O. Gokce, B. K. Lim, S. C. Fowler, R. C. Malenka and T. C. Sudhof (2014). "Autism-associated neuroligin-3 mutations commonly impair striatal circuits to boost repetitive behaviors." Cell **158**(1): 198-212.

189. Rudolph, U. and H. Mohler (2014). "GABAA receptor subtypes: Therapeutic potential in Down syndrome, affective disorders, schizophrenia, and autism." Annu Rev Pharmacol Toxicol **54**: 483-507.

190. Salcedo-Tello, P., A. Ortiz-Matamoros and C. Arias (2011). "GSK3 Function in the Brain during Development, Neuronal Plasticity, and Neurodegeneration." Int J Alzheimers Dis **2011**: 189728.

191. Samaco, R. C., C. Mandel-Brehm, H.-T. Chao, C. S. Ward, S. L. Fyffe-Maricich, J. Ren, K. Hyland, C. Thaller, S. M. Maricich and P. Humphreys (2009). "Loss of MeCP2 in aminergic neurons causes cell-autonomous defects in neurotransmitter synthesis and specific behavioral abnormalities." Proceedings of the National Academy of Sciences: pnas. 0912257106.

192. Samoriski, G. M. and C. D. Applegate (1997). "Repeated generalized seizures induce time-dependent changes in the behavioral seizure response independent of continued seizure induction." J Neurosci **17**(14): 5581-5590.

193. Scheffzek, K., M. R. Ahmadian, W. Kabsch, L. Wiesmuller, A. Lautwein, F. Schmitz and A. Wittinghofer (1997). "The Ras-RasGAP complex: structural basis for GTPase activation and its loss in oncogenic Ras mutants." Science **277**(5324): 333-338.

194. Scheffzek, K., A. Lautwein, W. Kabsch, M. R. Ahmadian and A. Wittinghofer (1996). "Crystal structure of the GTPase-activating domain of human p120GAP and implications for the interaction with Ras." Nature **384**(6609): 591-596.

195. Scoville, W. B. and B. Milner (1957). "Loss of recent memory after bilateral hippocampal lesions." J Neurol Neurosurg Psychiatry **20**(1): 11-21.

196. Sharma, S. R., X. Gonda and F. I. Tarazi (2018). "Autism Spectrum Disorder: Classification, diagnosis and therapy." Pharmacol Ther **190**: 91-104.

197. Shastri, L. (2002). "Episodic memory and cortico-hippocampal interactions." Trends Cogn Sci **6**(4): 162-168.

198. Siegel, M., C. A. Beresford, M. Bunker, M. Verdi, D. Vishnevetsky, C. Karlsson, O. Teer, A. Stedman and K. A. Smith (2014). "Preliminary investigation of lithium for mood disorder symptoms in children and adolescents with autism spectrum disorder." J Child Adolesc Psychopharmacol **24**(7): 399-402.

199. Singleton, M. K., M. L. Gonzales, K. N. Leung, D. H. Yasui, D. I. Schroeder, K. Dunaway and J. M. LaSalle (2011). "MeCP2 is required for global heterochromatic and nucleolar changes during activity-dependent neuronal maturation." Neurobiology of disease **43**(1): 190-200.

200. Sipila, S. T., K. Huttu, I. Soltesz, J. Voipio and K. Kaila (2005). "Depolarizing GABA acts on intrinsically bursting pyramidal neurons to drive giant depolarizing potentials in the immature hippocampus." J Neurosci **25**(22): 5280-5289.

201. Sipila, S. T., K. Huttu, J. Yamada, R. Afzalov, J. Voipio, P. Blaesse and K. Kaila (2009). "Compensatory enhancement of intrinsic spiking upon NKCC1 disruption in neonatal hippocampus." J Neurosci **29**(21): 6982-6988.

202. Southwell, D. G., R. C. Froemke, A. Alvarez-Buylla, M. P. Stryker and S. P. Gandhi (2010). "Cortical plasticity induced by inhibitory neuron transplantation." Science **327**(5969): 1145-1148.

203. Squire, L. R. (1992). "Memory and the hippocampus: a synthesis from findings with rats, monkeys, and humans." Psychol Rev **99**(2): 195-231.

204. Stell, B. M., P. Rostaing, A. Triller and A. Marty (2007). "Activation of presynaptic GABA(A) receptors induces glutamate release from parallel fiber synapses." J Neurosci **27**(34): 9022-9031.

205. Stiles, J. and T. L. Jernigan (2010). "The basics of brain development." Neuropsychol Rev **20**(4): 327-348.

206. Sung, K. W., M. Kirby, M. P. McDonald, D. M. Lovinger and E. Delpire (2000). "Abnormal GABAA receptor-mediated currents in dorsal root ganglion neurons isolated from Na-K-2Cl cotransporter null mice." J Neurosci **20**(20): 7531-7538.

207. Suresh, S. N., A. K. Chavalmane, V. Dj, H. Yarreiphang, S. Rai, A. Paul, J. P. Clement, P. A. Alladi and R. Manjithaya (2017). "A novel autophagy modulator 6-Bio ameliorates SNCA/alpha-synuclein toxicity." Autophagy **13**(7): 1221-1234.

208. Szabadics, J., C. Varga, G. Molnar, S. Olah, P. Barzo and G. Tamas (2006). "Excitatory effect of GABAergic axo-axonic cells in cortical microcircuits." Science **311**(5758): 233-235.

209. Tabuchi, K., J. Blundell, M. R. Etherton, R. E. Hammer, X. Liu, C. M. Powell and T. C. Sudhof (2007). "A neuroligin-3 mutation implicated in autism increases inhibitory synaptic transmission in mice." Science **318**(5847): 71-76.

210. Takayama, C. and Y. Inoue (2010). "Developmental localization of potassium chloride co-transporter 2 (KCC2), GABA and vesicular GABA transporter (VGAT) in the postnatal mouse somatosensory cortex." Neurosci Res **67**(2): 137-148.

211. Tang, X., J. Drotar, K. Li, C. D. Clairmont, A. S. Brumm, A. J. Sullins, H. Wu, X. S. Liu, J. Wang, N. S. Gray, M. Sur and R. Jaenisch (2019). "Pharmacological enhancement of KCC2 gene expression exerts therapeutic effects on human Rett syndrome neurons and Mecp2 mutant mice." Sci Transl Med **11**(503).

212. Tardin, C., L. Cognet, C. Bats, B. Lounis and D. Choquet (2003). "Direct imaging of lateral movements of AMPA receptors inside synapses." EMBO J **22**(18): 4656-4665.

213. Tassone, F., N. S. Choudhary, B. Durbin-Johnson, R. Hansen, I. Hertz-Picciotto and I. Pessah (2013). "Identification of expanded alleles of the FMR1 Gene in the CHildhood Autism Risks from Genes and Environment (CHARGE) study." J Autism Dev Disord **43**(3): 530-539.

214. Tchoumtchoua, J., M. Halabalaki, E. Gikas, A. Tsarbopoulos, N. Fotaki, L. Liu, S. Nam, R. Jove and L. A. Skaltsounis (2019). "Preliminary pharmacokinetic study of the anticancer 6BIO in mice using an UHPLC-MS/MS approach." J Pharm Biomed Anal **164**: 317-325.

215. Toyoizumi, T., H. Miyamoto, Y. Yazaki-Sugiyama, N. Atapour, T. K. Hensch and K. D. Miller (2013). "A theory of the transition to critical period plasticity: inhibition selectively suppresses spontaneous activity." Neuron **80**(1): 51-63.

216. Uvarov, P., A. Ludwig, M. Markkanen, S. Soni, C. A. Hubner, C. Rivera and M. S. Airaksinen (2009). "Coexpression and heteromerization of two neuronal K-Cl cotransporter isoforms in neonatal brain." J Biol Chem **284**(20): 13696-13704.

217. Uvarov, P., P. Pruunsild, T. Timmusk and M. S. Airaksinen (2005). "Neuronal K+/Cl- co-transporter (KCC2) transgenes lacking neurone restrictive silencer element recapitulate CNS neurone-specific expression and developmental up-regulation of endogenous KCC2 gene." J Neurochem **95**(4): 1144-1155.

218. Vaillend, C., R. Poirier and S. Laroche (2008). "Genes, plasticity and mental retardation." Behav Brain Res **192**(1): 88-105.

219. Vazquez, L. E., H.-J. Chen, I. Sokolova, I. Knuesel and M. B. Kennedy (2004). "SynGAP regulates spine formation." Journal of Neuroscience **24**(40): 8862-8872.

220. Verma, V., A. Mandora, A. Botre and J. P. Clement (2020). "Identification of an individual with a SYGNAP1 pathogenic mutation in India." Mol Biol Rep **47**(11): 9225-9234.

221. Verma, V., A. Paul, A. Amrapali Vishwanath, B. Vaidya and J. P. Clement (2019). "Understanding intellectual disability and autism spectrum disorders from common mouse models: synapses to behaviour." Open Biol **9**(6): 180265.

222. Verpelli, C. and C. Sala (2012). "Molecular and synaptic defects in intellectual disability syndromes." Curr Opin Neurobiol **22**(3): 530-536.

223. Vlaskamp, D. R. M., B. J. Shaw, R. Burgess, D. Mei, M. Montomoli, H. Xie, C. T. Myers, M. F. Bennett, W. XiangWei, D. Williams, S. M. Maas, A. S. Brooks, G. M. S. Mancini, I. van de Laar, J. M. van Hagen, T. L. Ware, R. I. Webster, S. Malone, S. F. Berkovic, R. M. Kalnins, F. Sicca, G. C. Korenke, C. M. A. van Ravenswaaij-Arts, M. S. Hildebrand, H. C. Mefford, Y. Jiang, R. Guerrini and I. E. Scheffer (2019). "SYNGAP1 encephalopathy: A distinctive generalized developmental and epileptic encephalopathy." Neurology **92**(2): e96-e107.

224. Vougogiannopoulou, K. and A. L. Skaltsounis (2012). "From Tyrian purple to kinase modulators: naturally halogenated indirubins and synthetic analogues." Planta Med **78**(14): 1515-1528.

225. Walensky, L. D., S. Blackshaw, D. Liao, C. C. Watkins, H. U. Weier, M. Parra, R. L. Huganir, J. G. Conboy, N. Mohandas and S. H. Snyder (1999). "A novel neuron-enriched homolog of the erythrocyte membrane cytoskeletal protein 4.1." J Neurosci **19**(15): 6457-6467.

226. Wang, C., C. Shimizu-Okabe, K. Watanabe, A. Okabe, H. Matsuzaki, T. Ogawa, N. Mori, A. Fukuda and K. Sato (2002). "Developmental changes in KCC1, KCC2, and NKCC1 mRNA expressions in the rat brain." Brain Res Dev Brain Res **139**(1): 59-66.

227. Wang, C. C., R. G. Held and B. J. Hall (2013). "SynGAP regulates protein synthesis and homeostatic synaptic plasticity in developing cortical networks." PLoS One **8**(12): e83941.

228. Wiesel, T. N. and D. H. Hubel (1963). "Effects of Visual Deprivation on Morphology and Physiology of Cells in the Cats Lateral Geniculate Body." J Neurophysiol **26**: 978-993.

229. Wiesel, T. N. and D. H. Hubel (1963). "Single-Cell Responses in Striate Cortex of Kittens Deprived of Vision in One Eye." J Neurophysiol **26**: 1003-1017.

230. Wiesel, T. N. and D. H. Hubel (1965). "Comparison of the effects of unilateral and bilateral eye closure on cortical unit responses in kittens." J Neurophysiol **28**(6): 1029-1040.

231. Wiesel, T. N. and D. H. Hubel (1965). "Extent of recovery from the effects of visual deprivation in kittens." J Neurophysiol **28**(6): 1060-1072.

232. Wijetunge, L. S., J. Angibaud, A. Frick, P. C. Kind and U. V. Nägerl (2014). "Stimulated emission depletion (STED) microscopy reveals nanoscale defects in the developmental trajectory of dendritic spine morphogenesis in a mouse model of fragile X syndrome." Journal of Neuroscience **34**(18): 6405-6412.

233. Williams, J. R., J. W. Sharp, V. G. Kumari, M. Wilson and J. A. Payne (1999). "The neuron-specific K-Cl cotransporter, KCC2. Antibody development and initial characterization of the protein." J Biol Chem **274**(18): 12656-12664.

234. Wolff, S. (2004). "The history of autism." Eur Child Adolesc Psychiatry **13**(4): 201-208.

235. Yao, H. B., P. C. Shaw, C. C. Wong and D. C. Wan (2002). "Expression of glycogen synthase kinase-3 isoforms in mouse tissues and their transcription in the brain." J Chem Neuroanat **23**(4): 291-297.